SPATIAL HETEROGENEITY IN *PSEUDOMONAS AERUGINOSA* BIOFILMS AND HOW IT AFFECTS ANTIBIOTIC TOLERANCE

By

Lee Alexander Richards

A dissertation submitted in partial fulfillment
of the requirements for the degree

of

Doctor of Philosophy

in

Engineering

MONTANA STATE UNIVERSITY
Bozeman, Montana

July 2006

APPROVAL

of a dissertation submitted by

Lee Alexander Richards

This dissertation has been read by each member of the dissertation committee and has been found to be satisfactory regarding content, English usage, format, citations, bibliographic style, and consistency, and is ready for submission to the Division of Graduate Education.

Philip S. Stewart

Approved for the Department of Chemical and Biological Engineering

Ron Larsen

Approved for the Division of Graduate Education

Joseph J. Fedock

STATEMENT OF PERMISSION TO USE

In presenting this dissertation in partial fulfillment of the requirements for a doctoral degree at Montana State University, I agree that the library shall make it available ot borrowers under the rules of the library. I further agree that copying of this dissertation is allowable only for scholarly purposes, consistent with "fair use" a prescribed in the U.S. Copyright Law. Requests for extensive copying or reproduction of the dissertation should be referred to Bell & Howell Information and Learning, 300 North Zeeb Road, Ann Arbor, Michigan 48106, to whom I have granted "the exclusive right to reproduce and distribute my dissertation in and from microform along with the non-exclusive right to reproduce and distribute my abstract in any format in whole or in part"

Lee Alexander Richards

July 2006

ACKNOWLEDGEMENTS

I would like to thank Frank Roe, Betsey Pitts, Garth Ehrlich, and Phil Stewart for their contributions to chapter 1 of this dissertation. Frank Roe and Betsey Pitts both contributed to the microelectrode data presented in Figure 2.1.

TABLE OF CONTENTS

TABLE OF CONTENTS CONTINUED

TABLE OF CONTENTS CONTINUED

LIST OF TABLES

LIST OF FIGURES

Figure Page

Figure Page

Figure Page

Figure Page

ABSTRACT

This dissertation presents evidence of heterogeneity within *Pseudomonas aeruginosa* biofilms and the effects of said heterogeneity on antibiotic tolerance. The existence of oxygen concentration gradients within the biofilm was confirmed. There were in fact regions within the biofilm that were nearly anoxic, this was confirmed by use of dissolved oxygen microelectrodes. The size of the aerobic zone within the biofilm agreed with the size of the active zone indicated by the use of an inducible green fluorescent protein. We found that anoxia could explain some of the biofilm's recalcitrance to the antibiotics ciprofloxacin and tobramycin, but the effects of anoxia were not adequate to explain all of an intact biofilm's tolerance to antimicrobial treatment. It was also apparent that glucose limitation was not a factor in biofilm recalcitrance.

In addition, dormancy within *Pseudomonas aeruginosa* biofilms was explored by use of a novel approach to labeling active and dormant cells within the biofilm using a strain of *P. aeruginosa* tagged with a stable, inducible, green fluorescent protein. Spatial patterns of activity were visualized by microscopy. Further, we found it possible to sort the active and dormant cells using a flow cytometer. It was thus possible to determine the relative viability of each population after treatment with the antibiotics tobramycin and ciprofloxacin. We found that dormant cells were much more tolerant to antibiotic treatment than were active cells within the same biofilm.

CHAPTER 1

INTRODUCTION

The first use of a microscope to observe organisms too small to see with the naked eye was by Robert Hook in 1664. In 1683, following Hook's groundbreaking observations of the fruiting structures of molds, Anthony van Leeuwenhoek wrote to the Royal Society of London describing the observations that he made with a self made microscope, in reality nothing more than a well made magnifying glass in reality. He wrote that he had observed what he called "animalcules" in great number, thus the study of bacteria began. Strangely enough, van Leeuwenhoek's first observations were on sessile cells existing on teeth, but for the next 300 years, research into the workings of bacteria were concentrated almost entirely on non attached planktonic bacteria. In the mid twentieth century ZoBell took a brief look at bacterial communities and their associations with surfaces (91,92). The study of bacteria existing in sessile communities encased in a matrix of extracellular polymeric substance, and attached to a surface, i.e. a biofilm was not explored in depth until the late 1970s (26). Since then the study of biofilms has come a long way. It is now thought that biofilms are the predominant form of bacterial existence in nature (22).

Biofilms have been implicated in a myriad of health related infections. Biofilms are known to be major factors in diseases such as endocarditis or inflammation of the inner layer of the heart (65) as well as bone infections (osteomyelitis) (12). In addition biofilms have even been found on things such as contact lenses (72). Biofilms are also

implicated in periodontal disease which is known to affect up to 90% of the world's population (64). Biofilms also play a large role in infections of the urinary tract (61). One of the most widespread medical problems associated with biofilms is the colonization of catheters (60,67,57) and other indwelling devices. Biofilms are capable of colonizing prosthetic heart valves (29) and implanted orthopedic devices (30). In addition, the organism *Pseudomonas aeruginosa* can colonize the lungs of persons with cystic fibrosis (21,34,44). These infections of the lung of CF patients are often very detrimental to the health of the patient. 95% of deaths associated with CF are due to respiratory disease, of which *P. aeruginosa* biofilms are the main pathogen (38). Biofilms are prevalent in such a wide ranging list of serious medical problems it is very obvious that their effective treatment has extremely important consequences.

In 1928 the discovery of penicillin by Sir Alexander Fleming led to the development of antibiotics as we know them today. This discovery led to the ability to treat a myriad of diseases that at the time were major causes of death among the population. In 1900 the four leading causes of death among the human population in the United States were influenza, pneumonia, tuberculosis, and gastroenteritis. In 2000 none of these ailments were even in the top 5 leading causes of death in the U.S. (56). With the invention of modern antimicrobial agents the control of bacteria existing in a suspended, planktonic state, is a relatively simple matter of diagnosis and treatment. The mechanisms of resistance which are employed by planktonic bacteria such as mutations to resistant phenotypes, employment of efflux pumps, and the use of modifying enzymes by the organism, are well known (79).

The elucidation of tolerance mechanisms and subsequent treatment of cells existing in the biofilm state is a much more complex matter than with planktonic cells. In 1984 Costerton elucidated the increased tolerance to biocidal agents of biofilms existing in several different environments (24). Since then, the tolerance of biofilms to antimicrobial agents has been well documented (2,4,16,19,20,23,32,36,37,63). The bacteria existing in a biofilm have many inherent advantages over free floating planktonic organisms. The most obvious difference is that the biofilm is supported by a matrix of extracellular polymeric substances (EPS) (22,25), this matrix may make up 50 to 90% of the biofilm's total organic carbon content (35). A biofilm's EPS matrix consists of up to 97% water (89) but it also contains proteins, DNA and lipids (39) though polysaccharides are the main non-water component of EPS (31, 45). The EPS helps facilitate the capture and subsequent accumulation of nutrients such as carbon and nitrogen (9). The highly hydrated state that the biofilm matrix exhibits may be very important to the biofilm. By surrounding itself in a hydrated matrix, the biofilm is better able to withstand environmental extremes. Thus, at times when nutrients or moisture are scarce, the biofilm is capable of sustaining itself longer than if it were absent the EPS matrix. EPS also plays a large role in the hydrodynamics that the biofilm is subjected to (75). The EPS matrix serves as the backbone for the biofilm structure. It allows the biofilm to develop into a physically diverse structure containing channels, interstitial voids, and large mushroom like structures (47,48,52,53). Walker and Keevil noted that biofilms growing on industrial water pipes existed in columns and stacks with a small thin layer of biomass attached to surfaces. This heterogeneity in structure caused areas of high

corrosion on the pipe walls (78). In a study by van Loosdrecht et al. it was found that biofilm structure is affected by substrate concentration as well as hydrodynamic conditions within the system in which the biofilm is grown (55). All this evidence leads to the conclusion that biofilms exist in many diverse and intricate forms, evolving to fit their environment and maximizing their potential to thrive and survive in that environment.

Knowing that the biofilm exists in a structured community forming a relatively thick film on a surface, the most intuitive explanation to the riddle of biofilms' tolerance to antimicrobial agents is that they do not completely penetrate into the biofilm. That is, not all cells are exposed to the antimicrobial and hence some are protected from killing. There has been much debate about this issue and there has been evidence in support of and against the theory that antimicrobials do not completely penetrate biofilms. Anderl et. al showed that ampicillin, an aminopenicillen, and ciprofloxacin, a fluoroquinolone, did in fact penetrate completely into *Klebsiella pneumoniae* biofilms(3). This result was confirmed by Zahller and Stewart (2002) via the use of transmission electron microscopy (TEM) (88). On the other hand, de Beer et. al found that chlorine penetration was retarded in a biofilm consisting of *Pseudomonas aeruginosa* and *Klebsiella pneumoniae* (28). Jefferson et al. used a novel approach of using a fluorescently labeled derivative of the glycopeptide vancomycin and confocal microscopy to view vancomycin penetration though *Staphylococcus aureus* biofilms (48). They found that vancomycin did penetrate through the biofilms, but it was slow to do so. Zhang and Stewart found that rifampin was able to completely penetrate *Staphylococcus epidermidis* biofilms (90). In another

study, Walters et al. found that tobramycin, an aminoglycoside antibiotic, and ciprofloxacin both penetrated *P. aeruginosa* biofilms (80). Grobe et al. reported that chlorine and glutaraldehyde both showed incomplete or slow penetration in *P. aeruginosa* biofilms (40). The penetration of antibiotics through *P. aeruginosa* biofilms is further complicated by the existence of alginate in the EPS matrix. It has been shown that penetration of antibiotics is inhibited by the presence of alginate (71). Nichols et. al. found that tobramycin penetration was inhibited by its binding to sodium alginate but the inhibition did not cause a substantial reduction in penetration time in *Pseudomonas aeruginosa* biofilms (62). Abdi-Ali et al. showed that the rate of permeation of several fluoroquinolone, β-lactam, and aminoglycoside antibiotics was reduced but not halted in alginate of *P. aeruginosa*, indicating that these antibiotics should eventually penetrate through *P. aeruginosa* biofilms (1). On the contrary, Hatch and Schiller showed that the diffusion of gentamicin, another aminoglycoside, and tobramycin were inhibited by a 2% suspension of *P. aeruginosa* alginate (42). Additionally, Shigeta et al. showed that aminoglycosides did penetrate *P. aeruginosa* biofilms but were slow to do so, where fluoroquinolone antibiotics were able to permeate the biofilm in a more rapid fashion (70). It is obvious that the issue of antibiotic penetration through biofilms is difficult to categorize and draw conclusions from. The important thing to note is that in nearly all cases where antibiotics were able to completely penetrate the biofilm, the biofilm was not completely killed. This is a very important result. If penetration was the sole factor to the biofilm's recalcitrance to antimicrobials, then treatment with antibiotics that do completely penetrate the biofilm should result in complete killing. This is not the case.

Another theory for explaining the tolerance of biofilms to antimicrobials is that the cells mutate into a resistant form. It has been shown that 1% of the genes within a *Pseudomonas aeruginosa* biofilm are expressed at different levels than those of planktonic cells (83). Some of these genes could lead to the antibiotic tolerance expressed by biofilms. When β-lactam antibiotics are introduced to the biofilm, genes for the production of alginate biosynthesis were up-regulated (6). This in effect could lead to greater tolerance to antimicrobials due to alginate's ability to bind to some antimicrobials and subsequently slow penetration into the biofilm, although the change in gene expression within biofilms does not appear to be the underlying reason for biofilm tolerance. When cells are grown in the biofilm state, then dispersed into suspension, and subsequently treated they have been found to be equally susceptible to antimicrobial treatment as planktonic cells (5,84). This would tend to agree with the idea that increased alginate production would help halt penetration of some antimicrobial agents allowing the biofilm more tolerance to treatment. If the biofilm were no longer surrounded by the alginate bearing EPS, cells would be fully exposed to antimicrobial agents. This does not change the fact that even when antibiotics have been shown to penetrate the biofilm, much of the biofilm is still able withstand treatment. Thus, changing gene expression within the biofilm probably leads to some properties of the biofilm aiding in its ability to resist antimicrobial treatment but it is not the entire reason for biofilm recalcitrance. It is the biofilm state of growth that ultimately leads to the tolerance of biofilms to antimicrobial agents.

The idea that the biofilm exists in a state of physiological heterogeneity is one that may ultimately explain some of the biofilms tolerance to antimicrobial agents. Since the biofilm has been established as a whole to have a very diverse structure, it would make sense that the cells within the biofilm would not all be existing in the same physiological state. The cells within the biofilm may be in differing states of protein synthetic activity, growth rate, and there may be localized nutrient deficiency within the biofilm.

Korber et al. showed that biofilms stained after treatment with the fluoroquinolone fleroxacin showed a heterogeneous pattern of staining with acridine orange (51). Kinniment and Wimpenny found that adenylate (a measure of the energetic status of living cells) levels changed throughout the biofilm, indicating that cells within the biofilm exist in a state of energetic heterogeneity (50). Caldwell et al. used confocal scanning laser microscopy (CSLM) to determine that there were areas of differing pH within *Vibrio parahaemolyticus* biofilms (18). Vroom et al. confirmed this finding by noting pH gradients in mixed species oral biofilms, using two photon excitation microscopy (77). Huang et al. showed that alkaline phosphatase (an enzyme used as an indicator of phosphate starvation) expression patterns were tied to nutrient availability, thus gene expression within the biofilm is affected by nutrient availability (46). Xu et al. showed that alkaline phosphatase activity was greatly limited by anaerobic conditions and confirmed that alkaline phosphatase activity was localized near the air interface in *Pseudomonas aeruginosa* biofilms (86). Prignet-Combaret et al. showed that there was a major change in gene expression patterns in developing *Escherichia coli* biofilms. In addition they determined that within the biofilm there exists oxygen limitation and

greater cell density and osmolarity conditions than in suspended planktonic cells (66). It is obvious that biofilms often exist in extremely varied conditions. It is these varied conditions that lead to the complexity of the biofilm in comparison to planktonic cells. Boles et al. noted extensive genetic diversity within cells of *P. aeruginosa* biofilms and hypothesized that this diversity was self induced and led to increased survival of biofilms when exposed to environmental stresses (10).

One of the most prevalent forms of heterogeneity within biofilms is the availability of oxygen. As early as 1983 Wimpenney and Coombs used microelectrodes to determined that there was in fact an oxygen gradient within colonies of *Bacillus cereus* (85). Boessmann et al. showed that there were distinct oxygen gradients within biofilms grown in airlift loop reactors (10). These data were confirmed by Hibiya et al. in environmental biofilms (43). Tresse et al. used a method of immobilizing *E. coli* in agar to determine that decreased oxygen availability increased biofilm tolerance to latamoxef, a β-lactam antibiotic, and tobramycin (76). It has also been shown by the use of microelectrodes that oxygen gradients in biofilms were affected by channels within the biofilms and that oxygen concentration is highly stratified within thick biofilms (68). That the biofilm differs as oxygen concentration differs is additionally supported by the observations of Sabra et al. They noted formation of membrane vesicles on the surface of *P. aeruginosa* increased when the biofilm was exposed to lower oxygen concentrations (69). This increase in production of membrane vesicles is an indicator of greater formation of B-band LPS (8). B-band LPS (as opposed to A-Band LPS) is one of the two lipopolysaccharides that *P. aeruginosa* can produce. The important thing to note from

this observation is that the biofilm is undergoing distinct changes due to a change in the partial pressure of oxygen around the biofilm.

Wentland et al. found that bacteria within biofilms were growing rapidly at the air interface but as the depth in the biofilm increased the growth rate of the cells decreased (82). Sternberg et al. showed that as biofilms of *Pseudomonas putida* age, the cells within the biofilm exist in differing states of growth, with some cells growing very slowly. They also reported that when nutrients were supplied to the slow growing cells, they could be stimulated to grow again (74). Brown et al. reported that some cells within the biofilm differ in their access to nutrients and exist in a slow-growing state (17). From these observations it is easy to come to the conclusion that cells within the biofilm exist in differing states of growth. Could this explain the biofilms tolerance to antimicrobial agents? Evans et al. noted that the tolerance to ciprofloxacin of cultures of both *E. coli* and *P. aeruginosa* grown in a chemostat was directly related to the growth rate of the cells (33). Ashby et al. found that biofilms were more susceptible to antibiotics known to be effective against non growing bacteria, indicating that at least part of the biofilm's recalcitrance was due to growth rate (7). Brooun et al. (2000) presented evidence that cells obtained from biofilms, and treated under conditions where growth was halted exhibited increased tolerance to tobramycin then did planktonic cells, but the decrease in killing was not enough to reconcile the intact biofilm's tolerance (13). Moyer and Morita showed that growth rate affected the concentrations of DNA, RNA, and protein within planktonic cells (59). This result is important in that it indicates that cells of differing growth rate are drastically different from each other. It very well may be that bacteria

within biofilms differ in similar ways depending on their spatial location with in the biofilm. Stenstrom et al. showed that starved cells had a reduced susceptibility to some antibiotics (73). Xu et al. observed gene expression and quantified the protein of RpoS (a stationary phase sigma factor) to determine that *P. aeruginosa* biofilms are much like stationary phase cultures (86). Biofilms may exist in a starved and or dormant state due to nutrient availability. That is, in certain locations within the biofilms cells may be lacking essential nutrients and this may induce them into an altered state as compared to cells with high anabolic activity.

This leads us to the concept of persistor cells. One explanation for the recalcitrance of biofilms is that there is a small population of cells within the biofilm that are inherently resistant to treatment with antimicrobial agents, and it is these cells that allow the biofilm to re-establish itself after treatment. Brooun et al. found that when *P. aeruginosa* biofilms were exposed to quinolones there emerged a very small population of the cells which were resistant to killing (12). It has been hypothesized that these "persistor" cells do not enter their protected state due to any lack of nutrients or other deficiencies but they are inherently predisposed to be resistant to antimicrobial killing (54). However, it has been shown that production of resistant cells is a function of the growth stage that the cells are in (49). When resistant cells are isolated and re-cultured the resulting culture is no more tolerant to treatment than average cells (58). In addition Harrison et al. presented evidence that there is a small population of cells within *P. aeruginosa* biofilms that were resistant to killing by high concentrations of metal cations (41).

Scope of This Dissertation

It is the scope of this thesis to explore two of the afore mentioned aspects of a biofilm's heterogeneity and the subsequent effect on tolerance to antibiotic treatment. The first aspect explored was oxygen availability. Dissolved oxygen microelectrodes were used to first confirm that there were in fact oxygen gradients within *Pseudomonas aeruginosa* biofilms. Patterns of anabolic activity were then mapped using an inducible green fluorescent protein tagged strain of *P. aeruginosa.* The effects of oxygen limitation were then explored in relation to tolerance to the antibiotics ciprofloxacin and tobramycin. It should be noted that Chapter 2 is a recreation of an article submitted for publication with coauthors Frank Roe, Betsey Pitts, Garth D. Ehrlich and Philip S. Stewart. It should also be noted that the data for figure 2.1 was generated by Frank Roe and Betsey Pitts.

In the second part of the concept of dormancy within the biofim was explored. Work by Wayne and Hayes suggest that tubercle bacilli enter a dormant state when exposed to anoxic conditions and it is this dormant state that aids in their recalcitrance to antimicrobials (81). In stationary phase cultures it has been noted that planktonic bacteria express a general stress response (GSR) in which bacteria become more tolerant to antimicrobial treatment (14). Brown and Smith theorized that in chronic biofilm infections bacteria experience slow growth and thus express a GSR. They also proposed that this may play a big role in recalcitrance of bacteria in biofilm infections (15). This idea of dormant cells within the biofilm being extremely tolerant to antimicrobials is

explore further in this work. By using a novel approach to label anabolically active and dormant cells within the biofilm, we have been able to visualize patterns of dormancy. In addition with the use of flow cytometry we have been able to quantify the susceptibility of dormant cells within the biofilm.

REFERENCES

1) Abdi-Ali, A.; Mohammadi-Mehr, M.; Alaei, A.A.; Bactericidal activity of various antibiotics against biofilm-producing *Pseudomonas aeruginosa*. International Journal of Antimicrobial Agents 2006, 27, 196-200

2) Allison, D.G.; Gilbert, P.; Modification by surface association of antimicrobial susceptibility of bacterial populations. Journal of Industrial Microbiology 1995, 15, 311-317

3) Anderl, J.N.; Franklin, M.J.; Stewart P.S. Role of antibiotic penetration limitation in *Klebsiella pneumonia* biofilm resistance to ampicillin and ciprofloxacin. Antimicrobial Agents and Chemotherapy 2000, 44, 1818-1824

4) Anwar, H; Dasgupta, M.K.; Costerton, J.W. Testing the susceptibility of bacteria in biofilms to antibacterial agents. Antimicrobial Agents and Chemotherapy 1990, 34, 2043-2046

5) Anwar, H.; van Biesen, T.; Dasgupta, M.; Lam, K.; Costerton, J.W.; Interaction of biofilm bacteria with antibiotics in a novel in vitro chemostat system. Antimicrobial Agents and Chemotherapy 1989, 33, 1824-1826

6) Ashby, M.J., Neale, J.E., Knott, S.J., Critchley, I.A., Effects of antibiotics on non-growing planktonic cells and biofilms of *Escheria coli*. Journal of Antimicrobial Chemotherapy 1994, 33(3), 443-452

7) Bagge, N.; Schuster, M.; Hentzer, M.; ciofu, O.; Givskov. M.; Greenberg, E.P.; Hoiby, N.; *Pseudomonas aeruginosa* biofilms exposed to imipenen exhibit changes in global gene expression and β-lactamase and alginate production. Antimicrobial Agents and Chemotherapy 2004, 48(4), 1175-1187

8) Beveridge, T.J.; Structure of Gram-negative cell walls and their derived membrane vesicles. Journal of Bacteriology 1999, 181, 4725-4733

9) Beveridge, T.J.; Makin, S.A.; Kadurugamuwa, J.L.; Li, Z.; Interactions between biofilms and the environment. FEMS Microbiology Reviews 1997, 20, 291-303

10) Boessmann, M.; Staudt, C.; Neu, T.R.; Horn, H.; Hempel, D.C.; Investigation and modeling of growth, structure, and oxygen penetration in particle supported biofilms. 2003, 26, 219-222

11) Boles, B.R.; Thoendel, M.; Singh, P.K.; Self generated diversity produces "insurance effects" in biofilm communities. Proceedings of the National Academy of Sciences of the United States of America 2004, 101(47), 16630-16635

12) Brady, R.A.; Leid, J.G.; Costerton, J.W.; Shirtliff, M.E.; Osteomyelitis: clinical overview and mechanisms of infection persistence. Clinical Microbiology Newsletter 2006, 28 (9), 65-72

13) Brooun, A.; Liu, S.; Lewis, K.; A dose-response study of antibiotic resistance in *Pseudomonas aeruginosa* biofilms. Antimicrobial Agents and Chemotherapy 2000, 44(3), 640-646

14) Brown, M.R.W.; Smith, A.W.; Dormancy and persistence in chronic infection: Role of the general stress response in resistance to chemotherapy. 2001 Journal of Antimicrobial Chemotherapy 48, 141-142

15) Brown, M.R.W.; Barker, J.; Unexplored reservoirs of pathogenic bacteria: Protozoa and Biofilms. Trends in Microbiology 1999, 7 (1) 46-50

16) Brown, M.R.W.; Gilbert, P.; Sensitivity of biofilms to antimicrobial agents. Journal of Applied Bacteriology 1993, 74, 87-97

17) Brown, M.R.W,; Allison, D.G.; Gilbert, P.; Resistance of bacterial biofilms to antibiotics: a growth-rate related effect? Journal of Antimicrobial Chemotherapy 1988, 22 (6), 777-780

18) Caldwell, D.E.; Korber, D.R.; Lawrence, J.R.; Confocal laser microscopy and digital image analysis in microbial ecology. Advances in Microbial Ecology 1992, 12, 1-67

19) Carpentier, B.; Cerf, O.; Biofilms and their consequences, with particular reference to hygiene in the food industry. Journal of Applied Bacteriology 1993, 75, 499-511

20) Ceri, H.; Olson, M.E.; Stremick, C.; Read, R.R.; Morck, D.; Buret, A.; The Calgary biofilm device: new technology for rapid determination of antibiotic susceptibilities of bacterial biofilms. Journal of Clinical Microbiology 1999, 37(6), 1771-1776

21) Costerton, J.W.; Cystic fibrosis pathogenesis and the role of biofilms in persistent infection. TRENDS in Microbiology 2001, 9(2), 50-52

22) Costerton J.W.; Lewandowski, Z,; Caldwell. D.E.; Korber, D.R.; Lappin-Scott, H.M.; Microbial biofilms. Annual Review of Microbiology 1995, 49, 711-745

23) Costerton, J.W.; Chang, K.J.; Geesey, G.G.; Ladd, T.I.; Nickel, J.C.; Dasgupta, M.; Marrie, T.J.; Bacterial biofilms in nature and disease. Annual Review of Microbiology 1987, 41, 435-464

24) Costerton, J.W.; The formation of biocide-resistant biofilms in industrial, natural, and medical systems. Developments in Industrial Microbiology 1984, 25, 363-372

25) Costerton. J.W.; Irvin, T.R.; The bacterial glycocalyx in nature and disease. Annual Review of Microbiology 1981, 35, 299-324

26) Costerton, J.W.; Geesey, G.G.; Cheng, K, J,; How bacteria stick. Scientific American 1978, 238, 86

27) De Beer, D.; Stoodley, P.S.; Lewandowski, Z.; Liquid flow and mass transport in heterogeneous biofilms. Water Resources 1996, 30(11), 2761-2765

28) De Beer, D.; Srinivasan, R.; Stewart, P.S.; Direct measurement of chlorine penetration into biofilms during disinfection. Applied and Environmental Microbiology 1994, 60(12), 4339-4344

29) Dickinson, G.M.; Bisno, A.L. Infections associated with indwelling devices: concepts of pathogenesis; infections associated with intravascular devices. Antimicrobial Agents and Chemotherapy 1989, 33(5), 597-601

30) Dickinson, G.M.; Bisno, A.L. Infections associated with indwelling devices: infections related to extravascular devices. Antimicrobial Agents and Chemotherapy 1989, 33(5), 602-607

31) Donlan, R.M.; Biofilms: microbial life on surfaces. Emerging Infectious Diseases 2002, 8(9), 881-890

32) Eng, R.H.K.; Padberg, F.T.; Smith, S.M.; Tan, E.N.; Cherubin, C.E. Bactericidal effects of antibiotics on slowly growing and nongrowing bacteria. Antimicrobial Agents and Chemotherapy 1991, 35, 1824-1828

33) Evans, D.J.; Allison, D.G.; Brown, M.R.; Gilbert, P.; Susceptibility of *Pseudomonas aeruginosa* and *Escherichia coli* biofilms towards ciprofloxacin: effect of specific growth rate. Journal of Antimicrobial Chemotherapy 1991, 27(2), 177-184

34) Field, T.R.; White, A.; Elborn, J.S.; Tunney, M.M.; Effect of oxygen limitation on the in vitro antimicrobial susceptibility of clinical isolates of *Pseudomonas aeruginosa* grown planktonically and as biofilms. European Journal of Clinical Microbiology and Infectious Disease 2005, 24, 677-687

35) Flemming, H.C.; Wingender, J.; Griegbe, M.C.; Physico-chemical properties of biofilms. In: Evans LV, editor. Biofilms: recent advances in their study and control. Amsterdam: Harwood Academic Publishers; 2000. p. 19–34

36) Gander, S.; Bacterial Biofilms: resistance to antimicrobial agents. Journal of Antimicrobial Agents and Chemotherapy 1996, 37, 1047-1050

37) Gilbert, P.; Collier, P.J.; Brown, M.R.W.; Influence of growth rate on susceptibility to antimicrobial agents: Biofilms, cell cycle, dormancy, and stringent response. Antimicrobial Agents and Chemotherapy 1990, 34, 1865-1868

38) Gilligan, P.H.; Microbiology of airway disease in patients with cystic fibrosis. Clinical Microbiology Reviews 1991, 4, 35-51

39) Goodwin, J.A.S.; Forster, C.F.; A further examination into the composition of activated sludge surfaces in relation to their settlement characteristics. Water Resources 1985, 19, 527-533

40) Grobe, K.J.; Zahller, J.; Stewart, P.S.; Role of dose concentration in biocide efficacy against *Pseudomonas aeruginosa* biofilms. Journal of Industrial Microbiology and Biotechnology 2002, 29, 10-15

41) Harrison, J.J.; Turner, R.J.; Ceri, H.; Persistor cells, the biofilm matrix and tolerance to metal cations in biofilm and planktonic *Pseudomonas aeruginosa* biofilms. Environmental Microbiology 2005, 7(7), 981-994

42) Hatch, R.A.; Schiller, N.L.; Alginate lyase promotes diffusion of aminoglycosides through the extracellular polysaccharide of mucoid *Pseudomonas aeruginosa*. Antimicrobial Agents and Chemotherapy 1998, 42(4), 974-977

43) Hibiya, K.; Nagai, J.; Tseuneda, S.; Hirata, A.; Simple prediction of oxygen penetration depth in biofilms for wastewater treatment. Biochemical Engineering Journal 2004, 19, 61-68

44) Hoiby, N.; Johansen, H.K.; Moser, C.; Song, Z.; Ciofu, O.; Kharazmi, A.; *Pseudomonas aeruginosa* and the in vitro and in vivo biofilm mode of growth. Microbes and Infection 2001, 3, 23-35

45) Horan, N.J.; Eccles, C.R.; Purification and characterization of extracellular polysaccharide from activated sludges. Water Resources 1986, 20, 1427-1432

46) Huang, C-T.; Xu, K.D.; McFeters, G.A.; Stewart, P.S.; Spatial patterns of alkaline phosphatase expression within bacterial colonies and biofilm in response to phosphate starvation. Applied and Environmental Microbiology 1998, 64(4), 1526-1531

47) Hunter, R.C.; Beveridge, T.J.; High Resolution Visualization of *Pseudomonas aeruginosa* PAO1 Biofilms by Freeze-Substitution Transmission Electron Microscopy. Journal of Bacteriology 2005, 22, 7619-7630

48) Jefferson, K.K., Goldmann, D.A.; Pier, G.B.; Use of confocal microscopy to analyze the rate of vancomycin penetration through *Staphylococcus aureus* biofilms. Antimicrobial Agents and Chemotherapy 2005, 49(6) 2467-2473

49) Karen, I.; Kaldalu, N.; Spoering, A.; Wang, Y.; Lewis, K.; Persistor cells and tolerance to antimicrobials. FEMS Microbiology Letters 2004, 230, 13-18

50) Kinniment, S.L.; Wimpenny, J.W.T.; Measurements of the distribution of adenylate concentrations and adenylate energy charge across *Pseudomonas aeruginosa* biofilms. Applied and Environmental Microbiology 1992, 58(5), 1629-1635

51) Korber, D.R.; James, G.A.; Costerton, J.W.; Evaluation of fleroxacin activity against established *Pseudomonas fluorescens* biofilms. Applied and Environmental Microbiology 1994, 60(5), 1663-1669

52) Lawrence, J.R.; Korber, D.R.; Hoyle, B.D., Costerton, J.W.; Caldwell, D.E. Optical sectioning of microbial biofilms. Journal of Bacteriology 1991, 173, 6558-6567

53) Lewandowski, Z.; Structure and function of biofilms. In Evans, L.V.; editor Biofilms: recent advances in their study and control. 2000 Amsterdam: Harwood Academic Publishers pp 1-17

54) Lewis, K.; Riddle of biofilm resistance. Antimicrobial Agents and Chemotherapy 2001, 45(4), 999-1007

55) van Loosdrecht, M.C.M.; Eikelbroom, D.; Gjaltema, A.; Mulder, A.; Tijhuis, L.; Heijnen, J.J.; Biofilm structures. Water Science and Technology 1995, 32, 35-43

56) Madigan, M.T.; Martinko, J.M.; Parker, J.; In Brock Biology of Microorganisms. 2003, New Jersey, Prentice Hall, Tenth Edition, pp. 7

57) Morris, N.S.; Stickler, D.J.; McLean, R.J.C.; The development of bacterial biofilms on indwelling urethral catheters. World Journal of Urology 1999, 17, 345-350

58) Moyed, H.S.; Bertrand, K.P.; hipA, a newly recognized gene of *Escherichia coli* K-12 that affects frequency of persistence after inhibition of murein synthesis. Journal of bacteriology 1983, 155(2), 768-775

59) Moyer, C.L.; Morita, R.Y.; Effect of growth rate and starvation-survival on Cellular DNA, RNA, and protein of psychrophilic marine bacterium. Applied and Environmental Microbiology 1989, 55(10), 2710-2716

60) Nakame, G.T.; Nishida, M.; Ohi, Y.; Bacterial biofilms and catheters in experimental urinary tract infection. International Journal of Antimicrobial Agents 1999, 11(3-4) 227-231, 237-239

61) Nakano, M.; Yasuda, M.; Yokoi, S.; Takahashi, Y.; Ishihara, S.; Deguchi, T.; In vivo selection of *Pseudomonas aeruginosa* with decreased susceptibilities to fluoroquinolones during fluoroquinolone treatment of urinary tract infection. Urology 2001, 58(1), 125-128

62) Nichols, W.W.; Dorrington, S.M.; Slack, M.P.E.; Walmsley, H.L.; Inhibition of tobramycin diffusion by binding to alginate. Antimicrobial Agents and Chemotherapy 1988, 32(4), 518-523

63) Nickel, J.C.; Ruseska, I.; Wright, J.B.; Costerton, J.W.; Tobramycin Resistance of *Pseudomonas aeruginosa* cells growing as a biofilm on urinary catheter material. Antimicrobial Agents and Chemotherapy 1985, 27, 619-624

64) Philstrom, B.L.; Michalowicz, B.S.; Johnson, N.W.; Periodontal diseases. Lancet 2005, 336, 1809-1820

65) Presterl, E.; Grisold, A. J.; Reichmann, S.; Hirschl,. A. M.; Georgopoulos, A.; Graninger, W.; *Viridans Streptococci* in endocarditis and neutropenic sepsis: Biofilm formation and effects of antibiotics. Journal of Antimicrobials and Chemotherapy 2005, 55(1), 45-50

66) Prigent-Combaret, C.; Vidal, O.; Dorel, C.; Lejeune, P.; Abiotic surface sensing and biofilm dependent regulation of gene expression in *Escherichia coli*. Journal of Bacteriology 1999, 181(19), 5993-6002

67) Raad, I.; Costerton, W.; Sabharwal, U.; Sacilowski, M.; Anaissie, W.; Bodey, G.P.; Ultrastructural analysis of indwelling vascular catheters: a quantitative relationship between luminal colonization and duration of placement. Journal of Infectious Disease 1993, 168, 400-407

68) Rasmussen, K.; Lewandowski, Z.; Microelectrode measurements of local mass transport rates in heterogeneous biofilms. Biotechnology and Bioengineering 1998, 59(3), 302-309

69) Sabra, W.; Lunsdorf, H.; Zeng, A,P.; Alterations in the formation of lipopolysaccharide and membrane vesicles on the surface of *Pseudomonas aeruginosa* PAO1 under oxygen stress conditions. Microbiology 2003, 149, 2789-2795

70) Shigeta, M.; Tanaka, G.; Komatsuzawa, H.; Sugai, M.; Suginaka, H.; Usui, T.; Permeation of antimicrobial agents through *Pseudomonas aeruginosa* biofilms: a simple method. Chemotherapy 1997, 43(5), 340-345

71) Slack, M.P.E.; Nichols, W.W., Antibiotic penetration of antibiotics through sodium alginate and through the exopolysaccharide of a mucoid strain of *Pseudomonas aeruginosa*. Lancet 1981, ii, 502-503

72) Slusher, M.M.; Myrvik, Q.N.; Lewis, J.C.; Gristina, A.G.; Extended wear lenses, biofilm, and bacterial adhesion. Archives of Ophthalmology 1987, 105(1), 110-115

73) Stenstrom, T.A.; Conway, P., Kjelleberg, S.; Inhibition by antibiotics of the bacterial response to long term starvation of *Salmonella tryphimurium* and the colon microbiota of mice. Journal of Applied Bacteriology 1989, 67(1), 53-59

74) Sternberg, C.; Christensen, B.B.; Johansen, T.; Nielson, A.T.; Andersen, J.B.; Givskov, M.; Molin, S.; Distribution of bacterial growth activity in flow-chamber biofilms. Applied and Environmental Microbiology 1999, 65(9), 4108-4117

75) Stoodley, P.K.; DeBeer, D.; Lewandowski, Z.; Liquid flow in biofilm systems. Applied Environmental Microbiology 1994, 60, 2711-2716

76) Tresse, O.; Jouenne, T.; Junter, G.A.; The role of oxygen limitation in the resistance of agar entrapped, sessile-like *Escherichia coli* to aminoglycoside and beta-lactam antibiotics. Journal of Antimicrobial Chemotherapy 1995, 36(3), 521-526

77) Vroom, J.M.; De Grauw, K.J.; Gerritsen, H.C.; Bradshaw, D.J.; Marsh, P.D.; Watson, G.K.; Birmingham, J.J.; Allison, C.; Depth penetration and detection of pH gradients in biofilms by two photon excitation microscopy. Applied and Environmental Microbiology 1999, 65(8), 3502-3511

78) Walker, J.T.; Keevil, C.W.; Study of microbial biofilms using light microscope technique. International Biodeterioration and Biodegradation 1994, 223-236

79) Walsh, C.; Molecular mechanisms that confer antibacterial drug resistance. Nature 2000, 406, 775-781

80) Walters, M.C.; Roe, F.; Bugnicourt, A.; Franklin, M.J.; Stewart, P.S.; Contributions of antibiotic penetration, oxygen limitation, and low metabolic activity to tolerance of *Pseudomonas aeruginosa* biofilms to ciprofloxacin and tobramycin. Antimicrobial Agents and Chemotherapy 2003, 47(1), 317-323

81) Wayne, L.G.; Hayes, L.G.; An in vitro model for sequential study of shiftdown of *mycobacterium tuberculosis* through two stages of nonreplicating persistence. Infection and Immunity 1996, 64(6), 2062-2069

82) Wentland, E.J.; Stewart, P.S.; Huang, C-T.; McFeters, G.A.; Spatial variations in growth rate within *Klebsiella pneumonia* colonies and biofilm. Biotechnology Progress 1996, 12(3), 316-321

83) Whiteley, M., Bangera, M.G.; Bumgarner, R.E.; Parsek, M.R.; Teitzel, G.M.; Lory, S.; Greenberg, E.P.; Gene expression in *Pseudomonas aeruginosa* biofilms. Nature 2001, 413, 860-864

84) Williams, I.; Venables, W.A.; Lloyd, D.; Paul, F.; Critchley, I.; The effects of adherence to silicone surfaces on antibiotic susceptibility in *Staphylococcus aureus*. Microbiology 1997, 143, 2407-2413

85) Wimpenny, J.W.; Coombs, J.P.; Penetration of oxygen into bacterial colonies. Journal of General Microbiology 1983, 129, 1239-1242

86) Xu, K.D.; Frankilin, M.J.; park, C-H,; McFeters, G.A.; Stewart, P.S.; Gene expression and protein levels of stationary phase sigma factor, RpoS, in continuously-fed *Pseudomonas aeruginosa* biofilms. FEMS Microbiology Letters 2001, 199, 67-71

87) Xu, K.D.; Stewart, P.S.; Xia, F.; Huang, C.; McFeters, G.A., Spatial physiological heterogeneity in *Pseudomonas aeruginosa* is determined by oxygen availability applied and environmental microbiology 1998, 64, 4035-4039

88) Zahller, J.; Stewart, P.S.; Transmission electron microscopic study of antibiotic action on *Klebsiella pneumoniae* biofilm. Antimicrobial Agents and Chemotherapy 2002, 46(8), 2679-2683

89) Zhang, X.Q.; Bishop, P.L.; Kupferle, M.J.; Measurement of polysaccharides and proteins in biofilm extracelluar polymers. Water Science Technology 1998, 37, 345-348

90) Zhang, Z.; Stewart, P.S.; Penetration of rifampin through *Staphylococcus epidermidis* biofilms. Antimicrobial Agents and Chemotherapy 2002, 46(3), 900-903

91) ZoBell, C.E.; The effect of solid surfaces upon bacterial activity. Journal of Bacteriology 1943, 46, 39-56

92) ZoBell, C.E.; Allen, E.C.; The significance of marine bacteria in the fouling of submerged surfaces. Journal of Bacteriology 1935, 29, 239-251

CHAPTER 2

CONTRIBUTIONS OF OXYGEN AND GLUCOSE LIMITATION TO *PSEUDOMONAS AERUGINOSA* BIOFILM TOLERANCE OF CIPROFLOXACIN AND TOBRAMYCIN

This work has been submitted to the journal Antimicrobial Agents and Chemotherapy, March 2006.

Authors: Lee Richards, Frank Roe, Betsey Pitts, Garth D. Ehrlich, and Philip S. Stewart

Abstract

The role of oxygen and glucose limitation in the protection of *Pseudomonas aeruginosa* biofilms from killing by the antibiotics tobramycin and ciprofloxacin was investigated in vitro. Biofilms were grown on a glucose minimal medium under low shear, continuous flow conditions in drip-flow reactors for three days, then challenged with either tobramycin or ciprofloxacin for 12 h. Bacteria in intact biofilms were less susceptible to the antibiotics than were cells challenged in suspension cultures. Steep oxygen concentration gradients were measured in the vicinity of the biofilm using microelectrodes and the expression of an inducible GFP was limited to a sharply demarcated band immediately adjacent to the oxygen source. These results showed that the biofilm contained regions of low oxygen concentration and low metabolic activity. A reaction-diffusion analysis showed that glucose was not depleted within the biofilm. The influence of oxygen and glucose availability on bacterial susceptibility was investigated

by manipulating the concentrations of these two substrates in planktonic cultures, by resuspending biofilms into medium either containing or lacking oxygen or glucose, and by manipulating the concentration of oxygen or glucose supplied to an intact biofilm during the antibiotic treatment period. These various tests yielded mixed results. It was concluded that oxygen limitation is one factor in the protection of *P. aeruginosa* biofilms from killing by tobramycin and ciprofloxacin, but is not, by itself, a sufficient explanation for the full extent of biofilm recalcitrance. Glucose limitation in these biofilms is unlikely and probably does not contribute to their reduced antibiotic susceptibility.

Introduction

One explanation for the chronic nature of some infections involving the opportunistic pathogen *Pseudomonas aeruginosa* is that this organism is adept at forming biofilms in which bacteria are protected from host defenses and from killing by antibiotics (6,11). The protection from antibiotics enjoyed by bacteria in biofilms probably depends on multiple factors (9,11). It has been shown that antibiotics do penetrate into the biofilm, yet bacteria are poorly killed (1,12). A plausible explanation for reduced antibiotic susceptibility in biofilms is that nutrient limitation leads to slow growth or stationary phase existence for many of the cells in a biofilm, reducing their antimicrobial susceptibility. In the case of *P. aeruginosa* growing in biofilms, oxygen limitation is known to occur readily in vitro (12,13,17) and has also been demonstrated in vivo in cystic fibrosis patients (15). Molecular biological evidence further suggests that *P. aeruginosa* in the cystic fibrosis lung experience anaerobic conditions (18). Oxygen

availability appears to modulate antibiotic action in *P. aeruginosa* (4,7,8), especially in the biofilm state (2). This article addresses the contribution of oxygen limitation, and also of glucose limitation, to the protection of biofilms formed by *P. aeruginosa* from killing by tobramycin and ciprofloxacin.

Materials and Methods

Strains, Media, and Antibiotics

Pure cultures of the *Pseudomonas aeruginosa* strain PAO1 were used for all experiments involving antibiotic treatment. Experiments investigating patterns of protein synthetic activity, used strain PAO1 (pAB1), containing a plasmid with an isopropylthio-beta-*D*-galactoside (IPTG) inducible gene for expression of a stable green fluorescent protein (GFP) (12). The vector control *P. aeruginosa* PAO1 (pPMF54) contained the same plasmid as pAB1, except that the GFP gene was not present. *P. aeruginosa* was grown in Pseudomonas basal medium (PBM) containing 0.2 g l^{-1} glucose for experiments measuring growth or antibiotic susceptibility. Inocula were grown in the same medium containing 1 g l^{-1} glucose. Bacteria were grown and experiments were conducted at 37^{o}C. Tobramycin sulfate was obtained from Sigma (St. Louis, MO) and ciprofloxacin hydrochloride was a gift of the Bayer Corporation (Leverkusen, Germany). Viable cell numbers were determined by colony formation on tryptic soy agar (TSA; Difco, Detroit, MI).

Biofilm Preparation

Biofilms were grown in drip-flow reactors (17). The medium used during treatment and growth was PBM with 0.2 g l^{-1} glucose as a carbon source. Drip-flow reactors consisted of four parallel chambers. The chambers were covered with polycarbonate windows containing a septum to allow for medium introduction through 22 gauge needles. The lid also contained a filtered air vent to allow sterile air to enter the reactor. Medium was pumped into the chambers at a flow rate of 50 ml hr^{-1}. The medium was allowed to drip onto stainless steel slides placed in the chambers of the reactor. The reactors were placed on a stand inclined at 10º from horizontal. After running down over the slide, spent medium drained out through a port at the bottom of each chamber. The stainless steel slides were 9.72 cm^2 in area. The reactors were inoculated by adding 1 ml of an overnight culture, grown to an OD_{600} of approximately 0.3 to 15 ml of PBM containing 1 g l^{-1} glucose covering the steel slide. The reactor was sealed by clamping the effluent tubes and the seeded medium was allowed to sit in the reactor for 18 hours while on a level surface. After this inoculation period, the reactor was inclined and flow was initiated. The entire drip-flow reactor was kept in a 37 ^oC incubator. Medium was warmed by passing silicone tubing through a grooved aluminum block kept in the incubator. The biofilms were grown in the drip flow reactors for 72 hours before treatment started.

Biofilm Growth Patterns

PAO1(pAB1) biofilms were grown for 72 hours in drip flow reactors. The medium was supplemented with 1 mM IPTG and flow continued. After 4 hours of induction by IPTG, biofilm-covered slides were removed from the reactor and cryoembedded in a tissue histology medium (17). Frozen sections were cut, deposited on glass microscope slides, and examined by confocal scanning laser microscopy with excitation at 488 nm and emission collected in a band from 500 to 530 nm. Dimensions of the biofilm and the gfp active zone were determined by image analysis using Scion Image software (Scion Corp., Frederick, Maryland). Some specimens were counterstained with rhodamine B. Biofilms were grown in the same way and again the GFP was induced with IPTG for 4 hours. Rhodamine B was introduced into the medium at a concentration of 5 $\mu g\ ml^{-1}$ for 30 min. The biofilms were rinsed with fresh medium for 30 min before cryoembedding.

Oxygen Concentrations in Biofilms

Oxygen concentration profiles in biofilms were measured with microelectrode technology described in detail elsewhere (12). The microelectrode manipulator was placed inside the incubator so that the measurements could be made at $37^{o}C$.

Biofilm Susceptibility

The killing of bacteria in biofilms was measured by introducing antibiotics into the growth medium feeding the drip-flow reactors. After 72 hours of growth in the absence of antibiotic, the desired antibiotic was added to the growth medium, and the flow

continued for an additional 12 hours. Tobramycin was applied at 10 μg ml^{-1} and ciprofloxacin at 1.0 μg ml^{-1}. Biofilm-covered steel coupons were removed from the reactor. Each biofilm was sampled by scraping the biomass from the coupon into 9 ml of pH 7.2 phosphate-buffered water and homogenizing for 1 min. The resulting cell suspension was serially diluted and viable bacteria were enumerated by drop-plating on TSA. Killing was reported as a log reduction or, when growth was observed, as a log increase. The log reduction was calculated relative to the cell count at time zero. Experiments were performed in at least triplicate.

In some susceptibility experiments, the availability of oxygen was altered by pumping either pure oxygen or pure nitrogen into the reactor headspace at flow rates ranging from 7 to 500 ml min^{-1}. When pure nitrogen was used, the growth medium was sparged with high purity nitrogen for 30 min prior to introduction into the reactor. Dissolved oxygen concentrations were measured using a Unisense (Vejlby, Denmark) dissolved oxygen probe.

Planktonic Susceptibility

The susceptibility of bacteria in suspension was measured by subculturing 1 ml of an overnight culture of *P. aeruginosa* PAO1 into 29 ml of PBM. The overnight cultures were grown in PBM with a glucose concentration of 1g l^{-1}. The inoculum from these cultures were taken when the OD_{600} were between 0.030 and 0.08 for the killing tests of cells experiencing exponential growth. The inoculum was taken at an OD_{600} greater

than 0.2 for the killing tests of cells in stationary phase. 1 ml aliquots from the overnight cultures were mixed with 29 ml of fresh PBM containing 1g l^{-1} glucose and antibiotics were added to start treatment. Cultures were placed in an orbital shaker at 37^{o}C and sampled over the course of 12 hours. The resulting cell suspensions were serially diluted and viable bacterial numbers were determined by plating on TSA. Experiments were performed in at least triplicate.

Bacteria resuspended from biofilms were also examined for their antibiotic sensitivity. 72 hour drip-flow biofilms were sampled from reactors, homogenized in phosphate buffer for 1 minute and resuspended in 30 ml of PBM to yield a cell density of approximately 3.0 x 10^{7} cells ml^{-1}. This suspension of bacteria was then processed as described above for the planktonic overnight culture to measure antibiotic killing. Samples treated in the absence of oxygen were added to 100 ml serum vials containing medium that had been sparged for 15 min with high purity nitrogen. Antibiotic solutions were also bubbled with nitrogen before addition to the media. After the resuspended bacteria were inoculated into the serum vials they were allowed to stand for four hours prior to antibiotic addition to ensure that all the residual oxygen had been scavenged by the bacteria. Experiments were performed in at least triplicate.

Results

Reduced Antibiotic Susceptibility of Biofilm Bacteria

P. aeruginosa cells grown in biofilms were protected from killing by tobramycin and ciprofloxacin, in comparison to growing planktonic bacteria. Both antibiotics rapidly and effectively reduced viable cell numbers in an aerobic, planktonic culture. After 12 h of treatment, the log reductions measured were 3.18± 1.79 and 4.84 ± 0.55 for tobramycin and ciprofloxacin, respectively. In contrast, neither antibiotic was very effective against biofilms of *P. aeruginosa*. After 12 h of exposure to antibiotic in continuously flowing medium, the log reductions in viable cell numbers were 0.72 ± 0.56 and 1.37 ± 0.06 for tobramycin and ciprofloxacin, respectively. These measurements were made with air in the headspace above the biofilm. The killing measured in the biofilm was less than the killing measured for planktonic cells for both agents, these differences were statistically significant ($P = 0.04$ and $P = 0.0004$ for tobramycin and ciprofloxacin, respectively)

Chemical and Physiological Heterogeneity in Biofilms

An oxygen microelectrode was used to demonstrate the presence of oxygen concentration gradients in this system (Figure 2.1A). The oxygen concentration in the flowing fluid above the biofilm was approximately 6 mg l^{-1} and the interface with air. Oxygen concentration decreased to 0.2 mg l^{-1} or less inside the biofilm. The oxygen concentrations shown in Figure 1A probably do not define the lower bound of oxygen concentration inside the biofilm because the electrode was positioned only partway into

the biofilm. Lowering the microelectrode further would have risked breaking it upon contact with the steel slide and was not attempted.

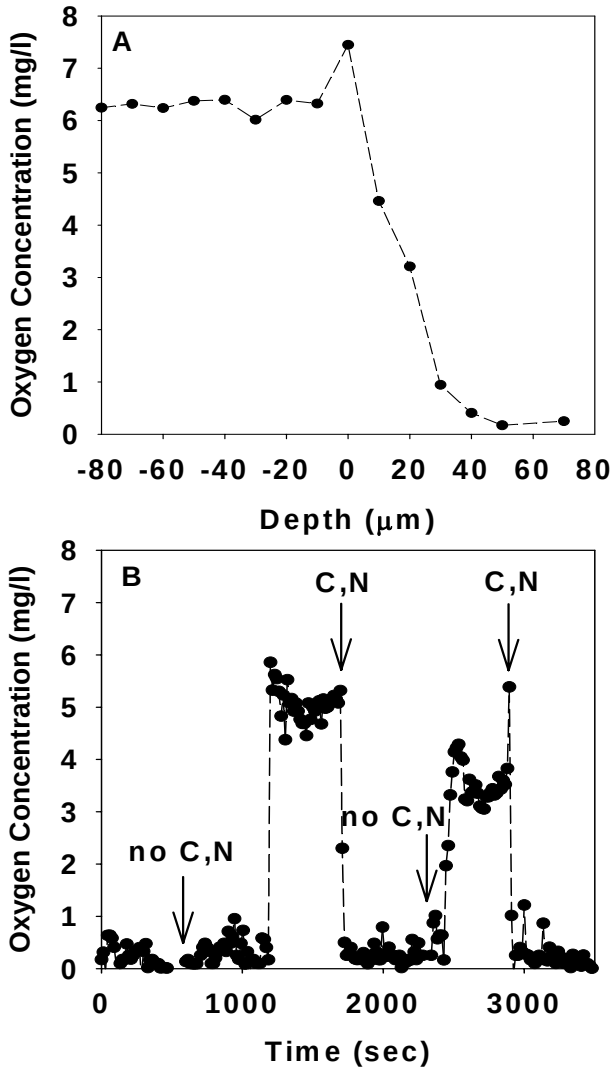

Figure 2.1 Oxygen concentrations in *Pseudomonas aeruginosa* biofilms. Panel A shows a representative oxygen concentration profile with depth in the biofilm. Zero on the x-axis corresponds to the bulk fluid-air interface. Negative positions are located in the headspace above the biofilm and positive positions are located inside the fluid film and biomass. Panel B shows the coupling between oxygen and glucose utilization. The oxygen microelectrode was positioned at a location within the biofilm where the oxygen concentration was low. The medium flowing over the biofilm was switched between one containing glucose and ammonium ion (C,N) and a medium lacking these constituents (no C,N) as indicated by the arrows. Data for this figure generated by Frank Roe and Betsey Pitts.

The utilization of oxygen by bacteria is coupled to their simultaneous uptake and oxidation of a carbon source. To investigate this coupling, the oxygen microelectrode was positioned at a depth part way into the biofilm where the oxygen concentration was less than 0.5 mg l^{-1} (Figure 2.1B). The medium flowing over the biofilm was then changed from complete PBM to PBM lacking glucose and ammonium chloride. Within a few minutes after switching to this starvation medium, the oxygen concentration in the biofilm abruptly rose to approximately 5 mg l^{-1}. When the complete medium containing glucose and the nitrogen source was restored, the oxygen concentration quickly dropped back to its previous low level. Upon switching once again to the starvation medium, the oxygen concentration again jumped up to a higher level. Restoring the complete medium again caused the oxygen concentration to fall. The same behavior was observed in a duplicate experiment. These experiments show that oxygen and nutrient utilization are interdependent.

The induction of a GFP has been used to reveal regions of active protein synthesis in biofilms (2,12,13). When this technique was applied to *P. aeruginosa* biofilms grown in drip-flow reactors, a stratified pattern of activity was observed (Figure 2.2). Expression of GFP was localized in a band at the top of the biofilm adjacent to the medium source of nutrients and oxygen. The dimension of the GFP-expressing zone averaged 66 ± 30 μm. The average thickness of the entire biofilm was 170 ± 78 μm. Results from these experiments and from controls are summarized in Table 2.1.

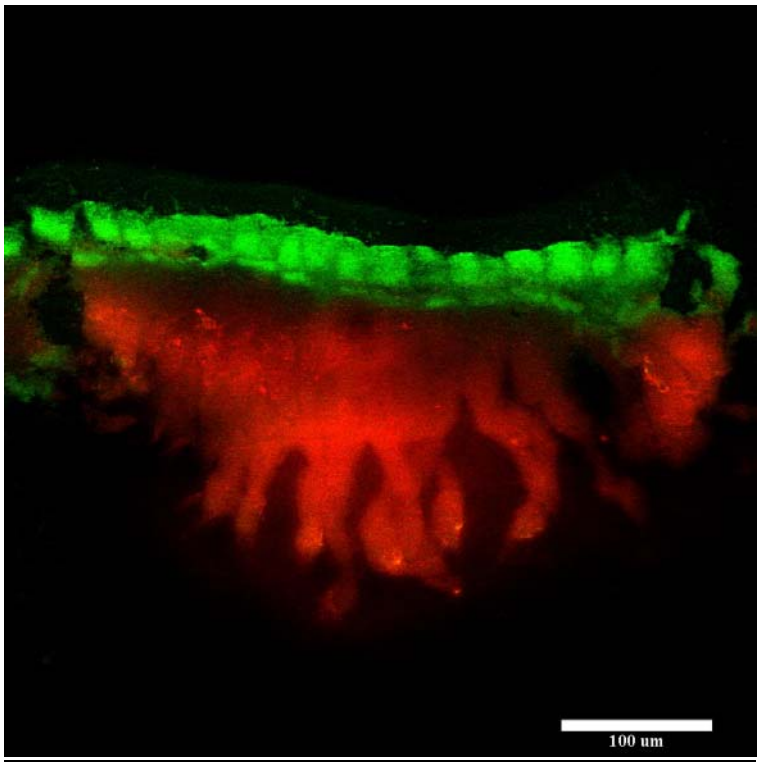

Figure 2.2 Spatial pattern of protein synthetic activity, as revealed by transient expression of an inducible GFP (green) in a *P. aeruginosa* biofilm grown in a drip-flow reactor. In this frozen section, the steel substratum was formerly at the bottom and the aerated nutrient medium at the top. Rhodamine B counterstaining (red) indicates the extent of the biofilm, independent of its activity.

Strain	IPTG	Biofilm Thickness (μm)	GFP Zone Dimension (μm)	Maximum Fluorescence Intensity (arbitrary)
PAO1(pAB1)	No	165 ± 100	None	24 ± 26
PAO1(pAB1)	Yes	170 ± 78	66 ± 30	166 ± 61
PAO1(pMF54)	Yes	120 ± 38	None	3 ± 1

Table 2.1 Biofilm thicknesses and dimension of the zone in which GFP was expressed. Plasmid pAB1 carries an IPTG-inducible GFP. Plasmid pMF54 is the vector control lacking GFP. The uncertainties indicated are standard deviations. Errors represent standard deviations of at least 3 sections from 3 separate biofilms of 3 measurements of thickness.

Tests of the Importance of Oxygen Availability for Antibiotic Susceptibility

It is our hypothesis that if oxygen availability were the sole determinant of antibiotic susceptibility, then resuspending bacteria from a biofilm into aerated medium should completely restore antibiotic sensitivity. On the other hand, resuspending bacteria from a biofilm into anaerobic medium should preserve the low level of susceptibility measured in the biofilm. Log reductions measured for biofilm bacteria resuspended into aerobic medium and treated with tobramycin or ciprofloxacin for 12 h were 3.90 ± 0.10 and 4.40 ± 0.53, respectively. This degree of killing was the same as that measured for planktonic, aerobic bacteria, indicating that susceptibility was indeed rapidly and fully restored upon dispersal of cells from the biofilm. On the other hand, log reductions measured for biofilm bacteria resuspended into anaerobic medium and exposed to antibiotics for 12 h were 3.69 ± 0.35 and 2.24 ± 0.36, for tobramycin and ciprofloxacin, respectively. These values were higher than the killing measured in the biofilm and found to be statistically significant for tobramycin ($P = 0.0004$) or for ciprofloxacin ($P = 0.07$) This shows that maintaining low oxygen tension was insufficient to preserve the low level of susceptibility afforded to intact biofilm cells.

If oxygen availability were the single most important determinant of antibiotic susceptibility, then one should be able to simulate the low susceptibility of biofilm cells by treating planktonic bacteria under strictly anaerobic conditions. Both antibiotics were able to kill bacteria under these conditions (Table 2.2). For both agents, the degree of killing determined for anaerobic, planktonic cells was less than for aerobic, planktonic

bacteria (Table 2.2) but greater than the killing measured for intact biofilms. There was a significant loss of viability when exponential phase planktonic cells were transferred to anaerobic conditions, even in the absence of antibiotics.

Growth Phase of Inoculum	Aerobic	Test Medium	Tobramycin Log Reduction	Ciprofloxacin Log Reduction	Untreated Control Log Reduction
Exponential	Yes	PBM	3.18 ± 1.03	4.84 ± 0.32	-2.53 ± 0.03
Exponential	No	PBM	3.97 ± 0.18	4.24 ± 0.25	1.74 ± 1.09
Stationary	Yes	PBM	3.95 ± 0.61	5.66 ± 0.07	-2.12 ± 0.50
Stationary	No	PBM	1.19 ± 0.26	3.62 ± 0.27	0.90 ± 0.17
Stationary	Yes	PBM lacking glucose	0.06 ± 0.08	3.99 ± 0.03	0.04 ± 0.01
Intact biofilm	Yes	PBM	0.72 ± 0.56	1.37 ± 0.06	-0.24 ± 0.12

Table 2.2 Antibiotic susceptibility of *P. aeruginosa* under various conditions of nutrient and oxygen availability. All tests were performed on planktonic cells, except for the intact biofilm result included for comparison. The uncertainty indicated is the standard error of the mean. Negative log reductions reported for the untreated control result from cell growth during the test period. Error represent standard deviations of at least 3 separate experiments.

The results of tests of the contribution of oxygen limitation to protection from antibiotic killing in biofilms are summarized in Table 2.3.

Test	Tobramycin	Ciprofloxacin
Oxygen is depleted in parts of the biofilm and metabolic activity in the biofilm is stratified	Yes	Yes
Bacteria resuspended from a biofilm into aerated medium rapidly and fully recover susceptibility	Yes	Yes
Bacteria resuspended from a biofilm into anoxic medium retain their low level of susceptibility	No	Partial
Planktonic (stationary phase) bacteria challenged in anoxic medium exhibit low susceptibility comparable to intact biofilm	Partial	No
Increased oxygen tension during treatment of a biofilm increases killing, decreased oxygen tension decreases killing	No	Partial

Table 2.3 Summary of the effects of oxygen limitation and growth rate to the protection of biofilm killing with tobramycin and ciprofloxacin. Yes indicates that the test was mostly satisfied, No indicates that the test was mostly not satisfied, and Partial indicates an intermediate result.

All of the previously presented experiments with planktonic bacteria were performed using inocula from exponential phase cultures. It can be theorized that planktonic phase cells in the exponential phase of growth are analogous to the most active cells existing in the biofilm, or the cells in the active zone, where as the planktonic cells existing in stationary phase would be a closer analogue to the biofilm cells residing outside the active zone. We questioned whether bacteria in stationary phase would show the same dependence on oxygen availability. When a stationary phase planktonic inoculum was treated with antibiotics, the killing measured was less than for exponential

phase planktonic cells (Table 2.2). It was also less than the killing measured for aerobic stationary phase cells (Table 2.2).

As an additional test of the role of oxygen in mediating biofilm resistance to antibiotics, the oxygen tension in the gas headspace above the biofilm during antibiotic treatment was varied. If oxygen limitation is responsible for biofilm protection, then increasing the oxygen concentration in the gas phase should increase biofilm susceptibility and decreasing the oxygen concentration in the gas phase should decrease biofilm susceptibility. Changing the oxygen concentration had no effect on biofilm susceptibility to tobramycin and only slight positive effect on ciprofloxacin action (Figure 2.3). The oxygen concentration in the bulk fluid as measured at the outlet of the reactor was increased to a value as high as 21 mg l^{-1}. A theoretical calculation of the oxygen penetration depth using the model described in Appendix B yielded an oxygen penetration depth of 233 μm when the bulk fluid oxygen concentration is 21 mg l^{-1}. Performing the same calculation when the bulk fluid oxygen concentration is 1 mg l^{-1} gives a penetration depth of 39 μm. These are drastically different results yet we see very little disparity of biofilms treated under either condition.

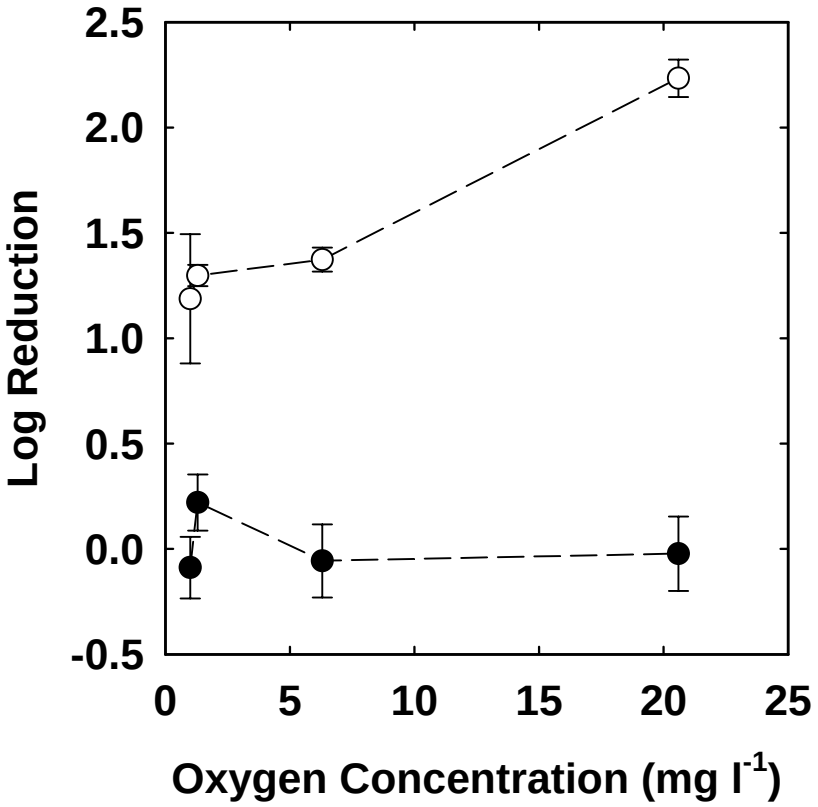

Figure 2.3 Antibiotic killing of *P. aeruginosa* in intact biofilms as a function of the oxygen concentration in the bulk fluid after the medium has exited the reactor. Data are for 12 h of ciprofloxacin (○) or tobramycin (●) treatment. In all cases the biofilm was grown in the presence of air for 72 h prior to antibiotic treatment. Only during the antibiotic treatment phase was the oxygen composition in the gas phase changed. Error bars represent standard deviations of at least 3 replicates.

Tests of the Importance of Glucose Availability for Antibiotic Susceptibility

Omitting glucose from the medium abolished killing of planktonic cells by tobramycin, but had little effect on the action of ciprofloxacin (Table 2.2). When biofilm bacteria were resuspended into medium lacking glucose and exposed to antibiotics, tobramycin was completely ineffective under aerobic conditions (log reduction 0.14 ± 0.26). The log reduction realized by ciprofloxacin under these conditions was 3.6 ± 0.32. These data suggest that depletion of glucose in the biofilm could account for protection against tobramycin in the biofilm state, if glucose depletion were to occur in a region where oxygen was still available. Glucose depletion would not appear to be sufficient to account for the reduced susceptibility of biofilm cells to ciprofloxacin. The results of tests of the contribution of glucose limitation to protection from antibiotic killing in biofilms are summarized in Table 2.4.

Test	Tobramycin	Ciprofloxacin
Glucose is depleted in parts of the biofilm	No	No
Bacteria resuspended from a biofilm into glucose-containing medium rapidly and fully recover susceptibility	Yes	Yes
Bacteria resuspended from a biofilm into medium lacking glucose retain their low level of susceptibility	Yes	No
Planktonic (stationary phase) bacteria challenged in glucose-free medium exhibit low susceptibility comparable to intact biofilm	Yes	No

Table 2.4 Summary of tests of the contribution of glucose limitation to protection from antibiotic killing in *P. aeruginosa* biofilms. Yes indicates that the test was mostly satisfied, No indicates that the test was mostly not satisfied, and Partial indicates an intermediate result.

Discussion

We hypothesized that oxygen limitation occurs in *P. aeruginosa* biofilms and that anoxia contributes to the reduced antibiotic susceptibility of biofilm bacteria. Steep oxygen concentration gradients were measured in the vicinity of the biofilm, with parts of the biofilm experiencing oxygen concentrations of 0.2 mg l^{-1} or less (Figure 2.1). The expression of an inducible GFP was limited to a sharply demarcated band immediately adjacent to the oxygen source. This band represented approximately 40% of the biofilm, indicating that as much as 60% of the biofilm could be anoxic and relatively inactive. These results are consistent with the first part of our hypothesis, namely, that oxygen limitation occurs in these biofilms. This conclusion is also consistent with previous studies of oxygen availability and spatial patterns of physiological activity in some other *P. aeruginosa* biofilms (12,13,16,17).

If oxygen or nutrient limitation alone is responsible for the reduced susceptibility of bacteria in biofilms, then it should be possible to duplicate this level of protection using planktonic cultures in which the environmental conditions are appropriately manipulated. To this end, we conducted experiments with planktonic cells in which oxygen availability, glucose availability, and growth phase of the inoculum were varied (Table 2.2). For both antibiotics, anoxia showed the largest effect when stationary phase planktonic cells were used. These experiments with planktonic cells suggest that the growth phase of the inoculum is as important as the availability of oxygen. These results

support the interpretation that oxygen availability is a partial, but incomplete, explanation for biofilm resistance to antibiotics.

Resuspended biofilm experiments show even more clearly that anoxia alone is not sufficient to preserve the high degree of protection maintained in intact biofilms. One would predict that if oxygen availability were the only factor determining susceptibility, then dispersing biofilm cells into anaerobic medium should preserve (or even enhance) the protection from antibiotics, compared to the intact biofilm. Bacteria dispersed from biofilms into aerated media did recover most of their susceptibility, showing that oxygen does modulate antibiotic sensitivity. These results suggest that physical disaggregation is at least as important as oxygen availability.

Experiments in which the oxygen concentration above the biofilm was increased or decreased had little impact on biofilm susceptibility to tobramycin and only a partial effect on biofilm susceptibility to ciprofloxacin (Figure 2.3).

What can be concluded from these experiments collectively, as summarized in Table 2.3, is that oxygen limitation is a partial, but incomplete, explanation for *P. aeruginosa* biofilm protection from antibiotics.

Having found that oxygen limitation alone does not appear to explain biofilm protection from antibiotic killing, it is natural to wonder whether limitation for the other important metabolic substrate, glucose, could be responsible for this protection. The short answer is: probably not. Glucose limitation in planktonic cultures conferred excellent protection against killing by tobramycin, but it did not afford similar protection against ciprofloxacin. Glucose limitation is not an adequate explanation for biofilm

tolerance of ciprofloxacin. More importantly, there is no basis for anticipating that glucose is actually limiting in any part of the biofilms that were grown in this study. This can best be appreciated by a simple calculation. As derived by Williamson and McCarty (14), the metabolic substrate that will first be depleted in a biofilm can be determined by calculating the dimensionless quantity:

$$\frac{D_{eG} S_G}{D_{eO_2} S_{O_2} Y_{GO_2}}. \quad (1)$$

This ratio is a measure of the relative diffusive fluxes of glucose and oxygen into the biofilm, where D_e denotes the effective diffusion coefficient of the respective substrate in the biofilm, S denotes the bulk fluid concentration of the respective substrate, and Y_{GO2} is the stoichiometric coefficient relating the consumption of glucose and oxygen. In the present case, we take the effective diffusion coefficients of oxygen and glucose to be 1.53 x 10^{-5} cm^2 s^{-1} and 2.69 x 10^{-6} cm^2 s^{-1}, respectively (10). The yield coefficient has been carefully measured, in biofilms of this bacterium, and is 2.25 g glucose per g oxygen (5). With the bulk fluid concentration of glucose at 200 mg l^{-1} and the bulk fluid concentration of oxygen at 6 mg l^{-1}, the quantity given in Equation 1 has a value of 2.6. This value being greater than 1 means that glucose is provided in excess and that oxygen is the limiting substrate.

The following describes our physical understanding of the concentration gradients in this particular biofilm system. In the aerobic layer, both oxygen and glucose are consumed. Once the oxygen has been depleted, utilization of glucose stops. Abundant glucose, approximately 125 mg l^{-1}, is predicted to be available at the bottom of the

biofilms studied in this investigation. We note that *P. aeruginosa* is unable to ferment glucose and that no alternative electron acceptor, such as nitrate, is present in the medium used in these studies. This analysis therefore argues against the hypothesis that glucose limitation leads to reduced antibiotic killing in these biofilms.

The coupling of glucose and oxygen utilization is evident in Figure 2.1B. When the carbon source is present, a low oxygen concentration prevails in the depths of the biofilm. When the carbon source is removed from the medium, oxygen levels increase sharply after a delay of several minutes. The increase is understood this way. The consumption of oxygen depends on having a steady source of electrons from an electron donor, in this case glucose. When the glucose is removed from the medium, the source of electrons is lost and oxygen respiration ceases. The likely explanation for the delay before this increase is observed is that the cells exhibit some endogenous respiration that can provide a source of electrons for a limited period of time. Once this internal reserve is exhausted, oxygen consumption stops and oxygen permeates throughout the biofilm. Immediately upon the restoration of glucose to the medium, the cells resume the coupled oxidation of glucose and reduction of oxygen. The concentration of oxygen inside the biofilm rapidly falls to the original low concentrations.

In an independent study using a different in vitro biofilm model, Borriello et al.. (2004) reported that oxygen limitation could account for 70 percent or more of the protection from six antibiotics observed in *P. aeruginosa* colony biofilms (2). This is a more definitive result for the role of oxygen in biofilm protection than the data reported in the current study justify. One explanation for this difference is that the oxygen effects

in the Borriello et al.. study were measured using aggregated cells – young biofilms that were exposed to antibiotics under aerobic or anaerobic conditions. This leads us to hypothesize that the full protection afforded by anoxia is only realized when cells are aggregated in an extracellular polymer matrix. In other words, oxygen limitation is a necessary, but not a sufficient condition for achieving full protection from antibiotics in a *P. aeruginosa* biofilm.

Acknowledgements

This work was supported by NIH awards R01GM067245-02 and R01DC04173-01A1 and by an award from the W. M. Keck Foundation.

REFERENCES

1. Anderl, J. N.; Franklin, M.J.; Stewart, P.S.; Role of antibiotic penetration limitation in *Klebsiella pneumoniae* biofilm resistance to ampicillin and ciprofloxacin. Antimicrobial Agents and Chemotherapy 2000, 44, 1818-1824

2. Borriello, G.; Werner, E.; Roe, F.; Kim, A. M.; Ehrlich, G. D.; Stewart, P.S.; Oxygen limitation contributes to antibiotic tolerance of *Pseudomonas aeruginosa* in biofilms. Antimicrobial Agents Chemotherapy 2004, 48, 2659-2664

3. Brown, M. R. W.; Allison, D. G.; Gilbert, P.; Resistance of bacterial biofilms to antibiotics: a growth-rate related effect? Journal of Antimicrobial Chemotherapy 1988, 22, 777-783

4. Bryant, R. E. ; Mazza, J.A.; Effect of the abscess environment on the antimicrobial activity of ciprofloxacin. American Journal of Medicine 1989, 87, (5A) 23S-27S

5. Characklis, W. G. Energetics and stoichiometry. In Biofilms, W. G. Characklis and K. C. Marshall, (eds.) 1990., pp.161-192. John Wiley & Sons, New York, N.Y.

6. Costerton, J. W.; Stewart, P.S.; Greenberg, E.P.; Bacterial biofilms: A common cause of persistent infections. Science 1999, 284, 1318-1322

7. Davey, P.; Barza, M.; Stuart, M.; Tolerance of *Pseudomonas aeruginosa* to killing by ciprofloxacin, gentamicin and imipenem in vitro and in vivo. Journal of Antimicrobial Chemotherapy 1988, 21, 395-404

8. Field, T. R.; White, A.; Elborn, J. S.; Tunney, M. M.; Effect of oxygen limitation on the in vitro antimicrobial susceptibility of clinical isolates of *Pseudomonas aeruginosa* grown planktonically and as biofilms. European Journal of Clinical Microbiology 2005, 24, 677-687

9. Mah, T. F.; Pitts, B.; Pellock, B.; Walker, G. C.; Stewart, P. S.; O'Toole. G. A.; A genetic basis for *Pseudomonas aeruginosa* biofilm antibiotic resistance. Nature 2003 426, 306-310

10. Stewart, P. S.; Diffusion in biofilms. Journal of Bacteriology 2003. 185, 1485-1491

11. Stewart, P. S.; Costerton, J. W.; Antibiotic resistance of bacteria in biofilms. Lancet 2001, 358, 135-138

12. Walters, M.C.; Roe, F. ; Bougnicourt, A. ; Franklin, M. J.; Stewart P. S.; Contributions of antibiotic penetration, oxygen limitation, and low metabolic activity

to tolerance of *Pseudomonas aeruginosa* biofilms to ciprofloxacin and tobramycin. Antimicrobial Agents and Chemotherapy 2003, 47, 317-323

13. Werner, E.; Roe, F.; Bugnicourt, A.; Franklin, M.; Heydorn, A.; Molin, S.; Pitts, B.; Stewart, P. S.; Stratified growth in *Pseudomonas aeruginosa* biofilms. Applied Environmental Microbiology 2004, 70, 6188-6196

14. Williamson, K..; McCarty, P. L.; A model of substrate utilization by bacterial films. Journal Water Pollution Control Federation 1976 48, 9-24

15. Worlitzsch, D.; Tarran, R.; Ulrich, M.; Schwab, U.; Cekici, A.; Meyer, K. C.; Birrer, P.; Bellon, G.; Berger, J.; Weiss, T.; Botzenhart, K.; Yankaskas, J. R.; Randell, S.; Boucher, R. C.; Döring. G.; Effects of reduced mucus oxygen concentration in airway *Pseudomonas* infections of cystic fibrosis patients. Journal of Clinical Investigation 2002, 109, 317-325

16. Xu, K. D.; McFeters, G. A.; Stewart, P. S.; Biofilm resistance to antimicrobial agents. Microbiology 2000, 146, 547-549

17. Xu, K. D.; Stewart, P. S.; Xia, F.; Huang, C.-T.; McFeters G. A.; Spatial physiological heterogeneity in *Pseudomonas aeruginosa* biofilm is determined by oxygen availability. Applied Environnemental Microbiology 1998, 64, 4035-4039

18. Yoon, S. S.; Hennigan, R. F.; Hilliard, G. M.; Ochsner, U. A.; Parvatiyar, K.; Kamani, M. C.; Allen, H. L.; DeKievit, T. R.; Gardner, P. R.; Schwab, U.; Rowe, J. J.; Iglewski, B. H.; McDermott, T. R.; Mason, R. P.; Wozniak, D. J.; Hancock, R. E. W.; Parsek, M. R.; Noah, T. L.; Boucher, R. C.; Hassett D. J.. *Pseudomonas aeruginosa* anaerobic respiration in biofilms: relationships to cystic fibrosis pathogenesis. Developmental Cell. 2002, 3, 593-603

CHAPTER 3

DORMANT CELLS WITHIN PSEUDOMONAS AERUGINOSA BIOFILMS ARE PROPTECTED FROM KILLIING BY ANTIBIOTIC TREATMENT

Abstract

It was hypothesized that *Pseudomonas aeruginosa* biofilms are protected from killing by antimicrobials due to the presence of dormant cells existing within mature biofilms. A *P. aeruginosa* strain containing a stable, inducible green fluorescent protein was used to visualize and characterize the anabolically dormant and active cell populations within the biofilm. Active cells were labeled by introduction of the inducing agent to mature biofilms. Only about 30 % of the cells within the biofilm turned bright, thus labeling the active cells with green fluorescence. Dormant cells were labeled by developing biofilms to maturity in the continuous presence of the inducer, then switching to media lacking the inducing agent. This produced a biofilm in which only the most dormant cells within the biofilm were bright after an extended period on media lacking the inducer. By disaggregating the biofilms and sorting each population it was possible to separate and collect populations based on GFP brightness. When plating the bright population of dormant cells for viability it was found that 17% of bright events, as counted by flow cytometry, produced colony forming units. Similarly when considering active cells, 21 % of bright events were found to be viable cells. This novel approach of

labeling cells by their anabolic state was used to explore the susceptibility of both dormant and active cells. Intact biofilms were treated as stated above to label active and dormant cells followed by treatment with antibiotics. After sorting into bright and dim populations it was then possible to plate each population of cells for viability, thus elucidating their susceptibility to either tobramycin or ciprofloxacin. When labeling dormant cells within colony biofilms as bright, ciprofloxacin and tobramycin produced log reductions of 0.39 and 0.08 respectively, in bright cells. Where as, the log reductions for both antibiotics were found to be 2.78 for non- labeled, active (dim) cells within the colony biofilm. When performing the converse of this experiment, labeling the active cells with GFP, the dormant (dim) cells experienced a 0.48 log increase when treated with ciprofloxacin and a 1.02 log increase when treated with tobramycin. This is in comparison to log reductions of 1.21 and 3.27 respectively for active (bright) cells. When dormant cells were labeled in drip flow reactors, tobramycin treatment resulted in a log reduction of 1.72 in active cells and only 0.63 in dormant cells. Ciprofloxacin exposure produced a log reduction of 2.48 in active cells and 1.32 in dormant cells. With the exception of the latter case, the increased susceptibility of active cells compared to dormant cells was found to be statistically significant. This suggests that the antibiotic tolerance expressed by *P. aeruginosa* biofilms is largely affected by dormant cells within the biofilm.

Introduction

Bacterial biofilms have been implicated in many persistent infections, such as colonization of the cystic fibrosis lung (8), endocarditis (13), osteomyelitis (2) and a host of nosocomial infections (7). It has also been shown that the biofilm state is the most prevalent mode of existence for bacteria in nature (6). The underlying challenge associated with this situation is that biofilms are inherently tolerant to antimicrobial treatment and subsequent killing. The reasons for this tolerance are likely complex and vary by situation. In Chapter 1 we showed that the ability of biofilms to survive through antibiotic treatment is a phenotypic change, when biofilm cells are disaggregated and resuspended in medium they are no more tolerant to antibiotics than cells grown in a planktonic culture (14). The most obvious explanation for this tolerance of cells within a biofilm state is that antibiotics do not penetrate into the biofilm. Since the biofilm is structured in an extracellular polymeric slime matrix, it can be theorized that antibiotics simply do not penetrate into the biofilm. Studies have been carried out that show at least some antibiotics do penetrate into biofilms, so the blanket tolerance that biofilms exhibit to antimicrobial agents can not be explained by penetration alone(1,15).

One idea is that biofilms are a compilation of cells in differing states of anabolic activity. A biofilm is a diverse environment with strata differing by several different means. We have shown in past work that the biofilm contains anoxic regions (14). It would also make sense that within the biofilm, there are cells of different age classes possibly exhibiting different characteristics than those formed earlier or later in the

process of biofilm growth. The diversity within the biofilm could result in cells differing drastically in their anabolic activity. The idea that there are a few cells within the biofilm that are tolerant to antibiotics has been explored in the past. It has been theorized that these "persistor" cells survive biocidal treatment, and subsequently repopulate the biofilm after treatment ceases (3). It has been hypothesized that these resistant cells are inherently predisposed to this state, that is they do not enter the resistant state in response to an environmental stimulus such as nutrient limitation and these are not simply slow growing cells (10). We will make no such claim in this work, we will further refer to the resistant cells as dormant cells to differentiate them from what has come to be called a persister cell. Elucidating the differences between these dormant cells and non tolerant cells within the biofilm has been a very difficult proposition for this is a condition exclusive to the biofilm state of growth, as soon as the biofilm is disturbed (resuspension of cells) the tolerant cells are not distinguishable from other cells that existed within the biofilm. We have devised a novel approach to labeling anabolically active and dormant cells using a strain of *Pseudomonas aeruginosa* tagged with an inducible green fluorescent protein (GFP). This labeling has allowed the exploration of the physical location of these cells within the biofilm. In addition, GFP labeling of bright and dormant cells within the intact biofilm has allowed us to elucidate the differences in susceptibility of these distinct populations.

Materials and Methods

Bacterial Strains, Media, and Antibiotics

Pseudomonas aeruginosa PAO1 pUTGm AraGfp was used in all experiments. This organism contains a plasmid with an inducible gene for expression of a stable green fluorescent protein (GFP). The plasmid also contains a gentamicin resistance marker. All inocula were grown for 18-24 hours in tryptic soy broth (TSB) (Beckton Dickinson and Company, Sparks, MD) with 15 μg ml^{-1} gentamicin sulfate. All colony biofilms were grown on tryptic soy agar (TSA) (Beckton Dickinson and Company, Sparks, MD). Drip flow biofilms were grown in Pseudomonas basal medium (PBM) containing 0.2 g l^{-1} glucose. Tobramycin sulfate was obtained from Sigma (St. Louis, MO) and ciprofloxacin hydrochloride was a gift of the Bayer Corporation (Leverkusen, Germany). Viable cell numbers were determined by colony formation on TSA.

Biofilm Preparation

Colony biofilms of *Pseudomonas aeruginosa* PAO1 pUTGm AraGfp were grown as described elsewhere(1). All biofilms were allowed to grow on membranes for 48 hours after inoculation, before any treatment was started.

Biofilms were grown in drip-flow reactors (17). The medium used during treatment and growth was PBM with 0.2 g l^{-1} glucose as the sole carbon source. Drip-flow reactors consisted of four parallel chambers. The chambers were covered with polycarbonate windows containing a septum to allow for medium introduction through 22 gauge needles. The windows also contained filtered air vents to allow sterile air to

enter the reactor. Medium was pumped into the chambers at a flow rate of 50 ml hr^{-1}. The medium was allowed to drip onto stainless steel slides placed in the chambers of the reactor. Spent medium drained out through a port at the bottom of each chamber after it was allowed to run down over the slide. The stainless steel slides were 9.72 cm^2 in area. The reactors were inoculated by adding 1 *m*l of an overnight culture, grown for 18 to 24 hours in TSB containing 15 μg ml^{-1} gentamicin sulfate, to 15 ml of PBM containing 1 g l^{-1} glucose covering the steel slide within the reactor chamber. The reactor was sealed by clamping the effluent tubes and the inoculated medium was allowed to sit in the reactor for an 18 hour batch phase while on a level surface. The effluent tubes were unclamped and the reactor was placed on a 10 degree inclined stand. The batch phase medium was allowed to flow out of the reactor chamber and flow was simultaneously started to the reactor. The entire drip-flow reactor was kept in a 37 ^oC incubator. Fresh medium containing 200mg l^{-1} glucose was allowed to drip onto the slide through a 22 gauge needle. Medium was pre-warmed by passing silicone tubing through a grooved aluminum block kept in the incubator. The biofilms were grown in the drip flow reactors for 72 hours before treatment.

Visualization of GFP Patterns in Biofilms

Bacteria in biofilms were induced to express GFP in two different protocols we have termed up-shift and down-shift. In the up-shift protocol, biofilms were grown to maturity in the absence of inducer. They were then exposed to media supplemented with arabinose and allowed to grow for an additional time before sampling. Down-shifted

colony biofilms were allowed to develop to maturity, 48 h, in the continuous presence of 2% arabinose. This created a population of cells which were loaded with GFP. These biofilms were then transferred to TSA plates lacking arabinose to down-shift for additional time periods.

The biofilms containing GFP were cryoembedded in a tissue histology medium(17). Frozen samples were sectioned into 5 μm thick slices and placed on glass microscope slides. The sections were examined using epiflourescent microscopy at an excitation wavelength between 465nm and 495nm, and an emission wavelength of 515nm to 555nm.

Flow Cytometry

Biofilms were grown and up-shifted or down-shifted as described above. Intact colony biofilms were disaggregated by placing the cells and the membrane in 9mL of phosphate buffered saline (PBS) and vortexing for 1 minute. The resulting cell suspensions were then serially diluted and analyzed in a Becton Dickinson FACSAria flow cytometer. The diluted cells were immediately taken to the flow cytometer and subsequently analyzed to minimize time between desegregation and analysis. Data was collected on GFP intensity with any cells exibiting an intensity over 100 on an arbitrary scale, collected as bright (GFP expressing cells) any events registered by the flow cytometer with an intensity below 100 were collected as dim cells (non-GFP expressing cells). The threshold of 100 was determined by first exploring the intensity behavior of un-induced *Pseudomonas aeruginosa* PAO1 pUTGm AraGfp. Biofilms were grown to

maturity and disaggregated. The intensity profile of these cells was recorded in the flow cytometer. It was found that un-induced cells of this organism, in fore mentioned growth conditions, almost exclusively express an intensity of less than 100 in the instrument that we used for these experiments. Cells were collected and scored as counts versus the overall population or percent of the whole population.

Antibiotic Treatment of Shifted Populations

Up-shifted and down-shifted biofilms were treated with either 10 μg ml^{-1} tobramycin sulfate or 1 μg ml^{-1} ciprofloxacin hydrochloride. In up-shift experiments, colony biofilms were grown to maturity (48 hours) then moved to TSA plates containing 2% arabinose for 12 hours to establish a GFP expressing population of cells. The colony biofilms were then moved to TSA plates containing 2% arabinose as well as antibiotics for 24 hours. These cells were then disaggregated and viable cells were enumerated by colony formation on TSA. Parallel samples were sorted on brightness into sterile tubes by flowcytometry. The resulting populations of sorted bright and dim cells were immediately plated for viability. The total time between desegregation of the cells and plating post sort was no more than one hour. Downshift experiments were performed with colony biofilms grown in the presence of arabinose for 48 hours then moved to TSA plates containing antibiotic for 24 hours. The same procedures were used to determine viable cell numbers in whole and sorted samples. Analogous downshift experiments were performed using drip flow biofilms. Biofilms were grown in drip flow reactors for 72 hours in PBM containing 1% arabinose. The medium was then switched to PBM

containing antibiotic but lacking arabinose. The medium was allowed to flow into the reactor for 24 hours. The resulting biofilms were then sampled as described above.

For cells processed using flow cytometry, log reductions were calculated by the following formula

$$-Log_{10}((\%P_t * \%p_t)/(\%P_u * \%p_u))$$

Where..

$\%P_t$ = percent of the total antibiotic treated population either bright or dim,

$\%p_t$ = percent of the antibiotic treated population either bright or dim that was viable as plated after sorting,

$\%P_u$ = percent of the total untreated population either bright or dim, and

$\%p_u$ = percent of the untreated population either bright or dim that was viable as plated after sorting.

Results and Discussion

This study made use of a *P. aeruginosa* strain containing an inducible GFP. This bacterium responds to the presence of the inducer, arabinose, by synthesizing a fluorescent protein. The GFP can then be detected by microscopy or flow cytometry. We used this construct as a tool for investigating the activity, and also inactivity, of bacterial cells. To insure that this strain of *P. aeruginosa* would not metabolize arabinose a culture was streaked on a PBM agar plate absent of both arabinose and glucose. A culture was then streaked on a PBM agar plate containing 1 g l^{-1} glucose. Another

culture was streaked on a PBM plate containing 1 g l^{-1} arabinose as the sole carbon source, this experiment was performed in triplicate. Growth was observed only on the plates containing glucose. This result shows that this strain of *P. aeruginosa* does not grow on arabinose.

Consider first some simple planktonic experiments that illustrate the behavior of this microorganism. When a planktonic culture of *P. aeruginosa* grown without the inducer was subcultured into fresh medium containing arabinose, the initially dark cells became fluorescent over the next several hours (Figure 3.1). After 12 h of growth under inducing conditions, 96% of the cells scored bright in a flow cytometric assay. This shows that in a growth environment with abundant nutrients, almost all of the bacterial cells actively synthesize new protein. When a stationary phase planktonic culture, grown in the absence of the inducer, was amended with arabinose there was little induction of GFP (Figure 3.1). Twelve hours after adding the arabinose, only about 6% of the bacteria scored bright for GFP expression. Most of the cells had presumably entered an inactive, or less active, state in which anabolism was arrested. The observation of a few bright cells is quite interesting in that it suggests that even under conditions where most of the bacteria have ceased protein synthesis, there was a subpopulation that was actively synthesizing new protein.

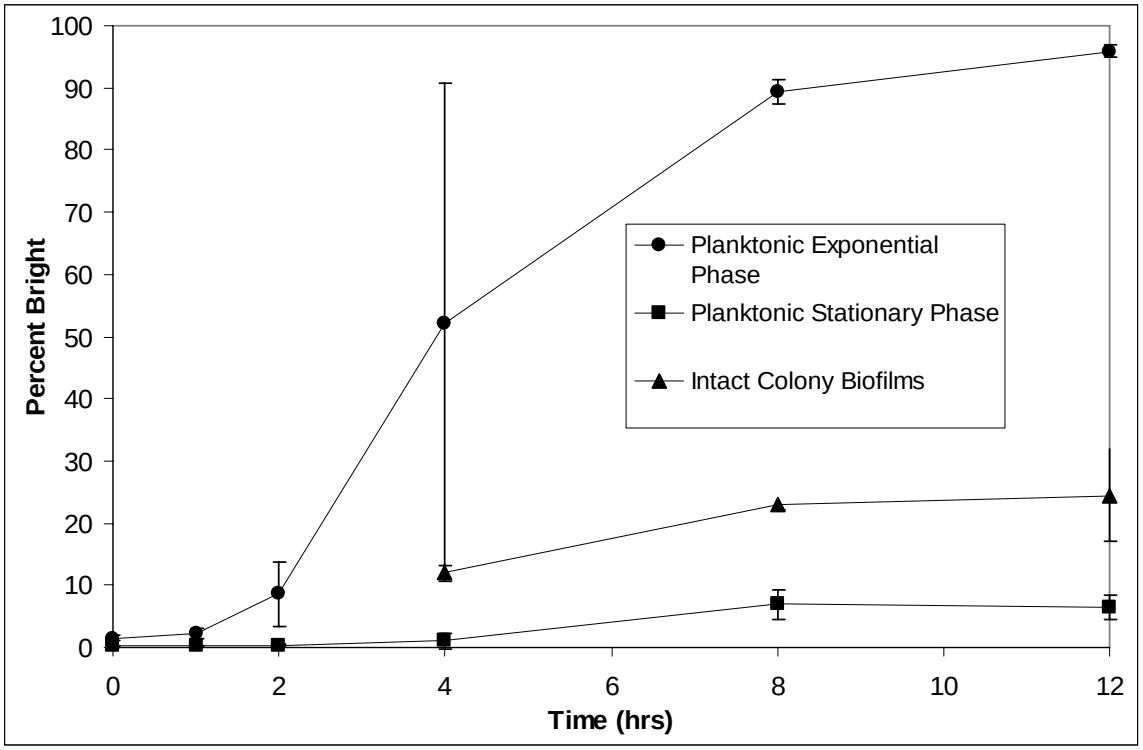

Figure 3.1 Dynamics of induction of GFP expression in *P. aeruginosa* cells in planktonic exponential phase (●), planktonic stationary phase (■), and intact colony biofilms (▲). Arabinose was added to the system at time zero. Vertical axis represents total percent of overall events that register as bright by flow cytometric analysis. Error bars represent standard deviations of at least 3 experiments.

When a *P. aeruginosa* colony biofilm was induced with arabinose, approximately 29% of the cells became bright with GFP after 12 h. This percentage did not increase appreciably upon prolonged incubation with arabinose (data not shown). This result suggests that only about a quarter of the bacteria in these colony biofilms were anabolically active. We considered four possible explanations for the dark state of the other three-quarters of the biofilm population. The first explanation is simply that about 70% of the bacteria in the biofilm were dead. To test this conjecture, we enumerated

viable bacteria (by plate counting) and total bacteria (by direct microscopic counts) in the same dispersed biofilm sample. Triplicate runs determined that 95 ± 6% of all cells were viable. This value rules out the explanation that most of the dark cells are dead. A second explanation is that three-quarters of the bacteria in the biofilm have lost the plasmid bearing the GFP gene. We therefore scored bacteria dispersed from biofilms for retention of the gentamicin marker borne on the plasmid. Colony counts on plates with and without gentamicin were nearly identical. To further confirm this result we disaggregated and plated colony biofilms grown on media lacking gentamicin, 100 colonies from this plating were then spotted on plates containing gentamicin. All 100 spots produced a colony. This shows that the plasmid is stable and therefore plasmid loss is not an explanation for the presence of dark cells within the biofilm. A third explanation is that all of the bacteria in the biofilm were synthesizing protein, but only those in the region adjacent to the air interface had sufficient oxygen to activate fluorescence of the GFP. This explanation is difficult to reconcile with the fact that *P. aeruginosa* do not grow at all on TSA in the absence of oxygen. The improbable scenario that is required is that the oxygen concentration in the depths of the biofilm was sufficient to support cellular protein synthesis but inadequate to allow for activation of GFP fluorescence. The fourth explanation is that 70 to 75% of the bacteria in the biofilm occupy a viable but inactive state. This is the explanation that is most consistent with our observations. It should be noted that even though nearly ¾ of the biofilm is in this inactive state, it is only a small portion of that population which we hypothesize to tolerant to antimicrobial agents.

Additional insight into the situation in the biofilm is provided by microscopic examination of frozen cross-sections of specimens induced for GFP expression (Figures 3.2 and 3.3). These images reveal that the zone of active GFP fluorescence is located along the air interface of colony biofilms (Figure 3.2). In colony biofilms, the dimension of the zone of GFP expression measured 68 ± 25 microns. This represents approximately 40% of the mean total thickness of these biofilms. Image analysis of the time course of fluorescence development in differing strata of colony biofilms (Figure 3.3) confirms that regions adjacent to the air interface expressed GFP whereas there was little GFP expression in the middle layer or in the region of the biofilm adjacent to the support membrane. These observations are consistent with the interpretation that only a fraction of the bacteria in the biofilm, localized predominantly along the air interface of colony biofilms, exhibit protein synthetic activity. The stratified activity patterns also demonstrate that arabinose permeated throughout the biofilm and induced bacteria at the opposite edge from which it was delivered.

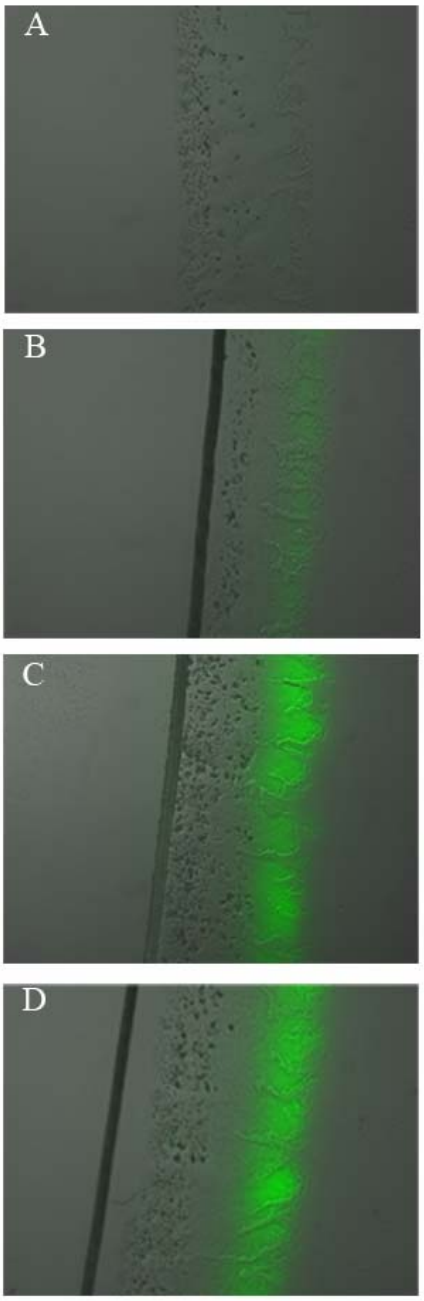

Figure 3.2 Spatial patterns of GFP induction in *P. aeruginosa* colony biofilms. Time zero (A), 4 hours of inductions (B), 12 hours of induction (C), and 24 hours of induction (D).

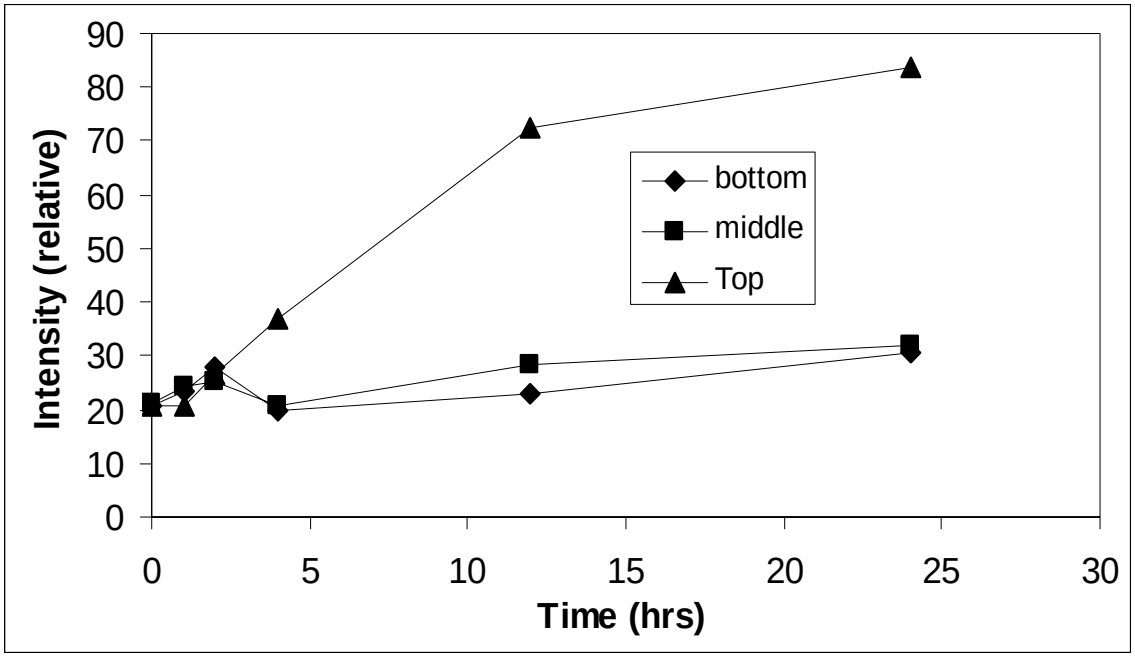

Figure 3.3 Image analysis of GFP induction, by strata within the biofilm. Bottom of the biofilm (♦) middle of the biofilm (■) and top of the biofilm (▲). Vertical axis represents relative intensity on an arbitrary scale.

While the preceding GFP induction experiments imply the presence of an inactive population of cells in the biofilm, these putative dormant cells remain invisible. We sought to positively tag the inactive cells in the biofilm population. To do this, colony biofilms were grown in the continuous presence of arabinose for 48 h after inoculation. The entire biofilm contained green fluorescence at this point (Figure 3.4A). These biofilms were then "downshifted" by transferring them to TSA plates lacking arabinose. There was a gradual loss of fluorescence over the next 48 h. GFP fluorescence diminished first in the region adjacent to the air interface, then fluorescence was lost in deeper regions of the biofilm (Figure 3.4B-D). This progression was also monitored by flow cytometry (Figure 3.4D-H), which revealed two peaks of cells, one bright and one

dim, that increased, and decreased in intensity, respectively. After 48 h of growth in the absence of the inducer, there remained a bright subpopulation that was evident by flow cytometry (Figure 3.4H) and as a trace of bright cells located predominantly along the membrane interface of the colony biofilm (Figure 3.4D). This is illustrated in the flowing figure.

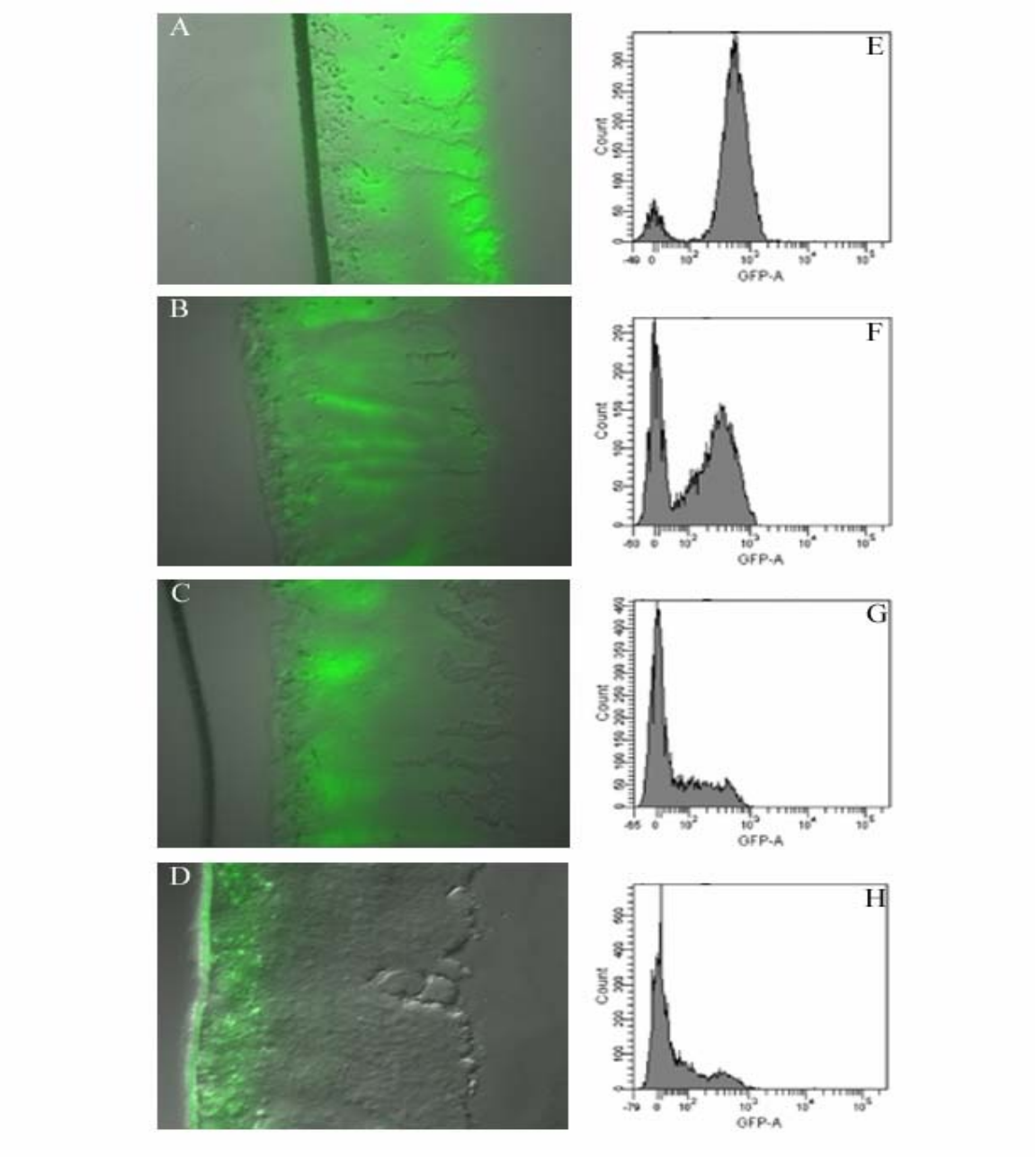

Figure 3.4 Visualization and flow cytometric analysis of GFP dynamics during biofilm down-shift. 3.4A- Entire biofilm loaded with GFP, Time 0. 3.4B- GFP loaded biofilm moved to plate lacking inducer (down-shift) T=24 hours. 3.4C- T=36 hours down-shift. 3.4D- T=48 hours down-shift. 3.4E- H Flow cytometric analysis of GFP loaded biofilm down-shifted for 0, 24, 36, and 48 hours.

Before interpreting the experiment shown in Figure 3.4, consider two mechanisms by which a cell loaded with GFP can lose fluorescence after being downshifted. The first mechanism is dilution through growth. Since there is no new production of GFP, the fluorescent protein present in the original population will be distributed equally among the progeny. A cell that doubles in mass and divides will yield two daughter cells, each of which has half the GFP content of the mother cell. After two doublings, the GFP content per cell would be one fourth that of the original cell. The second mechanism of GFP decay is protein degradation. This process could occur in both growing and non-growing cells, but it might be expected to be slower in a metabolically inactive cell.

With these mechanisms in mind, here is our interpretation of the sequence of the downshift experiment illustrated by the example of Figure 3.4. When growing on TSA, *P. aeruginosa* is an obligate aerobe. Growth is therefore localized along the air interface of the biofilm where oxygen is available. We know from previous studies that oxygen concentration gradients are present in colony and drip-flow *Pseudomonas aeruginosa* biofilms (14). GFP is expected to be diluted or degraded most rapidly in cells located in the growing and metabolically active regions of the biofilm. This is the zone adjacent to the air interface and this is exactly where GFP fluorescence first diminishes (Figure 3.4B). The decay of fluorescence is nearly complete in the aerobic layer of the biofilm after 36 h (Figure 3C) whereas GFP is still present in the bottom half of the biofilm. Even 48 h after the downshift from induced conditions, some bacteria in the colony biofilm, localized primarily but not exclusively along the membrane interface of the biofilm, remain bright. These bright cells cannot have been growing during the

downshift period or they would have diluted the GFP. Neither can there have been much degradation of GFP. These are putative dormant cells.

Cells that retain GFP fluorescence during prolonged incubation in the absence of inducer could be dormant cells, but these could also just be dead cells. To test this possibility, dispersed bacteria from a 48 h downshifted colony biofilm were sorted in the flow cytometer. Bright cells recovered in this way were plated to determine viability. The population of bright, putative dormant cells exhibited a similar level of viability to bright, active cells, labeled in an up-shift experiment. 21% of up-shifted bright events resulted in colony formation, compared to 17% for down-shifted cells. This suggests that the GFP containing bacteria persisting after a downshift are not merely dead cells. One published study supports this interpretation in that it was reported that GFP-tagged *Pseudomonas fluorescens* tend to rapidly lyse and thus lose their fluorescence once the cell dies (11).

The percentage of cells scored bright by flow cytometry in a downshifted colony biofilm decreased from 85% when first transferred to medium lacking the inducer to less than 1% after 72 h in the absence of arabinose (Figure 3.5). The time constant for this loss of fluorescence was 0.05 ± 0.01 h^{-1}. When a planktonic culture that was grown up in the presence of arabinose was subcultured into medium lacking the inducer, the cells rapidly lost fluorescence (Figure 3.5). This population, which was initially scored as 93% bright cells by flow cytometry, was completely devoid of bright cells after 8 h of growth in the absence of arabinose. The time constant for the decay of fluorescence in this population was 1.3 ± 0.4 h^{-1}. This is 26 times faster than the decay of the bright

population in a colony biofilm and is similar in magnitude to the maximum specific growth rate of the organism of $1.2 \pm 0.03\ h^{-1}$. These results indicate that the rate of dilution by growth and degradation of GFP in the biofilm is much slower than in a growing planktonic cultures. GFP is diluted and/or turned over in actively growing cells. In colony biofilms, the loss of GFP is relatively slow. When looking at this phenomenon further, via image analysis of the GFP intensity of the top, middle, and bottom of the biofilm we see that the time constant for GFP loss is $0.03 \pm 0.01\ h^{-1}$, $0.01 \pm 0.01\ h^{-1}$, and $-0.01 \pm 0.01\ h^{-1}$ respectively. This result further indicates that florescence intensity changes depending on where the cells are located within the biofilm, with the cells at the air-interface loosing fluorescence at a rate 3 times greater than the middle strata of the biofilm. It appears that the bottom of the biofilm at the membrane interface actually gains in intensity, but this could be attributed to error in the analysis of this data.

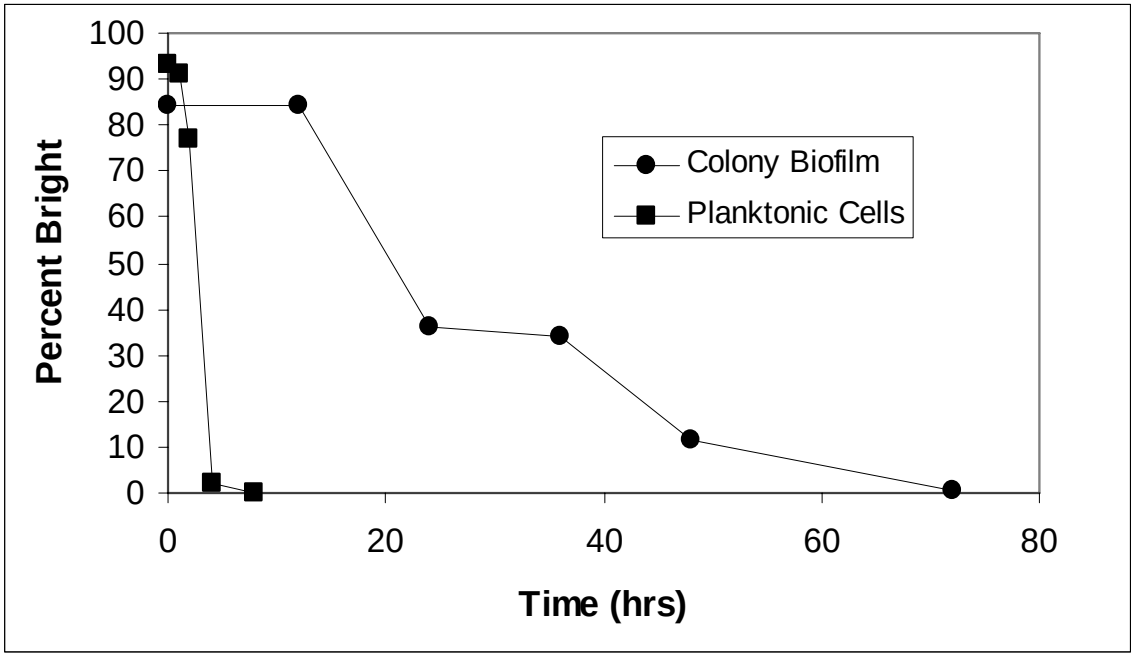

Figure 3.5 Dynamics of GFP loss in *P. aeruginosa* cells in exponential phase planktonic (■) and intact colony biofilms (●). Bacteria were initially loaded with GFP by growth in the presence of arabinose, and then transferred to media lacking the inducer at time zero.

We hypothesized that dormant cells in *P. aeruginosa* biofilms are less susceptible to killing by antibiotics compared to the remainder of the population. Colony biofilms and also biofilms developed in the continuous drip-flow reactor system were grown up for 48 h and 72 h, respectively. Coincident with introduction of antibiotic, which was either 10 mg ml^{-1} tobramycin or 1 mg ml^{-1} ciprofloxacin, the arabinose was removed from the nutrient source for a downshift experiment (Table 3.1) or amended to the medium with the inducer for 12 hours to establish a bright population for an up-shift experiment (Table 3.2). Biofilms were exposed to antibiotic for 24 h, then dispersed and sorted in the flow cytometer. Bright and dim populations were separated and plated to determine viability. In this way the relative susceptibility of different fractions of the

biofilm were quantified (Tables 3.1 and 3.2). In every case, the active fraction of the population was more susceptible than the putative dormant population. These results were statistically significant in all but one case. The dormant cells were found to be less susceptible whether the active population was positively labeled (up-shift experiment) or the dormant population was labeled (down-shift experiment). The same trends were observed in the colony biofilm system and in the drip-flow reactor biofilms. These data support the hypothesis that inactive bacteria harbored in *P. aeruginosa* biofilms are less susceptible to killing by tobramycin and ciprofloxacin.

Biofilm Type	Antibiotic	Log Reduction Active Cells	Log Reduction Dormant Cells	P value
Colony	Ciprofloxacin	2.78+/- 0.06	0.39+/-0.03	0.001
Colony	Tobramycin	2.78+/- 0.02	0.08+/-0.12	0.001
Drip Flow	Ciprofloxacin	2.48+/-0.58	1.32+/-0.47	0.184
Drip Flow	Tobramycin	1.72+/-0.28	0.63+/-0.38	0.019

Table 3.1 Differential antibiotic susceptibility of putative dormant and active *P. aeruginosa* in colony and drip-flow biofilms in downshift experiments. The population was sorted by flow cytometry into a GFP-bright fraction (putative dormant cells) and a GFP-dim fraction (active cells). Errors represent standard deviations of at least 3 replicates.

Biofilm Type	Antibiotic	Log Reduction Active Cells	Log Reduction Dormant Cells	P value
Colony	Ciprofloxacin	1.21+/-0.12	-0.48+/-0.21	0.002
Colony	Tobramycin	3.27+/- 0.61	-1.02+/-0.22	0.003

Table 3.2. Differential antibiotic susceptibility of putative dormant and active *P. aeruginosa* in colony biofilms in upshift experiments. The population was sorted by flow cytometry into a GFP-bright fraction (active cells) and a GFP-dim fraction (dormant cells). Errors represent standard deviations of at least 3 replicates.

Unfortunately, the calculation of log reduction in flow cytometric analysis such as this is not as straight forward as in other situations. The problem lies in the inability to close a cell balance around the measurements obtained by the flowcytometer. We found the task of finding a suitable counter stain that would register well in flow cytometric analysis and not interfere with the GFP channel, more difficult than expected. It was possible to determine the total number of counts entering the flowcytometer, it was also possible to determine the abort rate but since we were observing total cell counts via side scatter it was impossible to distinguish a dim cell from an anomaly registered as a count, e.g. pieces of dead cells or large un-dissolved aggregates of EPS. Thus we had to look at log reductions as a relative number related to percentages of bright and viable cells. The exact procedures for calculation have been previously outlined in the materials and methods section. This lack of absolute cell counts is reconciled in the fact that the log

reduction numbers relative to controls (bright and dim populations of untreated controls) produced data sufficiently informative.

During the upshift experiments, the dim cells show a negative log reduction, i.e. they increase when antibiotic treatment is carried out. This can be explained partly by the fact that as the bright cells were treated a fraction of those cells would succumb to the antibiotic and thus die. Subsequently, GFP expression would cease and the formerly bright cell would then become a dim cell thus causing an increase in the dim population of cells.

Conclusion

The idea of resistant, cells making up a small fraction of the biofilm has been explored in several venues (3,10,12). The mechanism which brings about the phenotypic state of persistence is still unclear. In stationary phase cultures it has been noted that planktonic bacteria express a general stress response (GSR) in which bacteria become tolerant to antimicrobial treatment (5). Brown and Smith theorized that in chronic biofilm infections bacteria experience slow growth and thus express a GSR. They also proposed that this may play a big role in recalcitrance of bacteria in biofilm infections (4). It may be that as the cells within the biofilm move into a stationary growth phase, a small number of bacteria express a GSR similar to stationary phase planktonic cells and thus manifest resistance to antimicrobials. These cells would be consistent with our hypothesis of resistant dormant cells. The idea that a biofilm consists of cells existing in different stages of growth including dormant cells and the prospect that slow growth rate

leads to reduced susceptibility of bacteria has been explored by other investigators (9). One of the reasons that infections of *mycobacterium tuberculosis* are so difficult to treat is that the organism enters a state of dormancy as it exists in isolated pockets of low oxygen concentration. In in-vitro situations this microaerophilic non-replicating condition has produced *mycobacterium tuberculosis* that was very resistant to antibiotic treatment (16). It may be that this dormant state is entered into due to oxygen limitation, or due to some other nutrient limitation. It may also be a product of the cell's growth stage. The mechanism for entrance into this protected dormant stage is not yet clear but the protection that it provides seems to be fairly evident.

It was shown that *P. aeruginosa* cells grown to stationary phase in a planktonic culture entered into an inactive state where anabolism ceased or was arrested as demonstrated by lack of GFP induction activity in most of the cells in the culture. We also observed this same state of inactivity within biofilms with only about 30% of the biofilm able to produce fluorescence after 12 hours of exposure to the inducer. Cells in the rest of the biofilm were in various states of inactivity, in which anabolism was slowed or halted. This hypothesis was explored in converse experiments where the biofilm was loaded with GFP throughout by continuous growth in the presence of the inducer and subsequently moved to media lacking the inducing agent. These experiments demonstrated that the fluorescence faded from the biofilm from the air interface down, with the last of the cells retaining fluorescence remaining at the membrane interface of the biofilm. Most of the inactive or dormant cells were located at the membrane interface of the biofilm. That is, they were at the bottom, where it can be hypothesized that these

dormant cells were the oldest cells within the biofilm. These last cells retaining fluorescence were the cells exhibiting the least amount of anabolic activity, the most dormant cells within the biofilm. It is not clear why these cells enter this dormant state within the biofilm. There are several factors which may contribute to the dormancy of these cells. Dormancy may be induced by lack of oxygen available to the cells, it may also be that the oldest cells within the biofilm are triggered into this protected dormant state. The stability of the plasmid bearing the GFP was explored and shown to be very stable, thus the results cannot be attributed to plasmid loss. We have therefore established that there is a substantial amount of heterogeneity of the anabolic activity within the biofilm including populations of dormant cells.

We hypothesized that the dormant cells within the biofilm were less susceptible to antibiotic treatment than the active cells. By using the previously mentioned means of up-shifting (labeling active cells with GFP) and down-shifting (labeling dormant cells with GFP) we were able to explore the effects of antibiotic treatment on these two distinct populations of cells. By treating both up-shifted and down-shifted intact biofilms with antibiotics and subsequently sorting the treated populations in a flow cytometer we determined that in almost every case, dormant cells were much less susceptible to antibiotic treatment than active cells. This overall trend was maintained with colony biofilms as well as drip flow biofilms.

These results are very powerful in that they suggest that much of the biofilms tolerance to antibiotics may be attributed to the presence of anabolically dormant cells within the biofilm.

REFERENCES

1) Anderl, J.N.; Franklin, M.J.; Stewart P.S. Role of Antibiotic Penetration Limitation in *Klebsiella pneumonia* Biofilm Resistance to Ampicillin and Ciprofloxacin. Antimicrobial Agents and Chemotherapy 2000, 44, 1818-1824

2) Brady, R.A.; Leid, J.G.; Costerton, J.W.; Shirtliff, M.E.; Osteomyelitis: Clinical Overview and Mechanisms of Infection Persistence. Clinical Microbiology Newsletter 2006, 28 (9), 65-72

3) Brooun, A. Liu, S. Lewis, K. A Dose-Response Study of Antibiotic Resistance in *Pseudomonas aeruginosa* Biofilms. Antimicrobial Agents and Chemotherapy 2000, 44, 640-646

4) Brown, M.R.W.; Barker, J.; Unexplored Reservoirs of Pathogenic Bacteria: Protozoa and Biofilms. Trends in Microbiology 1999, 7 (1) 46-50

5) Brown, M.R.W.; Smith, A.W.; Dormancy and Persistence in Chronic Infection: Role of the General Stress Response in Resistance to Chemotherapy. 2001 Journal of Antimicrobial Chemotherapy 48, 141-142

6) Costerton, J.W.; Lewandowski, Z.; Caldwell, D.E.; Korber, D.R.; Lappin-Scott, H.M.; Microbial Biofilms. Annual Review of Microbiology 1995, 49, 711-745

7) Costerton, J.W.; Stewart, P.S.; Greenberg, E.P.; Bacterial Biofilms: A Common Cause of Persistent Infections. Science 1999, 284, 1318-1322

8) Costerton, J.W.; Cystic Fibrosis Pathogenesis and the Role of Biofilms in Persistant Infection. Trends in Microbiology 2001, 9 (2), 50-52

9) Gilbert, P.; Collier, P.J.; Brown, M.R.W.; Influence of Growth Rate on Susceptibility to Antimicrobial Agents: Biofilms, Cell Cycle, Dormancy, and Stringent Response. 1990 Antimicrobial Agents and Chemotherapy 34 (10) 1865-1868

10) Lewis, K.; Riddle of Biofilm Resistance. 2001 Antimicrobial Agents and Chemotherapy 45 (4) 999-1007

11) Lowder, M., A. Unge, N. Maraha, J. K. Jansson, J. Swiggett, and J. D. Oliver. 2000. Effect of starvation and the viable-but-nonculturable state on green

fluorescent protein (GFP) fluorescence in GFP-tagged *Pseudomonas fluorescens* A506. Appl Environ Microbiol **66**:3160-3165.

12) Moyed, H. S.; Bertrand, K.P.; *hip*A a Newly Recognized Gene of Escherichia Coli K-12 That Affects Frequency of Persistance After Inhibition of Murien Synthesis. Journal of Bacteriology 1983, 155 (2) 768-775

13) Presterl, E.; Grisold, A. J.; Reichmann, S.; Hirschl,. A. M.; Georgopoulos, A.; Graninger, W.; Viridans Streptococci in Endocarditis and Neutropenic Sepsis: Biofilm Formation and Effects of Antibiotics. Journal of Antimicrobials and Chemotherapy 2005 55(1):45-50

14) Richards, L.; Pitts, B.; Roe, F.; Ehrlich, G.D.; Stewart, P.S.; Contribution of Oxygen and Glucose Limitation to *Pseudomonas aeruginosa* Biofilm Tolerance of Ciprofloxacin and Tobramycin. Submitted to Antimicrobial Agents and Chemotherapy 2006 (CHAPTER 2)

15) Walters, M.C.; Roe, F.; Bugnicourt, A.; Franklin, M.J.; Stewart, P.S.; Contributions of Antibiotic Penetration, Oxygen Limitation, and Low Metabolic Activity to Tolerance of *Pseudomonas aeruginosa* Biofilms to Ciprofloxacin and Tobramycin. Antimicrobial Agents and Chemotherapy 2003, 47, 317-323

16) Wayne, L.G.; Hayes, L.G.; An In Vitro Model for Sequential Study of Shiftdown of *Mycobacterium tuberculosis* through Two Stages of Nonreplicating Persistence. 1996 Infection and Immunity 64 (6) 2062-2069

17) Xu, K.D.; Stewart, P.S.; Xia, F.; Huang, C.; McFeters, G.A., Spatial Physiological Heterogeneity in *Pseudomonas aeruginosa* is Determined by Oxygen Availability. Applied and Environmental Microbiology **1998,** *64*, 4035-4039

CHAPTER 4

CONCLUSIONS

The scope of this thesis encompassed two main thrusts in my research at the Center for Biofilm Engineering. First, in chapter 2 the theme of oxygen limitation within the biofilm and its effects on the tolerance of *Pseudomonas aeruginosa* biofilms was explored. In chapter 3 we explored dormancy within the biofilm and the effects of said dormancy on the biofilm ability to tolerate antimicrobial treatment.

We established that there were distinct strata of oxygen concentrations within the biofilm. This was established by the use of a strain of *Pseudomonas aeruginosa* tagged with an inducible green fluorescent protein (GFP). By inducing the GFP in mature biofilms and analyzing the subsequent images we were able to calculate an active zone for the biofilm's protein synthesis. We theorized that the active area of the biofilm was the zone where oxygen was available to the cells. Profiling of dissolved oxygen concentration showed similar stratification of oxygen concentrations.

It was our goal to establish the relationship between oxygen availability and antibiotic susceptibility. If the reason for the biofilms recalcitrance to antimicrobials was entirely due to oxygen deficiency, then treating planktonic cells under anoxic conditions should allow for complete protection. Experiments were performed with planktonic cells in which oxygen availability, glucose availability, and growth phase of the inocula were varied. We treated the cultures under varying conditions including differences in oxygen availability as well as growth rate. We found that anoxia alone could not entirely explain

the tolerance of intact biofilms to these antibiotics. In addition to experiments performed with planktonic cells we dispersed biofilms and treated them in suspension and found that susceptibility was then comparable to that of planktonic cells. Hence it is truly the biofilm state that allows for recalcitrance. We also performed experiments by increasing or decreasing the oxygen tension above intact biofilms. These experiments yielded little change in biofilm susceptibility to tobramycin regardless of the oxygen conditions in the biofilm's headspace. There was a small increase in susceptibility for intact biofilms treated with ciprofloxacin in an oxygen rich environment. Hence we established that while oxygen may play a role in biofilm recalcitrance it is not the only factor that leads to antibiotic tolerance of *Pseudomonas aeruginosa* biofilms. In addition, we explored the possibility that glucose may somehow be limited to the biofilm. We concluded from theoretical calculations and experimental evidence that it is highly unlikely that glucose is at all limited within the biofilm.

The second theme of this dissertation explored the idea of dormant cells within the biofilm. We hypothesized that the biofilm harbored inactive or dormant cells that were highly resistant to antimicrobial challenge. In the past it has been difficult to elucidate the differences in the susceptibility of cells that differed spatially within the biofilm. We developed a novel approach of labeling active and dormant cells within *Pseudomonas aeruginosa* biofilms using GFP. Using this method it was possible to visualize patterns of anabolic activity within the biofilm. We found that the most anabolically active cells within the biofilm were located in upper portions of the biofilm adjacent to the air interface. The least active or dormant cells were located in a small

region near the bottom of the biofilm. Using flowcytometry we were able to sort cells according to their anabolic activity (analogous to presence or lack of GFP production). Using this novel technique we determined that dormant cells within *Pseudomonas aeruginosa* biofilms are much less susceptible to antibiotic treatment than are active cells.

Although putative dormant cells were shown to be tolerant to treatment by both ciprofloxacin and tobramycin, we still do not know how the cells enter the dormant state. We showed in Chapter 2 that there were oxygen concentration gradients within the biofilm and the aerobic zone of the biofilm closely resembles the active zone of the biofilm. It may be that the cells are triggered to enter and exit the dormant state through extended periods of oxygen depletion, or a combination of that and other factors yet undetermined. We have shown that oxygen only plays a partial role in antibiotic tolerance it may be that it only plays a partial role in the cell's entrance into and exit from the dormant state.

Implications

The implications of this work are far reaching in the field of biofilm research. This work concludes that oxygen availability is not the only factor regarding biofilm tolerance to the antibiotics ciprofloxacin and tobramycin. This result will allow future researchers to concentrate on other approaches towards elucidating the reasons that biofilms are tolerant to antimicrobial treatment. In addition the heterogeneity of the biofilm was confirmed in respect to oxygen concentration and levels of dormancy within the biofilm. It is important to note that biofilms are complicated systems and we must

think about them as so when contemplating methods for uncovering the intricacies associated with their recalcitrance.

The conclusion that the biofilm harbors dormant cells and those cells are in effect more resistant to antibiotic treatment than active cells, is quite significant. Knowing this to be the case, it may be possible to establish the mechanism for their recalcitrance and in turn develop methods of killing dormant cells. If treatment strategies can be developed to target these dormant cells it may be possible to more effectively control biofilms.

Biofilm recalcitrance is very problematic, especially in the health care industry. Since it is so difficult to effectively treat biofilms, infections within the human body often cause the patient severe trauma or even death. The reasons for a biofilms' tolerance to antimicrobial agents have proven to be very diverse and difficult to elucidate. This thesis contributes to our overall knowledge base regarding biofilms. These contributions are pieces of the puzzle that will ultimately be put together in order to determine how to effectively control biofilms and thus advance medicine to the point where controlling a biofilm infection is a simple matter of diagnosis and routine treatment.

Future Work

The most pressing issue when it comes to future work is the additional analysis of dormant cells within the biofilm. With the ability to separate dormant cells from active cells with a flowcytometer it will also be possible to explore the gene expression of each respective population. By analyzing what genes are up-shifted and downshifted in dormant cells verses active cells it may be possible to determine exactly the factors that

cause dormant cells to be more tolerant to antibiotics. And thus open the door for developing treatment strategies to target those cells.

In addition it would be useful to determine if the same patterns of dormancy were seen in other organisms in addition to *Pseudomonas aeruginosa*. Treatment and susceptibility patterns to other antimicrobial agents would also be advantageous to explore. In this thesis we have looked at the tolerance of dormant cells to only two antimicrobial agents to one species of bacteria. It should be confirmed that the patterns of dormancy reach to differing situations.

The last recommendation I have for future work is to find out if the dormant cells require the biofilm state to manifest recalcitrance. Can they be effectively treated when they are sorted and suspended or do they retain their tolerance to antimicrobial agents? Up until now, all of the data that we have collected has led to the conclusion that the tolerance of the biofilm is multifaceted and linked to the biofilm state of growth. If these dormant cells remain tolerant even when not in the biofilm state it would mean that the biofilm state of growth may not actually be as important a factor to biofilm recalcitrance as once believed.

Relating spatial heterogeneity within the biofilm would also prove to be helpful in understanding how oxygen and dormant cells are distributed throughout the biofilm. Measurements of active zones should be made with the physical location of the sample noted i.e. top of drip flow coupon, middle, bottom etc. This way we would know if the active zone is larger or smaller closer and further from where the nutrients enter and if it differed in channels or in thick places in biofilms.

In addition to laboratory experiments it would be advantageous to add this dormant mode of growth to improve accuracy of computer biofilm models. Computer models are often very helpful in elucidating differences in a system. Changes can be made to parameters within the model and the results can be obtained often within minutes. This is a much more efficient means of testing perturbations in experimental conditions since a wet experiment doesn't have to be fully set up and biofilms allowed to grow over a period of several days. Of course it is best to confirm results obtained from computer models by additional experiments in the laboratory. That this dormant state of existence does in fact occur in *Pseudomonas aeruginosa* biofilms has been established, models that take dormancy into account could help elucidate how important the tolerance of the small number of dormant cells is to overall biofilm recalcitrance. Computer simulations including and excluding dormant cells could be run and the results compared to get a measure of protection that dormant cells provide the biofilm.

APPENDICES

APPENDIX A

STAIN UPTAKE OF *PSEUDOMONAS AERUGINOSA* BIOFILMS

Introduction

The purpose of the work outlined in this appendix was to elucidate the stain uptake of *Pseudomonas aeruginosa* cells and ultimately shed some light on the permeability of those cells within a biofilm. Our hypothesis was that *P. aeruginosa* cell membranes were more permeable in planktonic culture than those within a biofilm, ultimately leading to the biofilm's inherent tolerance to antimicrobials. It has been shown in the past that antibiotics do in fact penetrate through biofilms yet they are still tolerant to antibiotic treatment relative to planktonic cells (1,4,8,7). Our hypothesis could help explain this phenomenon, in that the antibiotic would be available to the cells but not able to penetrate through their membranes. That is, cells within the biofilm were inherently less permeable to antibiotics than planktonic, suspended cells.

Although a considerable amount of time and effort was expended on this research and many experiments were conducted, we decided to abort further efforts to explore the issue of cell permeability. It did not appear that this research vector was going to lead to publishable material. The results we obtained were not as expected and we found the problem to be more convoluted than expected. This material is noted here in an attempt to record our efforts towards gaining understanding of *P. aeruginosa* cell permeability, it may prove useful for future researchers as a reference of what we have tried and the results that were obtained.

We decided to test this hypothesis of reduced cell permeability within biofilms by experimenting with stain uptake of biofilms and planktonic cells. The first approach that

we took was to use Syto® 9 to explore the stain uptake properties biofilms. Syto® 9 is a membrane permeable nucleic acid stain that should stain all cells within the biofilm. The thought was that Syto® 9 would allow us to stain the entire biofilm and then compare the stain uptake characteristics of biofilm cells to those of planktonic cells. We theorized that we would be able to determine rate of stain uptake by comparing image time courses of biofilms and planktonic cells as they were exposed to stain for specified periods of time. We also planned to compare maximum brightness to determine the total amount of stain present in each cell. The thought was that less permeable cells would take up stain slowly, but the final concentration of stain would be the same as the less permeable cell. Theoretically stain uptake of cells only differing in permeability should have the same endpoint, the changes should be seen in the rate of uptake. Syto® 9 was used because it has been widely used in the LIVE/DEAD® Bac*Light*™ bacterial viability and counting kit. This staining kit has been used in several different studies to determine the viability of biofilm cells (3,5,6). We found the staining characteristics of biofilms proved to be very unsatisfactory using Syto® 9.

Since Syto® 9 proved to be unsatisfactory for the task of elucidating permeability of biofilm cells, we decided to try another nucleic acid stain, acridine orange. The uptake properties were in fact more rapid for acridine orange, but we were still not able to make any conclusions from this research. Uptake of Rhodamine B was also briefly explored. Experiments were suspended and efforts were redirected towards other projects.

Those experiments performed in hopes of determining permeability of biofilm cells are recorded and results are outlined here.

Materials and Methods

Bacterial Strain and Media

All experiments were performed with *Pseudomonas aeruginosa* strain PAO1. All inocula and planktonic cultures were grown for 18-24 hours in tryptic soy broth (TSB) (Beckton Dickinson and Company, Sparks, MD). Colony biofilms were grown on tryptic soy agar (TSA) (Beckton Dickinson and Company, Sparks, MD). Colony biofilms of *Pseudomonas aeruginosa* PAO1 were grown as described elsewhere (2). All biofilms were allowed to grow on membranes for 48 hours after inoculation, before any exposure to stain.

Staining

Syto® 9, propidium iodide, and acridine orange were obtained from Molecular Probes (Carlsbad, Ca). Syto 9 was used at a concentration of 5 mM. Acridine orange was used at a concentration of 50 μg/ml or 0.17 mM. Intact biofilms were stained by placing them membrane side down on Millipore™ Cellulosic absorbent pad discs (Fischer Scientific, Pittsburg, PA), saturated with TSB containing the appropriate stain. When biofilms were subjected to longer exposure times, after 12 hours of exposure they were moved to fresh pads saturated in TSB containing the proper concentration of stain. Biofilms were placed in petri dishes in large, partially sealed bags containing water saturated paper towels. This was done in order that humidity could be kept high and drying of the biofilm would be kept at a minimum throughout the staining period.

Stain uptake of rhodamine B (obtained from Sigma-Aldrich, St Louis, Mo.) was explored as well. Rhodamine B was added to TSA in the proper concentrations while it was still liquid, plates were poured and allowed to set up, resulting in rhodamine B impregnated TSA plates. Mature biofilms were placed on the rhodamine B impregnated plates and allowed to stain intact. Polycarbonate membranes with a porosity of 0.2 μm (Poretics Corp., Livermore, Ca.) were placed on top of the biofilm, 6mm paper discs (Becton Dickinson and Company, Cockeysville, MD) were placed above the top membrane. The paper discs were placed on top of the biofilms in this manner at the start of staining. The discs were removed at specific time points and placed in sterile water. The samples were vortexed and subsequently the adsorption was read in a Turner Designs TD-700 fluorometer. In this manner it was possible to determine the amount of time it took for rhodamine B to completely penetrate the biofilm.

Visualization of Biofilms and Image analysis

The stained biofilms were cryoembedded in a tissue histology medium (9). Frozen samples were sectioned into 5 μm thick slices and placed on glass microscope slides. The sections were examined using epiflourescent microscopy. The images were analyzed using MetaMorph® software (Molecular Devices Corp., Sunnyvale, Ca.). Cross sections were examined for maximum brightness in a given region using the line scan feature. The line scan was made 100 pixels wide and measurements were taken such that nearly the entire biofilm in the image was registered. MetaMorph® averages the intensity across the entire 100 pixel width. The maximum intensity registered in the line

scan was recorded. In order to see patterns of staining in samples with differing brightness, it was often necessary to capture images with differing exposure times. All graphs representing comparisons in average maximum brightness have been standardized to 100 ms exposure time. That is, if an image was taken with an exposure time of 50 ms the average maximum intensity would be multiplied by two to compare to an image taken with an exposure time of 100 ms. All images presented are the result of overlaying an epiflourescence image over a transmission image thus they are compilations of two images at the same spot on the frozen section.

Results and Discussion

As seen in Figure A.1 colony biofilms were grown to maturity and stained intact, on a pad disc saturated with TSB containing 5 mM Syto® 9. Biofilms were then removed and cryoembedded at specific times throughout the stain exposure period. The resulting images show a distinct stratification of staining, concentrated near the membrane interface (on the left hand side of all images presented). This was the case even after 24 hours of exposure to the stain (Figure A.1D). It is clear that even after extended periods of staining, cells within the biofilm are not taking up the stain uniformly.

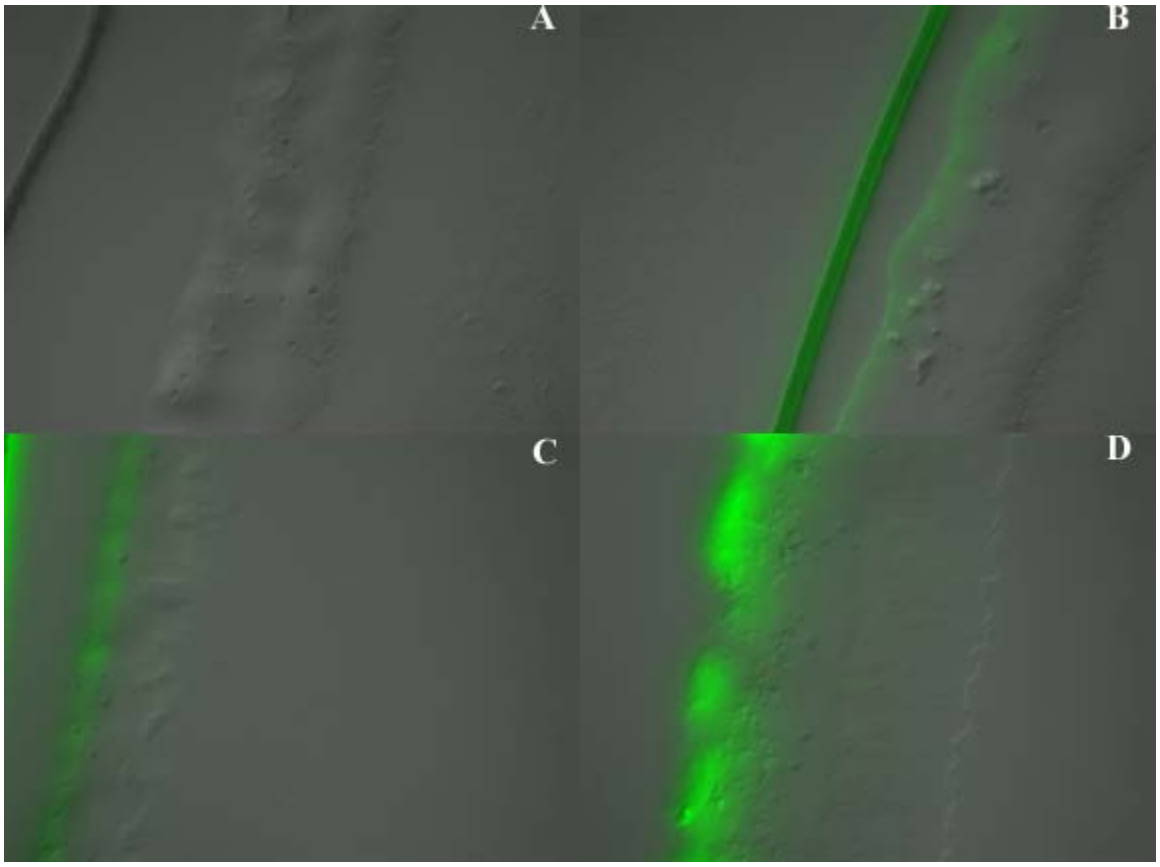

Figure A.1 Intact colony biofilm time course of staining with Syto 9 on pad discs. Images are presented with the substrate/membrane on the left hand side of the picture. A) biofilm before exposure to stain. B) 4 hours of exposure C) 12 hours of exposure D) 24 hours of exposure.

Pseudomonas aeruginosa cells were grown then stained in suspension over a time course. The cells were then rinsed in phosphate buffered saline two times and filtered onto a membrane. Cryoembedding then took place in the same manner as intact biofilms. By imaging planktonic and resuspended cells in this manor it was possible to directly compare the images to those of intact biofilms. Figure A.2 shows the time course of staining planktonically grown cells in suspension. It is apparent that the staining is uniform throughout the cells and maximum brightness occurs in a very short period of

time. It is important to note that the exposure times for the images differed from those of the the previous images. Overall brightness can not be compared visually from the images presented here. The images are shown to give a representation of staining patterns only.

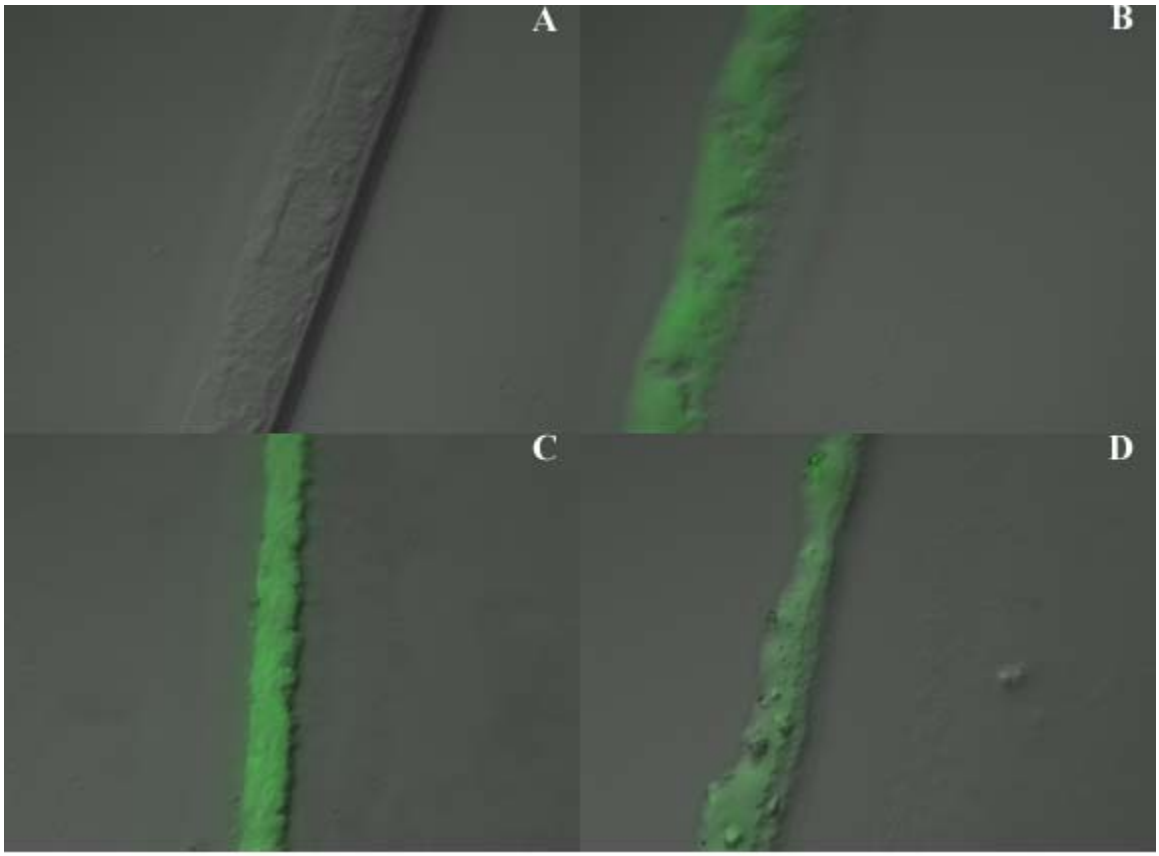

Figure A.2. Time course of images after Syto® 9 staining of planktonic cells in suspension. Cells were washed and filtered onto membranes for imaging. These images were extremely bright and taken with a reduced exposure time, thus the brightness is relative to pictures only in this series. A) Unstained cells B) 10 minutes of staining C) 30 minutes of staining C) 2 hours of staining.

Disaggregated biofilm cells were stained in suspension in order to determine if there was something inherent to the cells themselves, rather than the biofilm state of growth, that caused poor uptake of the stain. As you can see from Figure A.3 stain uptake was rapid and resulted in bright cells similar to planktonic cells stained in suspension. The pattern of staining was uniform throughout the cells.

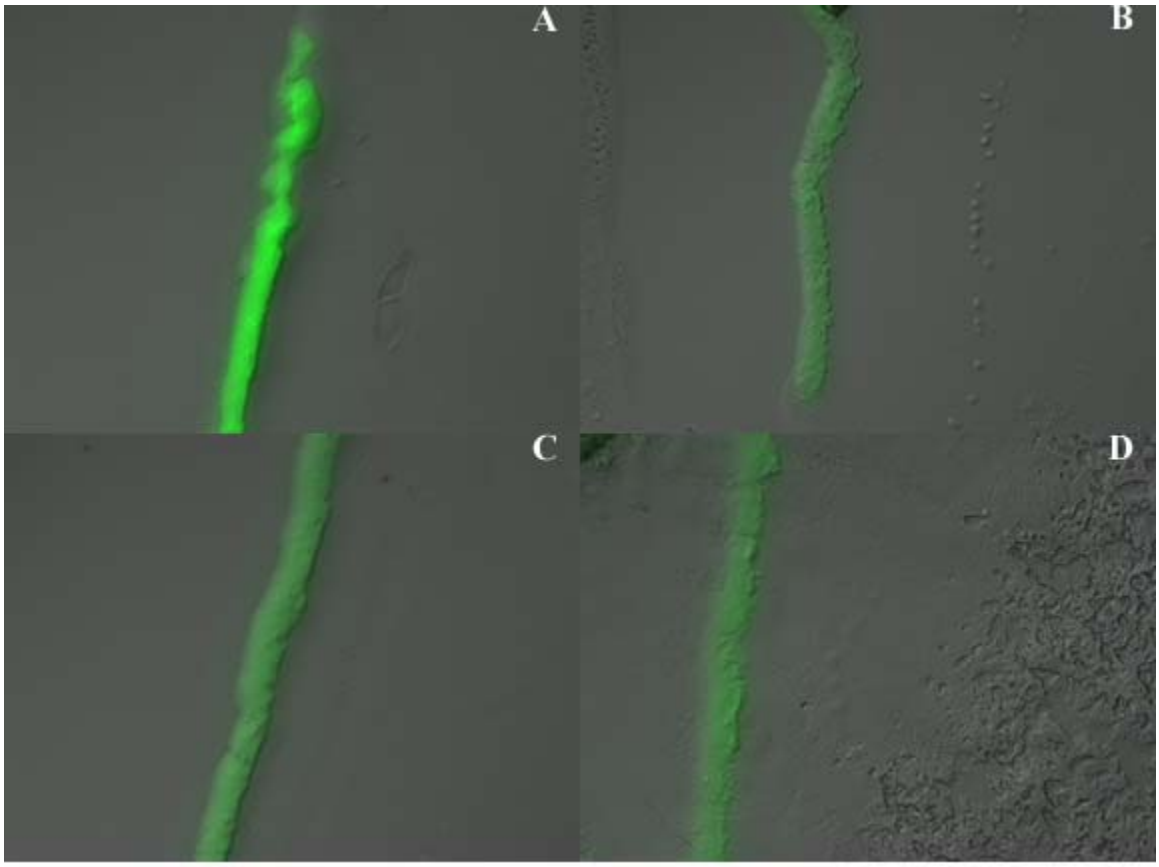

Figure A.3. Time course of cells grown in a biofilm, disaggregated and stained in solution. A) after 10 minutes of staining B) 30 minutes of staining C) 1 hour of staining D) 2 hours of staining

In order to further elucidate the difference in stain uptake characteristics between planktonic cells and biofilm cells, It was necessary to compare planktonic cells stained on a membrane to those of the intact biofilms. Cultures were grown planktonicly, rinsed and filtered onto membranes, the membranes were placed on filter pads for staining just as the intact biofilms had been. A time course of images was then taken (Figure A.4). It is apparent that very little staining of the cells took place even though these were planktonic cells. The cells did take up a very small amount of stain, i.e. they were slightly brighter than controls placed on pads with TSB only (not shown). The stain uptake did not appear to take place in a stratified pattern.

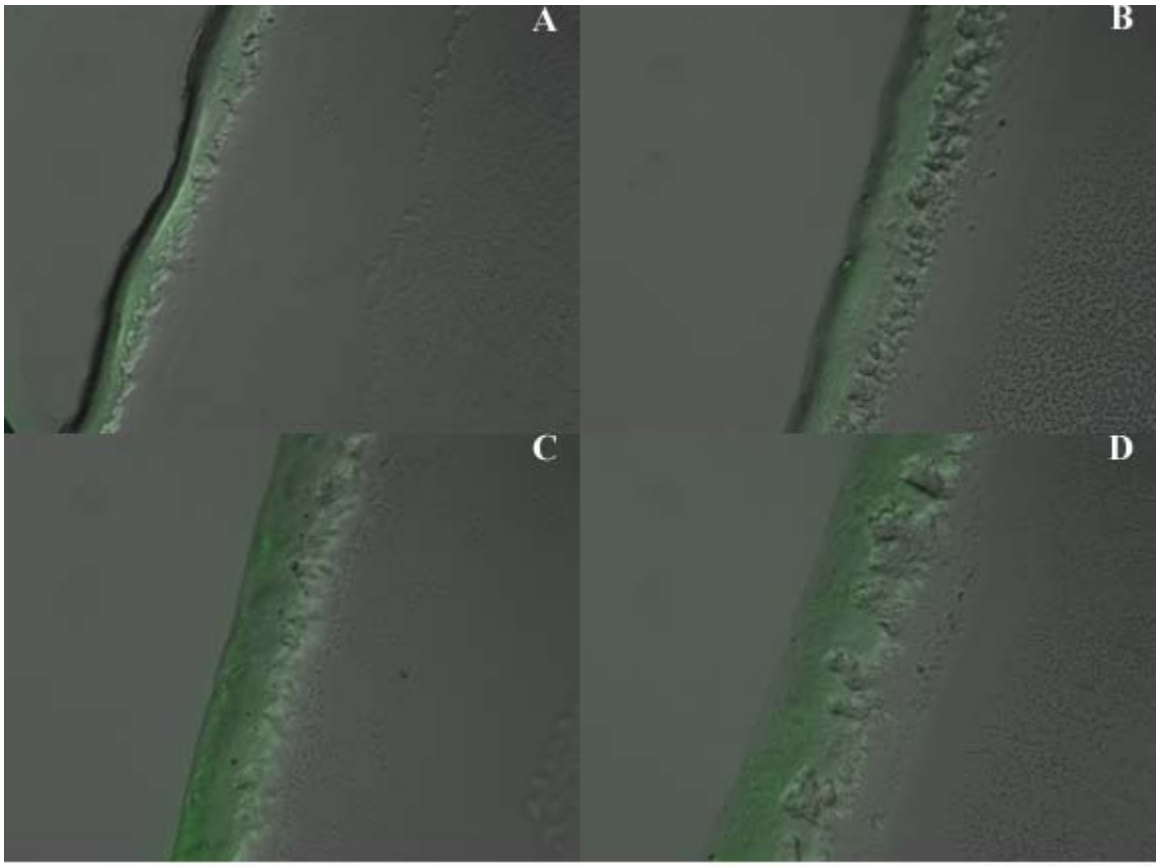

Figure A.4 Time course of images after Syto® 9 staining of planktonic cells stained on a membrane. A) after 10 minutes of staining B) 1 hour of staining C) 4 hours of staining D) 9 hours of staining

This same experiment was repeated but with cells grown in the biofilm state, then disaggregated and filtered back onto a membrane. After filtering the cells on a membrane they were then stained by placing them on a stain saturated filter pad. The image time course is shown in Figure A.5. It is curious that the 9 hour time point does seem to have experienced thorough staining, but there is no evidence of this staining in any other time points.

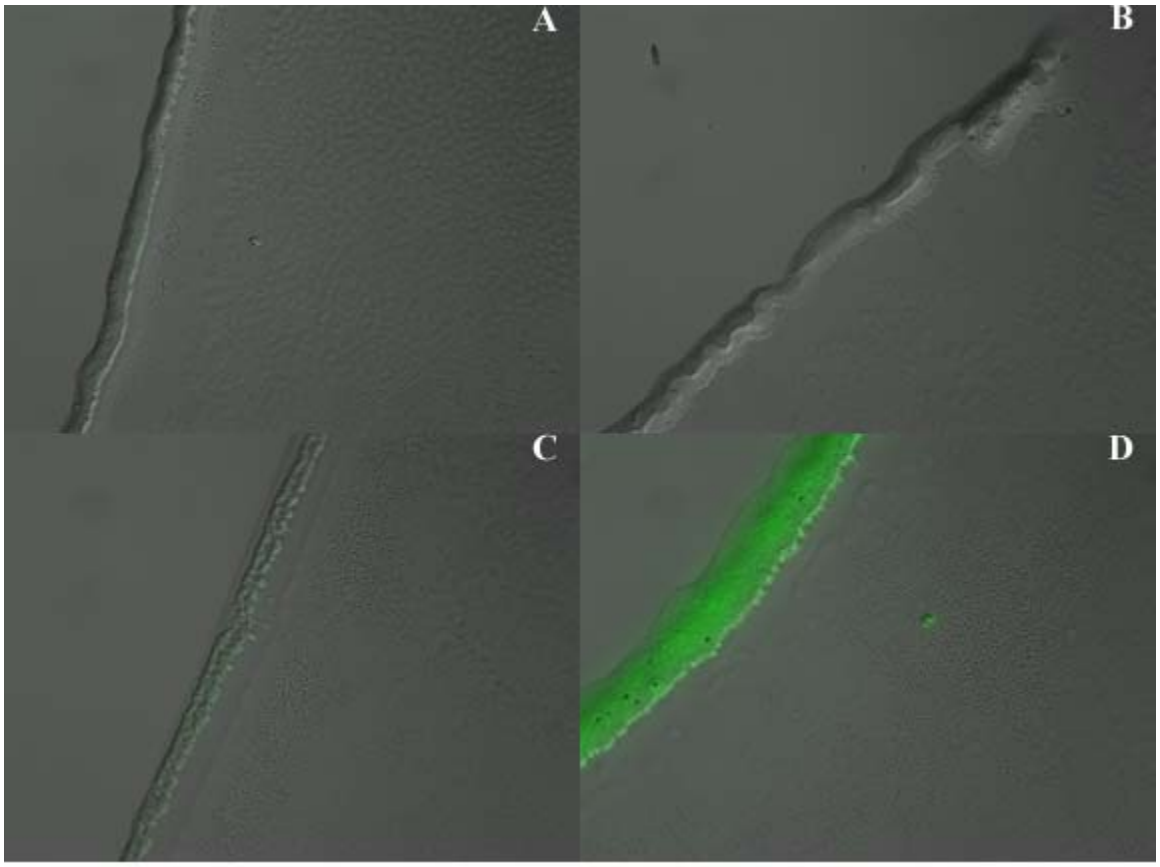

Figure A.5 Time course of images after Syto® 9 staining of biofilm cells stained on a membrane after disaggregation and subsequent filtering. A) 10 minutes of exposure to stain B) 1 hour of exposure to stain C) 4 hours of exposure to stain D) 9 hours of staining.

Planktonic and resuspended biofilm cells did not take up stain very well when stained on a membrane. If the reason that the cells did not take up the stain was that the membranes were less permeable, then cells fixed with glutaraldehyde to increase the permeability of the cell membranes, would show improved staining characteristics. This in fact did not turn out to be the case. When cells were fixed with glutaraldehyde and stained in suspension they rapidly took up the stain, and they stained very bright. When fixed planktonic cells were stained on a membrane, stain uptake was very slow and

resulted in very low overall brightness. In effect, there was very little difference between unfixed and fixed planktonic cells when they were stained on membranes. The image analysis of planktonic and biofilm cell staining is summarized in figures A.6 and A.7 respectively.

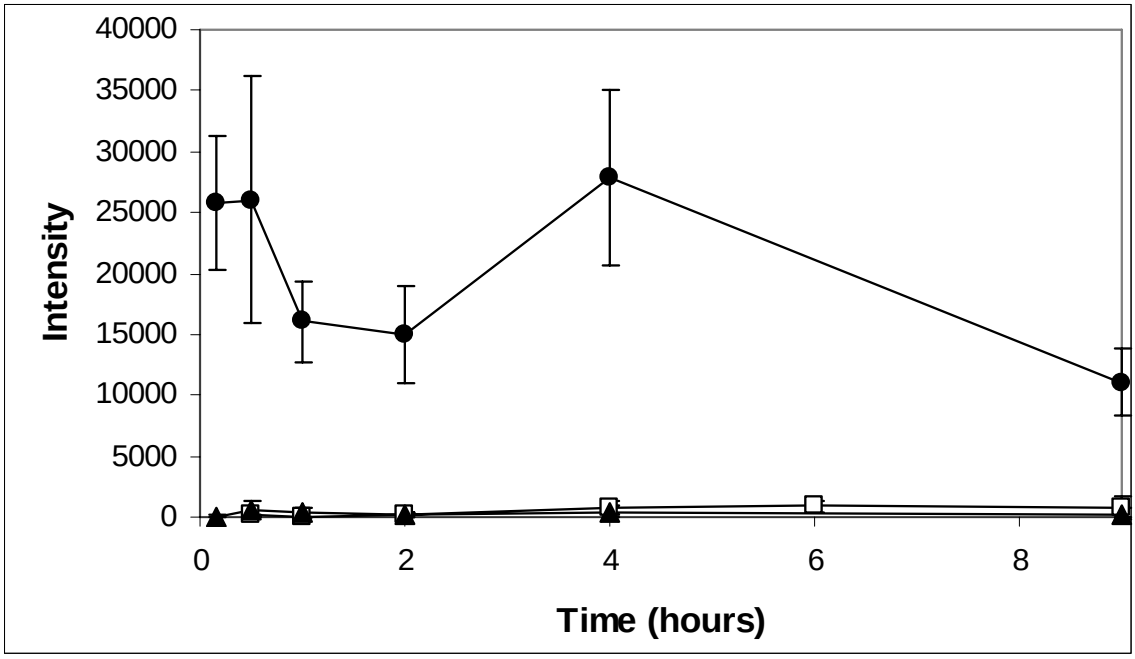

Figure A.6. Summary of staining image analysis of biofilm cells. Biofilm cells disaggregated and stained in suspension (●). Biofilm cells stained intact (□). Biofilm cells disaggregated, re-filtered onto a membrane and stained (▲). Error bars represent standard deviations of at least 3 replicates.

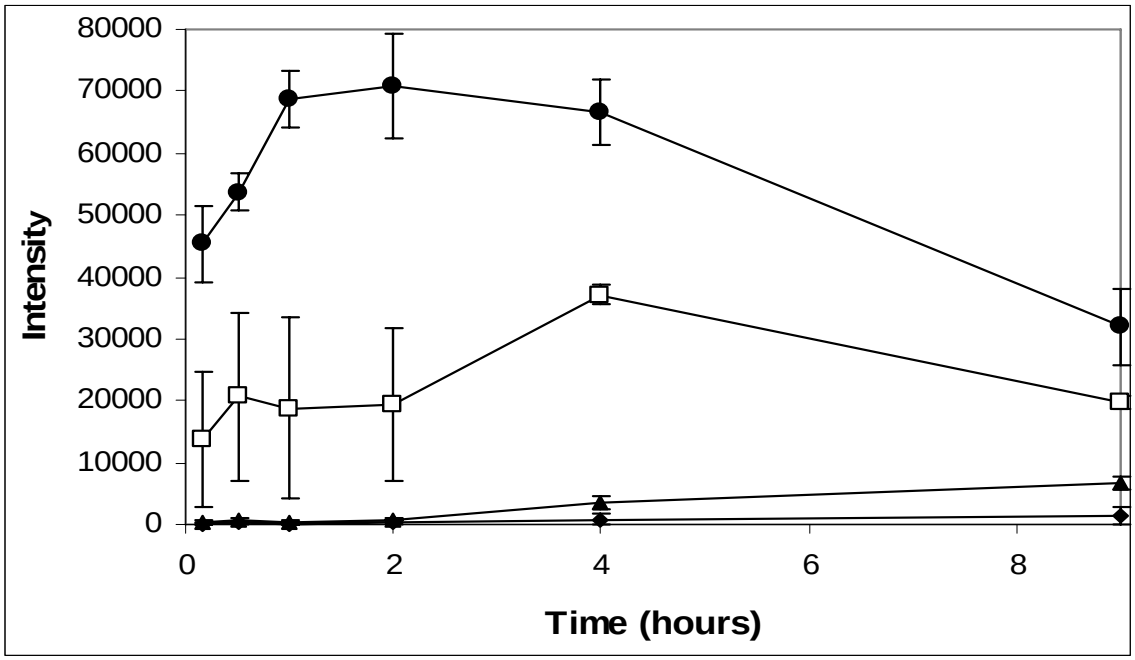

Figure A.7. Summary of staining image analysis in planktonic cells. Planktonic cells stained in suspension (□). Planktonic cells filtered onto a membrane and stained (♦). Planktonic cells fixed with 5% glutaraldehyde and stained in solution (●). Planktonic cells fixed with 5% glutaraldehyde and stained on a membrane (▲).Error bars represent standard deviations of at least 3 replicates.

It is clear that cells stained in suspension absorb the stain in a rapid fashion and stain very bright. Cells stained on membranes showed very little stain uptake. Fixed cells stained in suspension proved to stain much brighter than unfixed cells. This is curious in that we would expect all cells to reach about the same maximum intensity due to the fact that the driving force for stain to diffuse into the cells would be the same for cells that differed only in membrane permeability.

It appeared that there was some sort of barrier to stain penetration when cells were stained on membranes. To see if stain would penetrate from the top of the biofilm two separate experiments were devised. The first was to place a drop of TSB containing stain

on top of the biofilm and examine how the stain would penetrate. Figure A.8 is an example of such an experiment. Staining occurred about half way through the biofilm. This was greater penetration than we saw when the biofilm was stained from the bottom, however complete staining was still not observed.

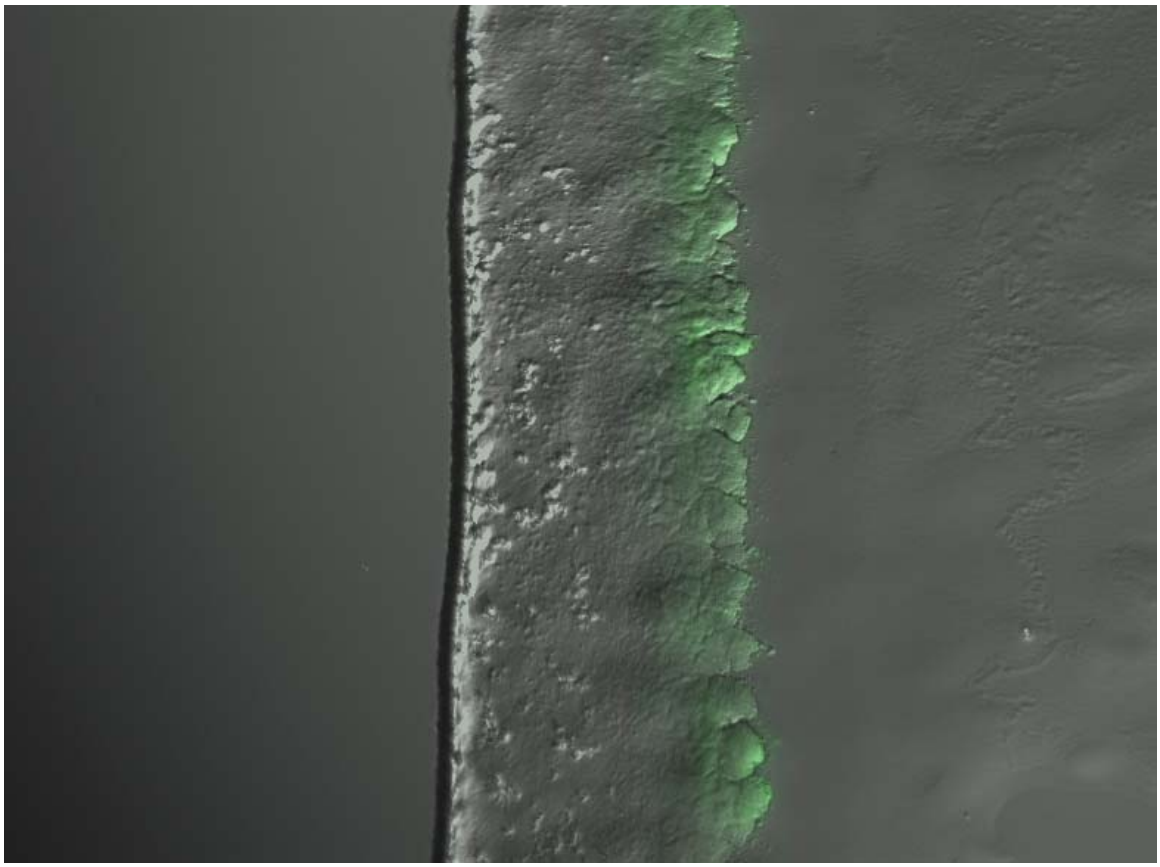

Figure A.8 Image of intact biofilm. a drop of TSB containing Syto® 9 was placed on top of the biofilm and allowed to soak in for 4 hours.

The second method used to stain the biofilm from the top was to place a dry pad disc under the biofilm then place a fresh membrane on top of the biofilm then a pad disc saturated with TSB containing Syto® 9 on top of the fresh membrane. A schematic of

this is shown in Figure A.9. This would give the biofilm an opportunity to absorb stain from the top and allow any excess stain to drain into the dry pad disc. An image of a biofilm stained for 4 hours in this manor can be seen in Figure A.10. It is apparent that the stain was absorbed by the membrane but did not penetrate into the biofilm.

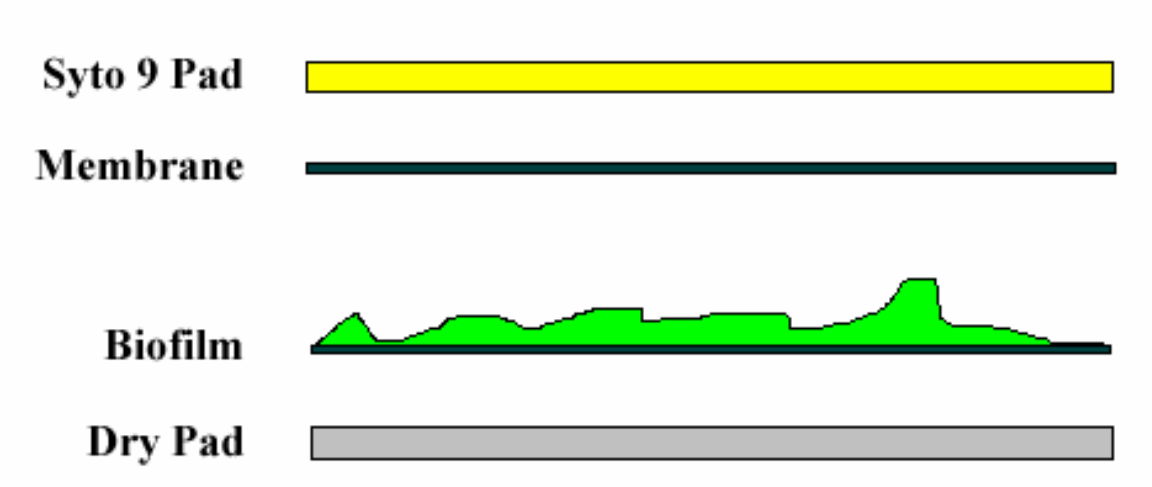

Figure A.9 Diagram of staining biofilm from the top. Disc pad saturated with TSB containing Syto® 9 placed on top of membrane, these were subsequently placed on top of the biofilm which was supported by a dry pad disc.

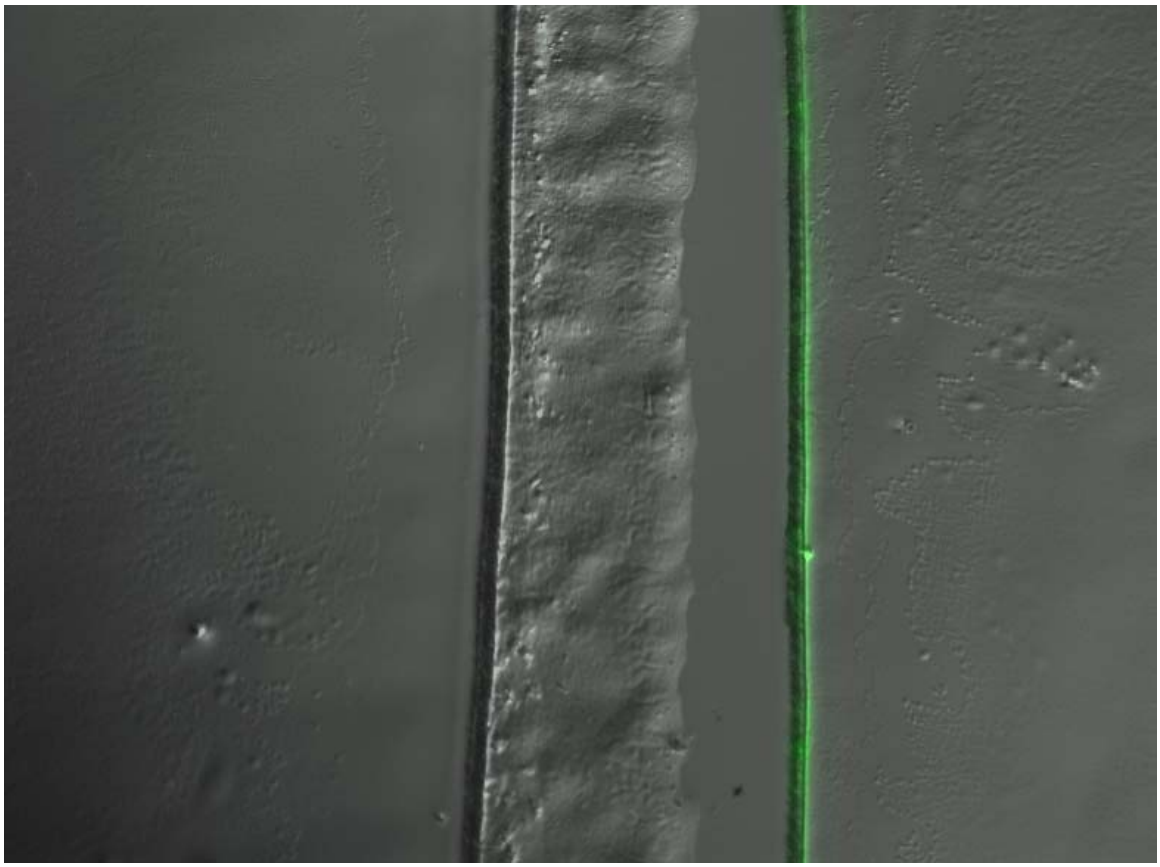

Figure A.10 Biofilm stained by placing a stain saturated pad disc on top of a fresh membrane and subsequently placing on top of the biofilm. The separation of the top membrane (right) is an artifact of the cutting and subsequent mounting of the frozen section.

At times it appeared that Syto® 9 was not penetrating through the polycarbonate membrane, but this was not the case. In some cases, there was apparent staining of cells stained on the membranes so the stain must have been at least partially, penetrating through the polycarbonate membranes. Since Syto® 9 is frequently used in conjunction with propidium iodide to stain live and dead cells using the LIVE/DEAD® Bac*Light*™ bacterial viability and counting kit, we decided to explore the staining characteristics of propidium iodide in intact biofilms (Figure A.11).

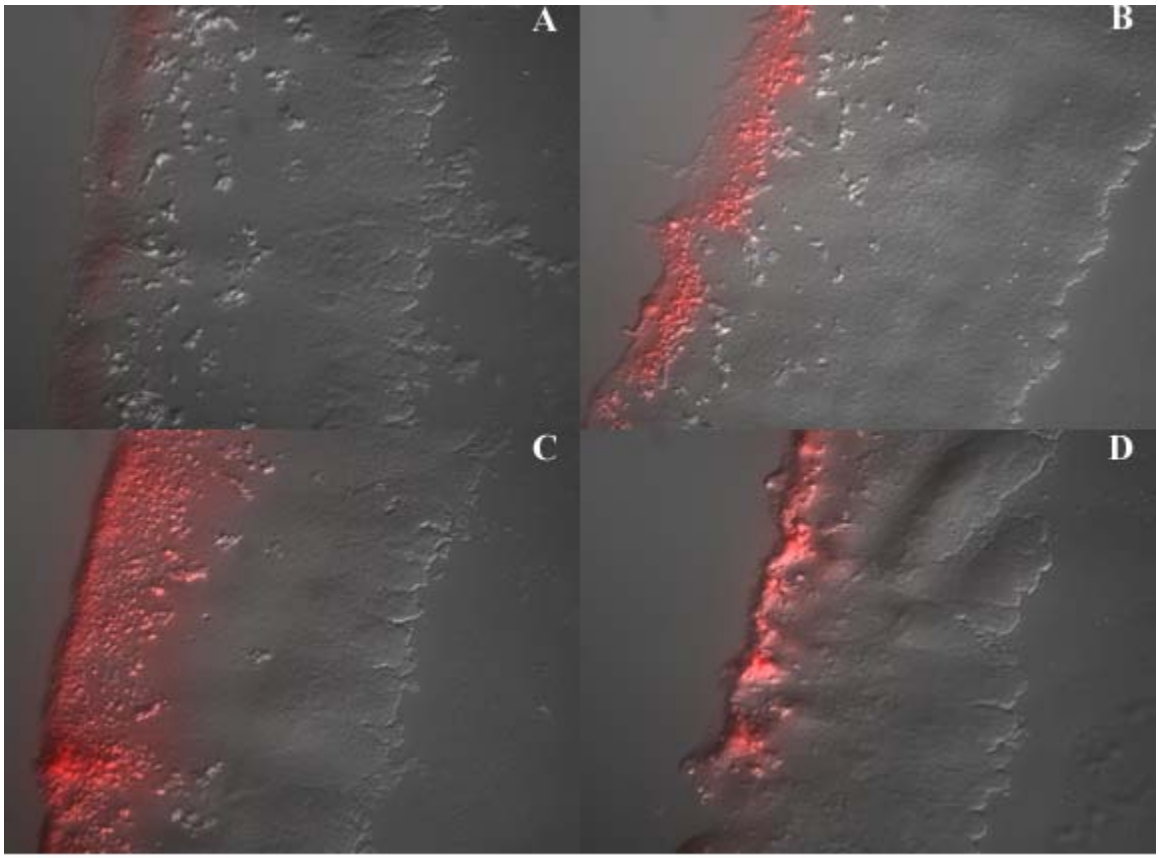

Figure A.11 Time series of intact biofilms stained on pad discs saturated with TSB containing 0.3mM propidium iodide. A) Biofilm exposed to stain for 10 minutes B) 30 minutes C) 4 hours D) 9 hours.

Propidum iodide is a cell inpermeant nucleic acid stain, it should stain only those cells that have compromised membranes. Staining of the biofilm commenced immediately upon introduction to propidium iodide but the stratified pattern of staining was still apparent. These were live, actively growing biofilms so we would expect less staining with propidium iodide than with Syto® 9. That is, propidium iodide should only

penetrate cells with compromised membranes (dead cells), where Syto® 9 should penetrate all cells, live and dead.

After these convoluted results with Syto® 9 and propidium iodide we decided to use another nucleic acid stain, acridine orange to repeat some of the experiments. Acridine orange did show an increased tendency to penetrate biofilms, but even after 9 hours of exposure, images of biofilms still indicated a stratified pattern of staining (FigureA.12). Biofilms were stained with acridine orange in an intact state, disaggregated in suspension, as well as disaggregated and stained on a membrane. Planktonic cells were stained in suspension as well as after being filtered onto a membrane (images not shown). These experiments resulted in images that were similar to the previous set of analogous experiments performed with Syto® 9. Acridine orange did result in more rapid and complete staining of the biofilm but the planktonic cells still stained much brighter than biofilm cells (even those at the membrane interface) and stain uptake patterns were still quite convoluted.

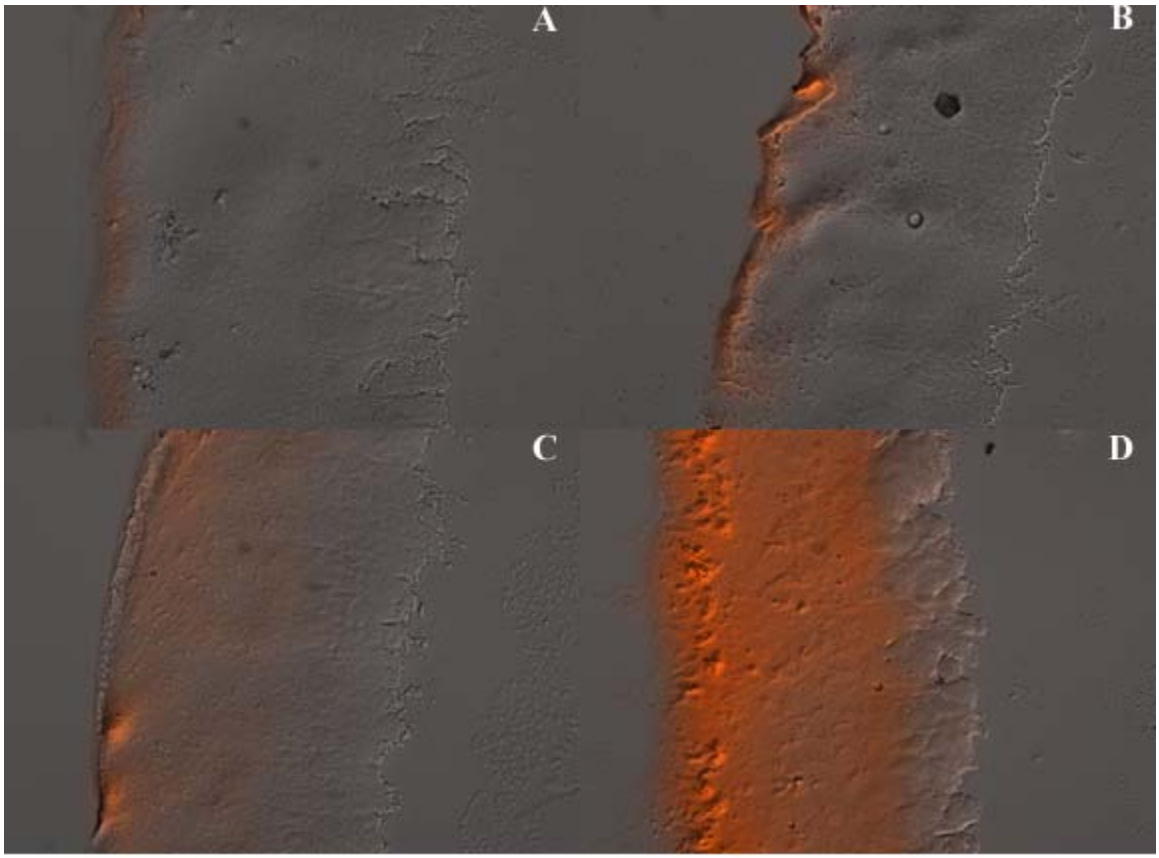

Figure A.12. Time course of staining of intact biofilms by acridine orange. A) image taken after 10 minutes of exposure to a filter pad saturated with acridine orange in TSB B) 2 hours of exposure C) 4 hours D) 9 hours.

The staining characteristics of rhodamine B were explored briefly. A time course of intact biofilm staining was taken (Figure A.13), it was apparent that rhodamine B did in fact penetrate completely through the biofilm. This was confirmed by analysis of paper discs placed on top of the biofilm during staining. The discs were taken off the top of the biofilm at time points during staining and placed in sterile water. The water was then placed in a flourometer and analyzed for presence of rhodamine B. In this manor it was possible to determine that rhodamine B fully penetrates the biofilm within 2 hours

(Figure A.14). It must be noted that rhodamine B is not a nucleic acid stain and thus does not need to enter the cells of the biofilm for the stain to appear bright.

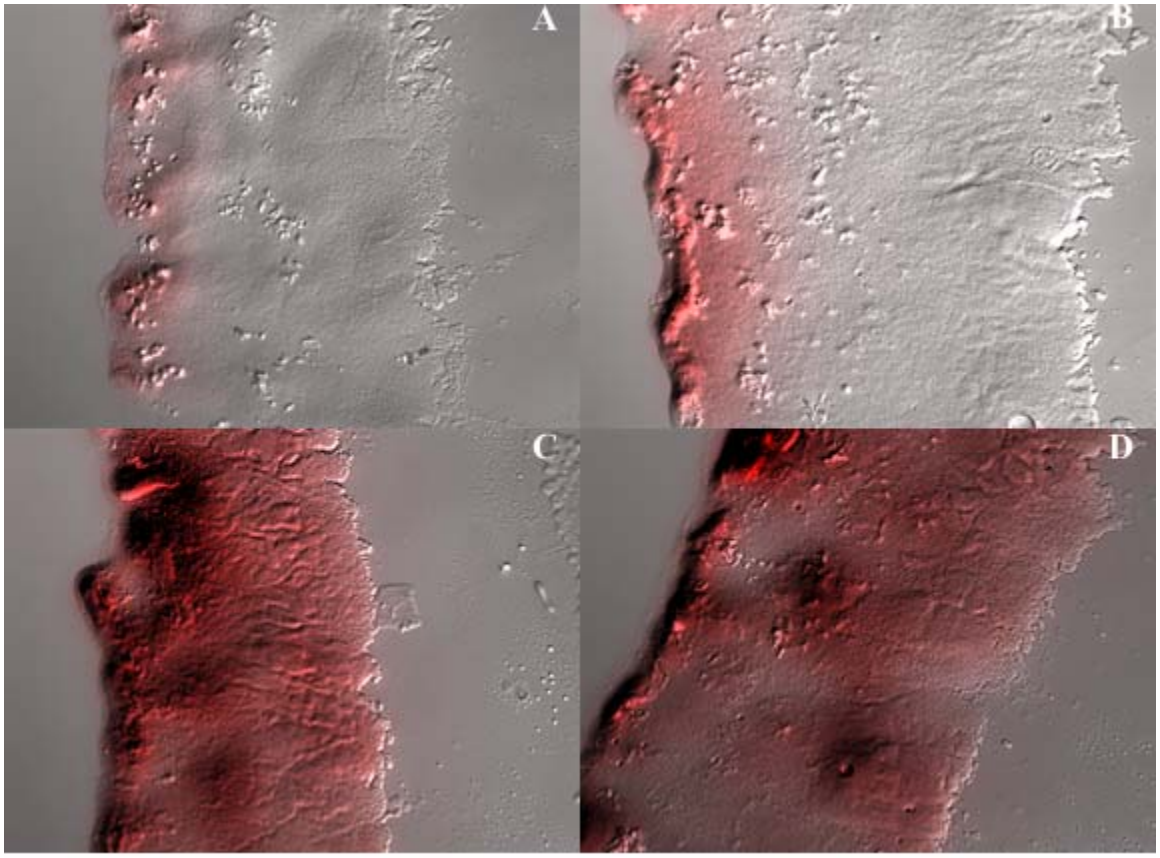

Figure A.13 Time course of images taken of intact biofilms stained by placing the mature biofilms on plates containing rhodamine B for A) 10 minutes B) 30 minutes C) 4 hours D) 9 hours.

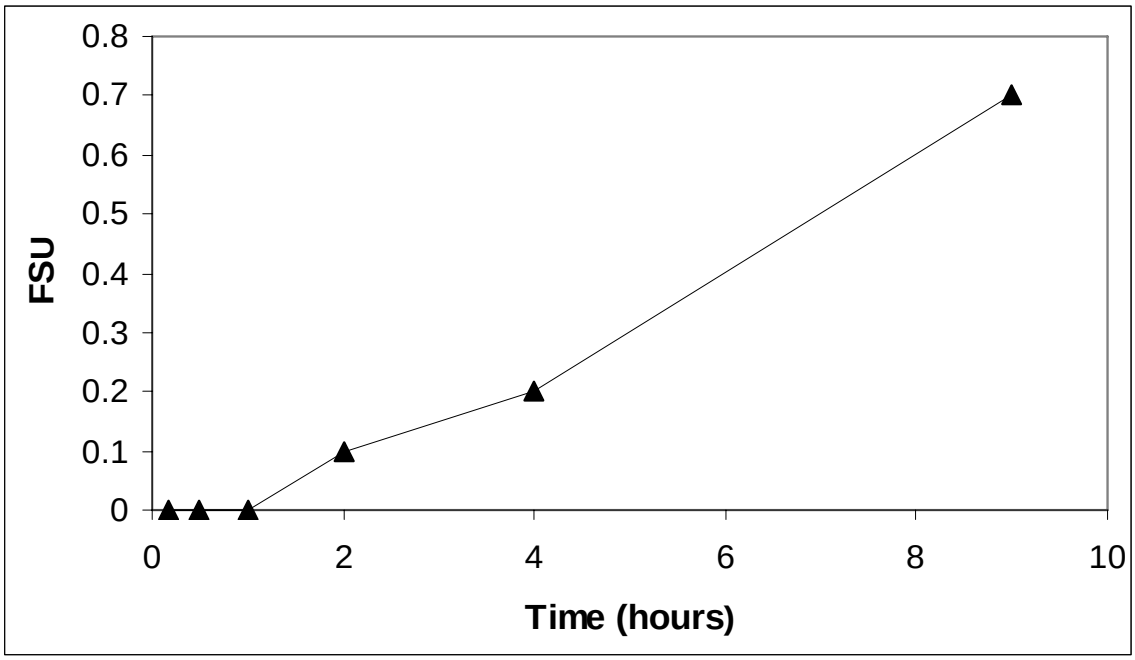

Figure A.14 Time course of readings taken in fluorometer from discs placed on top of biofilms to absorb rhodamine B. Rhodamine B was introduced to the biofilm by dissolving in TSA before cooling thus impregnating the plates with the proper amount of dye.

Conclusion

It was shown that rhodamine B does actually penetrate the biofilm in a fairly rapid fashion. It did not appear that Syto® 9, propidium iodide, or acridine orange actually penetrated completely through the biofilm. It was apparent that acridine orange was able to stain the cells in a more rapid fashion than Syto® 9. Acridine orange and Syto® 9 have similar molecular weights (301.82, and about 250 to 300 respectively), so it copuld be theorized that they should penetrate through the biofilm in a similar manor. That is, if molecular weight were the most important factor in the stains transport through the biofilm. There are of course other factors such as electrostatic interactions, that play into

the affinity of a substance to travel through a biofilm. The molecular weight of rhodamine B is actually greater than that of Syto® 9 or acridine orange, a direct comparison cannot be made here though since rhodamine B is not a nucleic acid stain.

This method of testing our hypothesis that biofilm cells were less permeable than planktonic cells proved to be less than fruitful. The results were not clear and led to more questions than answers. It is apparent though that staining of intact *P. aeruginosa* biofilms with the LIVE/DEAD® Bac*Light*™ bacterial viability and counting kit may result in false results since neither Syto® 9 nor propidium iodide penetrate the biofilm in its entirety.

REFERENCES

1) Abdi-Ali A.; Mohammadi-Mehr M.; Agha Alaei Y. Bactericidal activity of various antibiotics against biofilm-producing Pseudomonas aeruginosa. International Journal of Antimicrobial Agents. 2006 Mar;27(3):196-200

2) Anderl, J.N.; Franklin, M.J.; Stewart P.S. Role of Antibiotic Penetration Limitation in Klebsiella pneumonia Biofilm Resistance to Ampicillin and Ciprofloxacin. Antimicrobial Agents and Chemotherapy 2000, 44, 1818-1824

3) Hu, Z.; Hidalgo, G.; Houston, P.L.; Hay, A.G.; Shuler, M.L.; Abruna, H.D.; Ghiorse, W.C.; Lion, L.W.; Determination of spatial distributions of zinc and active biomass in microbial biofilms by two-photon laser scanning microscopy. Applied Environmental Microbiology. 2005, 71(7) 4014-4021

4) Jefferson, K.K.; Goldmann, D.A.; Pier, G.B.; Use of confocal microscopy to analyze the rate of vancomycin penetration through Staphylococcus aureus biofilms. Antimicrobial Agents and Chemotherapy 2005, 49(6), 2467-73

5) Macedo, A.J.; Kuhlicke, U.; Neu, T.R.; Timmis, K.N.; Abraham, W.R.; Three stages of a biofilm community developing at the liquid-liquid interface between polychlorinated biphenyls and water. Applied Environmental Microbial Microbiology. 2005, 71(11) 7301-7309

6) Neut, D.; Hendriks, J.G.; van Horn, J.R.; van der Mei, H.C.; Busscher, H.J.; Pseudomonas aeruginosa biofilm formation and slime excretion on antibiotic-loaded bone cement. Acta Orthopaedica. 2005, 76(1) 109-114

7) Shigeta, M.; Tanaka, G.; Komatsuzawa, H.; Sugai, M.; Suginaka, H.; Usui, T.; Permeation of antimicrobial agents through Pseudomonas aeruginosa biofilms: a simple method. Chemotherapy 1997, 43(5) 340-345

8) Walters, M.C.; Roe, F.; Bugnicourt, A.; Franklin, M.J.; Stewart, P.S.; Contributions of antibiotic penetration, oxygen limitation, and low metabolic activity to tolerance of Pseudomonas aeruginosa biofilms to ciprofloxacin and tobramycin. Antimicrobial Agents and Chemotherapy 2003, 47(1), 317-23

9) Xu, K.D.; Stewart, P.S.; Xia, F.; Huang, C.; McFeters, G.A., Spatial Physiological Heterogeneity in Pseudomonas aeruginosa is Determined by Oxygen Availability Applied and Environmental Microbiology 1998**,** 64, 4035-4039

APPENDIX B

NUMERICAL SOLUTION TO OXYGEN DIFFUSION THROUGH THE BIOFILM

Introduction

A model of the drip flow biofilm was developed in order to compare a mathematical model of oxygen distribution above and within the biofilm to the data that were obtained via microelectrodes. The biofilm was modeled as a flat slab, with a stagnant fluid film over it. Convection within the biofilm and the fluid film was considered to be negligible. It has been noted that within the cell cluster of a biofilm the only transport mechanism present is diffusion (1,15). Modeling the biofilm with a stagnant fluid layer above it is a generalization of the many conditions that exist within a given biofilm region. Imaging of biofilms has shown that they consists of many different geometries, including channels, cell clusters and voids within aggregates of cells (2,6,8,9,10). These differing structures lead to varying fluid velocities related to the biofilm system (10). Fluid velocity ranges from laminar flow in channels to nearly stationary liquid in other areas of the biofilm system (16,14). A flat slab biofilm and a stagnant liquid layer above the biofilm is used here as a one representation of the biofilm.

Several attempts were made to fit the model to the data by altering parameters that were either not clear or not recorded for this system, namely biofilm density and fluid film thickness.

Discussion

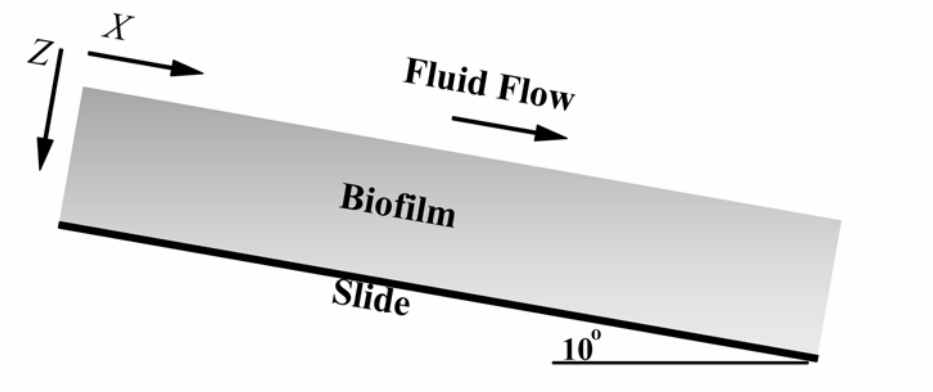

Figure B.1 Coordinate geometry of drip flow biofilm on 10^o incline.

If we take the biofilm to be a flat slab on a 10^o incline, we can solve for the average velocity over a cross section of the inclined film from the following equation

$$< v_x >= \frac{\rho g \delta^2 \cos\beta}{3\mu} \quad (3)$$

We can calculate the mass flow rate of a falling film by the following equation

$$w = \int_0^W \int_0^\delta \rho v_x dz dy = \rho W \delta < v_x >= \frac{\rho^2 g W \delta^3 \cos\beta}{3\mu}$$

Where..

ρ = density of nutrient medium (0.99 g cm^{-3})

W = width of slide (1.2 cm)

g = gravitational acceleration (998 cm s^{-2})

δ = thickness of the falling film

β = 90^o – angle of incline (80^o)

μ = viscosity of nutrient medium at 37^o C (0.00692 g cm^{-1} s^{-1})

w = mass flow rate (0.014 g s^{-1} based on 50 ml hr^{-1})

Rearranging this to solve for film thickness

$$\delta = \sqrt[3]{\frac{3\mu w}{\rho^2 g W \cos\beta}}$$

and calculating this quantity with the above parameter values gives, $\delta = 113\mu m$

The approximate time for oxygen to equilibrate diffusively across the fluid film can be estimated by

$$t \approx \frac{\delta^2}{D_{aq}}$$

The diffusion coefficient of oxygen in water at 25°C has been recorded as 20.0*10^{-6} cm^2 s^{-1} (7). The relationship between temperature and diffusivity is as follows

$$\frac{D_{aq}\mu}{T} = C$$

Where..

C = constant

D_{aq} = diffusivity of oxygen in water at 30°C

From this, diffusivity of oxygen in water at 37°C is calculated to be 26.8*10^{-6} cm^2 s^{-1}.

A good approximation for the effective diffusivity of oxygen in the biofilm can be calculated by the ratio $\frac{D_e}{D_{aq}} = 0.6$ (12)

Taking temperature into account, this yields an effective diffusivity of oxygen within the biofilm of $16.8*10^{-6}$ cm^2 s^{-1} at 37°C.

We know the average fluid velocity is given by

$$< v_z >= \frac{\rho g \delta^2 \cos\beta}{3\mu}$$

So the entrance length, or the length down the slide that it takes for oxygen to equilibrate by diffusion from the top of the fluid layer to the bottom, is given by

$$t < v_z >= \frac{\rho g \delta^4 \cos\beta}{3\mu D_{aq}} = \lambda$$

For our film of a thickness of 113 μm, $\lambda = 4.94$ cm

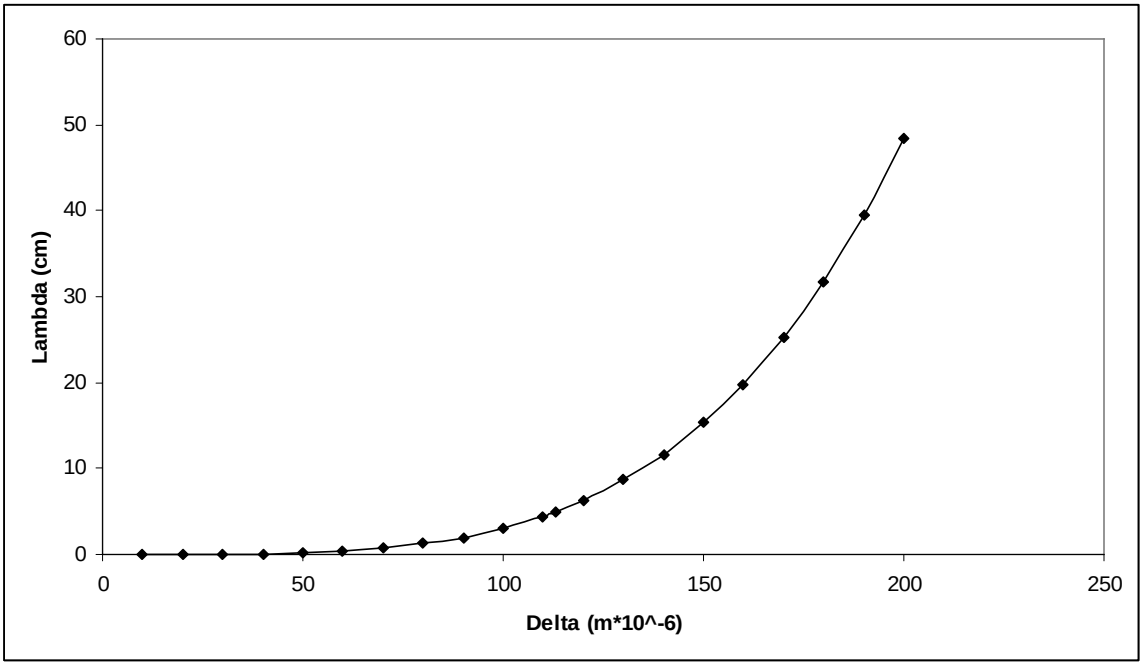

Figure B.2 Plot of the entrance length λ in centimeters versus the film thickness δ in micrometers.

It is clear that the entrance length is fairly short until the film thickness reaches about 60μm. The entrance length is 4.94 cm for our film thickness of 113 μm. That is a substantial distance when you consider that the dimensions of the slide are 8.1 cm by 1.2 cm. On the other hand, if the film was only 70μm thick the entrance length would only be about 0.7 cm.

Knowing the film thickness we can calculate the Reynolds number.

The Reynolds number is given by

$$\mathrm{Re} = \frac{4\delta < v_z > \rho}{\mu}$$

calculating using a theoretical film thickness of 113 μm, Re = 6.6

When..

Re<20 laminar flow with negligible rippling

20<Re<1500 laminar flow with pronounced rippling

Re>1500 turbulent flow

From this calculation it is obvious that this system of a flat slab on an incline produces laminar flow with negligible rippling, but we know that the biofilm is not a flat slab and the fluid film thickness is not uniform since the biofilm has high and low spots where the film may be thicker or thinner. From the previous calculation of the entrance length, with a 113 μm fluid film, of approximately 5 cm means that a model that takes into account the convection within the biofilm, would yield the most accurate results for the first half of the biofilm. On the other hand anywhere the fluid film is substantially thinner the model would not fit since diffusion would be the dominant force to transport oxygen through the fluid. When the fluid film gets thinner diffusion becomes the dominate force for oxygen transport. It is important to note that on the actual biofilm, the fluid film is most likely very heterogeneous with thin and thick areas. The goal of this section of the thesis is to fit a curve to the oxygen concentration profile presented in figure 2.1A. That figure is presented again here for the sake of discussion.

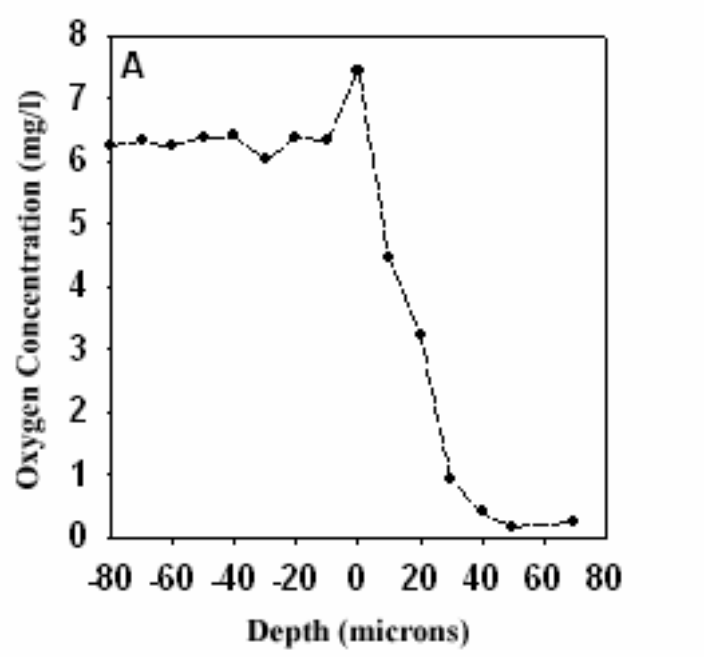

Figure B.3 Oxygen profile within biofilm cluster measured by dissolved oxygen microelectrode.

The flat area of the graph is in the airspace above the fluid film. It is difficult to differentiate the fluid film from the biofilm in this figure but the fluid film should yield a linear oxygen concentration profile, where the biofilm should produce a curved oxygen concentration profile. The curved geometry present within the biofilm is due to the reaction that is taking place by the biofilm consuming oxygen. From this graph it is possible to estimate the fluid thickness above the biofilm as a maximum of about 30 μm. Since the film above the biofilm is very thin it makes more sense to model this system using a stagnant film model where diffusion is the predominant form of oxygen transport rather than a model that takes convection into account.

This model presented here is of a flat slab biofilm with a stagnant fluid film above it. It is valid for areas where the film is in general less than 100 μm thick.

We will start by modeling the fluid layer above the biofilm. Diffusion of oxygen through this stagnant layer can be modeled by assuming a steady state concentration of oxygen above the biofilm C_O^o. We will also assume that all transport is by diffusion perpendicular to the substratum. A steady state mass balance around this yields the differential equation

$$D_{aq}\frac{d^2C_O^f}{dz^2}=0$$

Where..

C_O^f = concentration of oxygen within the fluid film

z = distance from fluid/air interface

The first boundary condition we will use is

$$C_O^f = C_O^o \quad \text{at} \quad z=0$$

Integrating this equation and implementing the boundary condition yields

$$D_{aq}\frac{d\ C_O^f}{dz}=C_1$$

This is the flux of oxygen through the fluid film. If we integrate again we get the concentration of oxygen spatially with respect to the z axis in the biofilm

$$C_O^f = \frac{C_1}{D_{aq}}z + C_O^o$$

where C_1 is an arbitrary constant to be solved for after further problem development.

We will model the oxygen transport through the biofilm again as a strictly diffusive mechanism with all transport perpendicular to the substratum. The biofilm will

be modeled as a flat slab. A flat slab is rarely the geometry present in actual biofilms but will serve as a good approximation for our purposes. Oxygen consumption within the biofilm will be considered to follow zero order Monod kinetics. A mass balance yields

$$D_e \frac{d^2 C_O}{dz_b^2} - k_O = 0$$

Where..

D_e = diffusivity of oxygen through the biofilm at 30°C

C_O = concentration of oxygen within the biofilm

z_b = distance from fluid/biofilm interface

k_O = oxygen Monod coefficient

Using the following boundary conditions

$$C_O = C_O^s \quad \text{at} \quad z_b = 0$$

$$\frac{d\ C_O}{dz_b} = 0 \ \text{ at } \ z_b = a$$

Where..

C_O^s = concentration of oxygen at the biofilm/fluid interface

a = penetration depth of oxygen within the biofilm

Integrating this equation once yields

$$D_e \frac{d\ C_O}{dz_b} = k_O z + C_2$$

Where..

C_2 = arbitrary constant

We can solve for C_2 using the second (no flux) boundary condition, yielding

$$D_e \frac{d\ C_O}{dz_b} = k_O z_b - k_O a$$

This equation represents the flux of oxygen anywhere within the biofilm.

The solution to the equation for diffusion of oxygen within the biofilm is as follows

$$C_O = \frac{k_O}{2D_e} z_b{}^2 - \frac{k_O a}{D_e} z_b + C_O^s$$

We know that the flux of oxygen going through the biofilm interface is the same on both sides of the interface

$$D_e \frac{d\ C_O}{dz_b} = D_{aq} \frac{d\ C_O^f}{dz}$$

We can therefore solve for the diffusion at the surface of the biofilm layer at z_b=0

$$D_e \frac{d\ C_O}{dz_b} = -k_O a$$

Thus

$$D_{aq} \frac{d\ C_O^f}{dz} = C_1 = -k_O a$$

The oxygen concentration within the fluid layer can be represented as

$$C_O^f = \frac{-k_O a}{D_{aq}} z + C_O^o$$

The specific reaction rate for anabolism of oxygen within the biofilm is given as

$$k_O = \frac{\mu_{\max} X_b}{Y_{xO}}$$

Where..

$\mu_{\max}$ = maximum specific growth rate

X_b = biofilm cell density

Y_{xO} = oxygen yield coefficient

The maximum specific growth rate has been determined by experiments performed in our lab to be approximately 0.74 hr^{-1} (data not shown) under similar conditions.

The cell density within the biofilm X_b is $4.7 * 10^{-3}$ g of carbon ml^{-1}.(13)

The oxygen yield coefficient for Pseudomonas Aeruginosa biofilms has been recorded as 0.9 g carbon g^{-1} oxygen. (4)

Using these values we can calculate k_O

$k_O = 3.86 * 10^{-3}$ g $hr^{-1}ml^{-1}$.

Using these parameters and the following formula we can now calculate the oxygen penetration depth that should be expected within the biofilm.

$$a = \left(\frac{2D_e C_O^s}{k_o}\right)^{1/2} \quad (5)$$

We can calculate the maximum penetration depth possible in our system using an oxygen concentration at the surface of the biofilm. It should be noted that this is the same equation that we get when solving for the penetration depth *a* in the equation that we derived for the oxygen concentration within the biofilm.

$C_O^s = 6.0$ mg l^{-1}

Calculating for the maximum penetration depth we get $a = 134$ μm

The oxygen gradient within the fluid film will affect the penetration depth since penetration depth within the biofilm is dependent on the concentration of oxygen present on the surface C_O^s. From figure B.3 we know the concentration of oxygen at certain points in the fluid film and biofilm. If we assume the fluid film is 30 um thick then from figure B.3 the concentration of oxygen at the surface of the biofilm C_O^s is approximately 1 mg/l, thus we can back calculate the penetration depth. Performing this operation we get a penetration depth of approximately 54 um. This is of course much deeper than we see in our dissolved oxygen microelectrode analysis. Attempting to model this system using our fore mentioned model and a fluid film thickness of 30 μm we obtain the following profile.

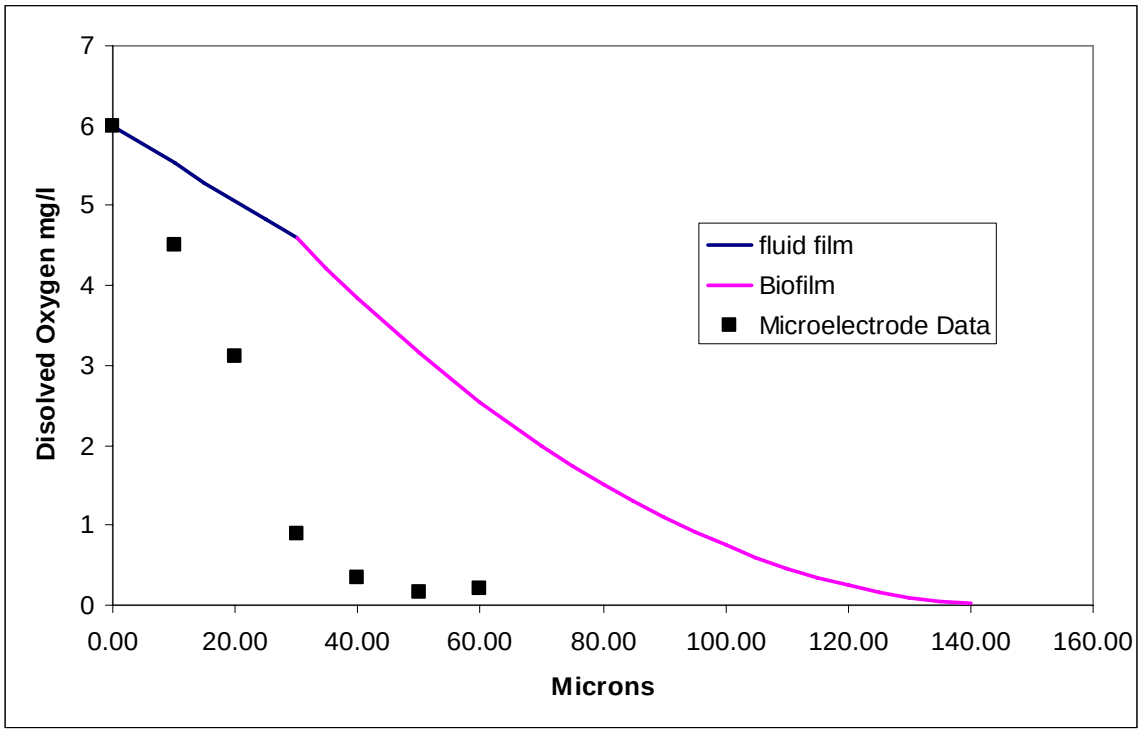

Figure B.4 Profile in fluid layer and biofilm layer. Model data represented with lines. The data from the microelectrode analysis (▲) is added as a reference. Fluid layer of 30 µm, hence the biofilm layer starts at 30 µm. The value of 60 µm on the graph represents 30 µm into the biofilm.

This representation is clearly not in agreement with the microelectrode data. This model shows that oxygen should penetrate about 117 µm into the biofilm. In chapter 2 we saw evidence of oxygen penetrating to around 60 µm into the biofilm using GFP expression.

One possible reason for the disparity between the model presented in figure B.4 and the data presented in B.3 may be a difference in biofilm density X_b. The number used here ($4.7 * 10^{-3}$ g of carbon ml^{-1}) may vary quite a bit from the actual density of the biofilm used in the microelectrode analysis. Biofilms are often quite different when grown under different conditions and a drip flow biofilm may have a different density

than one grown in another reactor system. We have not determined the actual density of the drip flow biofilms that we used for these experiments. Using the parameters and previous model and changing the density of the biofilm to 0.272 g of carbon ml^{-1} we get the following dissolved oxygen concentration curve.

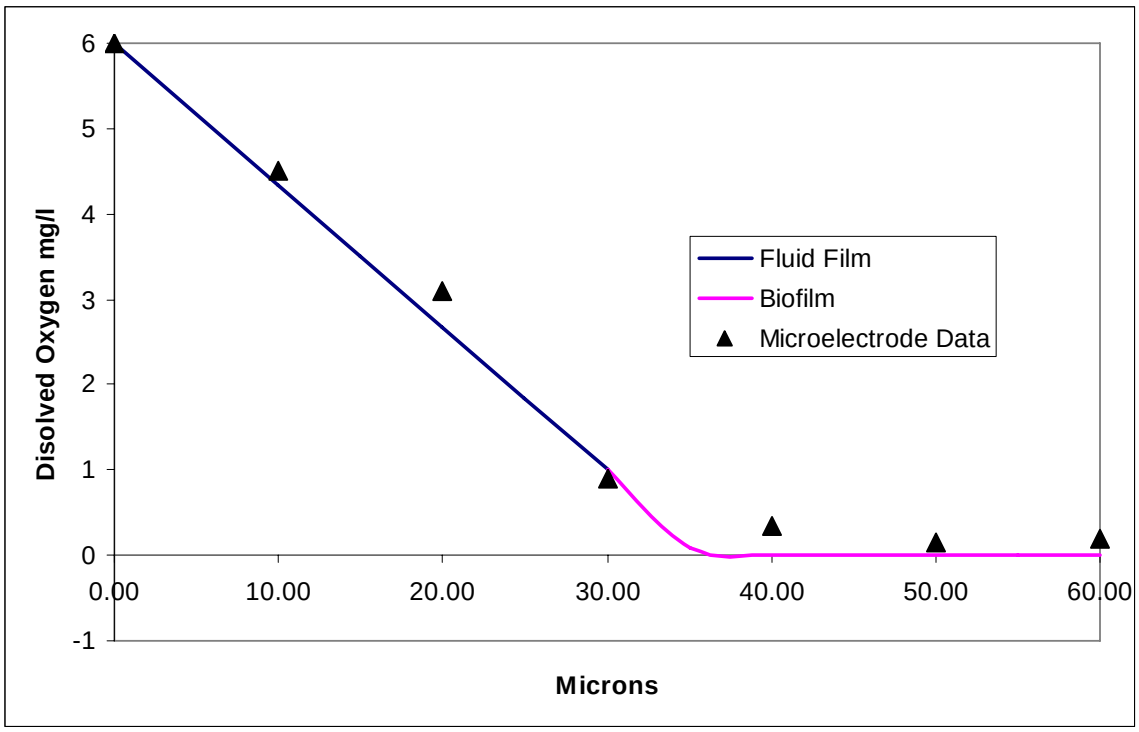

Figure B.5 Profile in fluid layer and biofilm layer using a biofilm density of 0.272 g of carbon ml^{-1}. Model data represented with lines. The data from the microelectrode analysis (▲) is added as a reference. Fluid layer of 30 µm hence the biofilm layer starts at 30 µm. The value of 60 µm on the graph represents 30 µm into the biofilm

This profile better represents the microelectrode data than the previous model using a smaller value for biofilm density. Of course the value for the biofilm density of 0.272 g of carbon ml^{-1} is substantially higher than the density recorded in the literature and is most unlikely. This biofilm density yields a penetration depth of approximately 7 um into the biofilm. This is a very improbable scenario.

It may be that the fluid film above the biofilm is actually closer to 20 um in depth. Using 20 µm as the fluid thickness and 3mg/L as the concentration of oxygen at the biofilm/fluid interface yields the following profile.

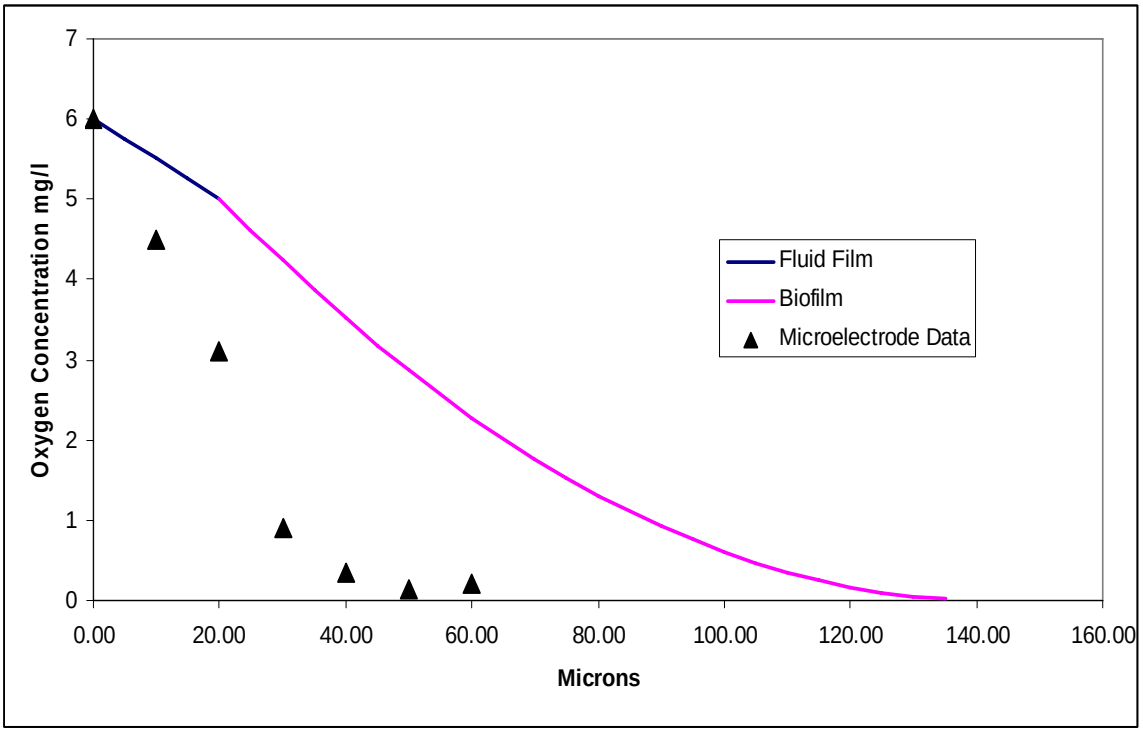

Figure B.6 Profile in fluid layer and biofilm layer. Fluid layer of 20 µm, hence the biofilm layer starts at 20 µm. Model data represented with lines. The data from the microelectrode analysis (▲) is added as a reference. The value of 60 µm on the graph represents 40 µm into the biofilm.

Again there is clearly a disparity between the data and the mathematical fit. It should be noted that the slope of the line that represents the oxygen concentration is not changing. The reader will recall the formula for the dissolved oxygen gradient in the fluid film is given by

$$C_O^f = \frac{-k_O a}{D_{aq}} z + C_O^o$$

Hence the slope is determined by the diffusion coefficient and the reaction coordinate k_o (the penetration depth is a function of reaction coordinate). The diffusion coefficient is well explored in biofilms of very similar structure (7). The reaction coordinate is again a product of yield coefficient, reaction rate and biofilm density. As stated earlier the parameter that is most suspect in this scenario is the biofilm density. Figure B.7 illustrates varying the biofilm density in the model..

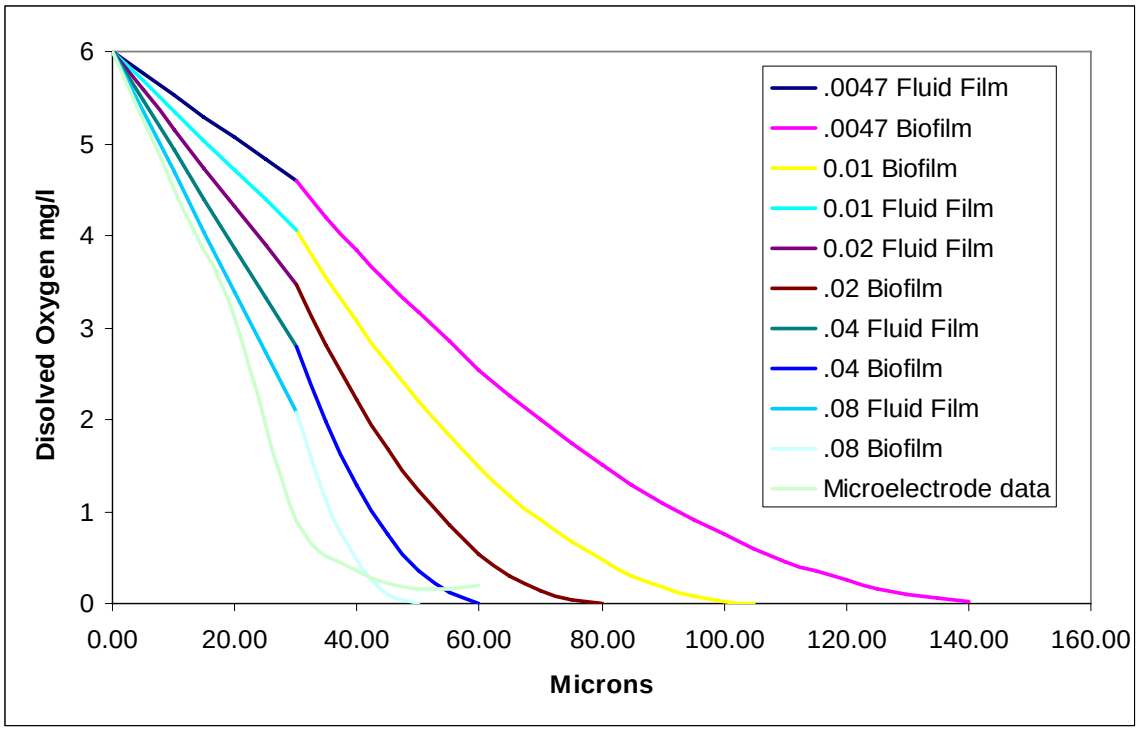

Figure B.7 Graph illustrating the effects of changing biofilm density on the mathematical model. Biofilm density recorded in key in units of g of carbon ml^{-1}.

From figure B.7 it is apparent that if the density number that we used for calculation of the model ($4.7 * 10^{-3}$ g of carbon ml^{-1}) is off there could be substantial

error entered into the model. By increasing the biofilm density it is possible to get a much better fit to the experimental data that was collected.

Another aspect that could vary in our system is the fluid film thickness. There are not enough data points from the dissolved oxygen microelectrode to determine exactly where the biofilm/fluid interface is. It is clear from the curve that the film is no thicker than 40 µm in thickness due to the curvature of the graph in the region past 40 µm. The following figure shows the behavior of the model when biofilm density is held constant and the fluid film thickness is varied.

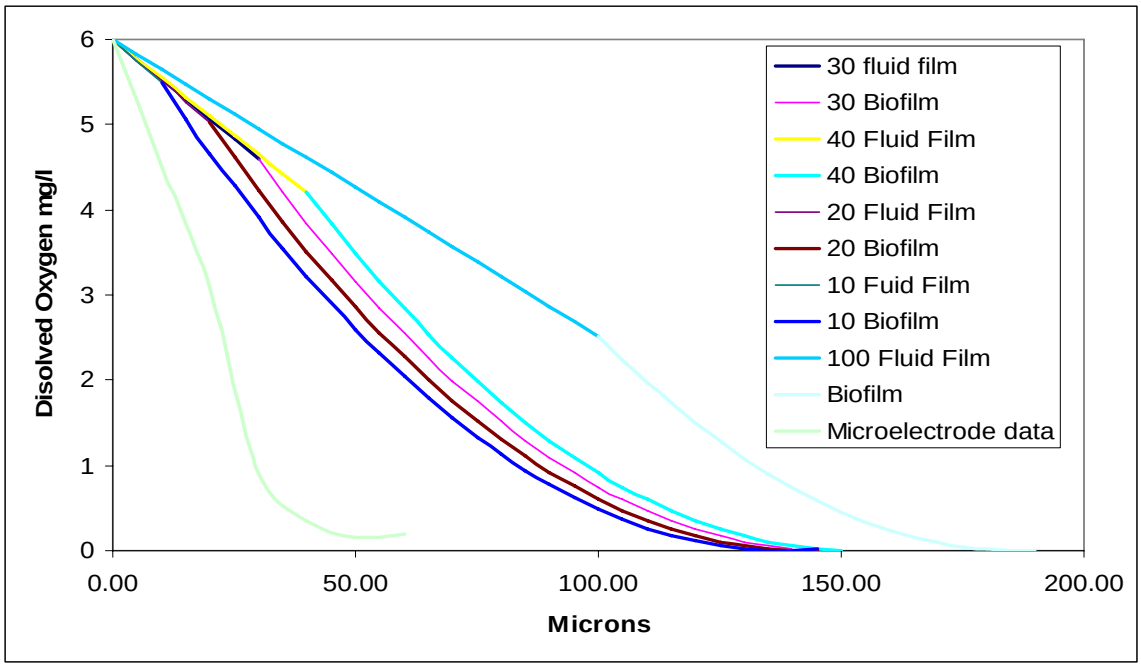

Figure B.8 Graph illustrating the effects of changing fluid film thickness above the biofilm. Fluid film thickness represented in key, units are µm.

It is clear from the figure B.8 that varying the fluid film thickness above the biofilm makes a very small difference in improving the model fit to the experimental

data. It is apparent that changing the biofilm density is more likely to result in a better fit of the data. The 100um fluid film thickness was put in as a reference to show how a substantially thicker film would affect the model.

Perhaps the best fit of the data can be obtained by using the mathematical model derived above, assuming a fluid thickness of 20 μm and varying the biofilm density. From this we can obtain a best fit to the data using the method of least squares.

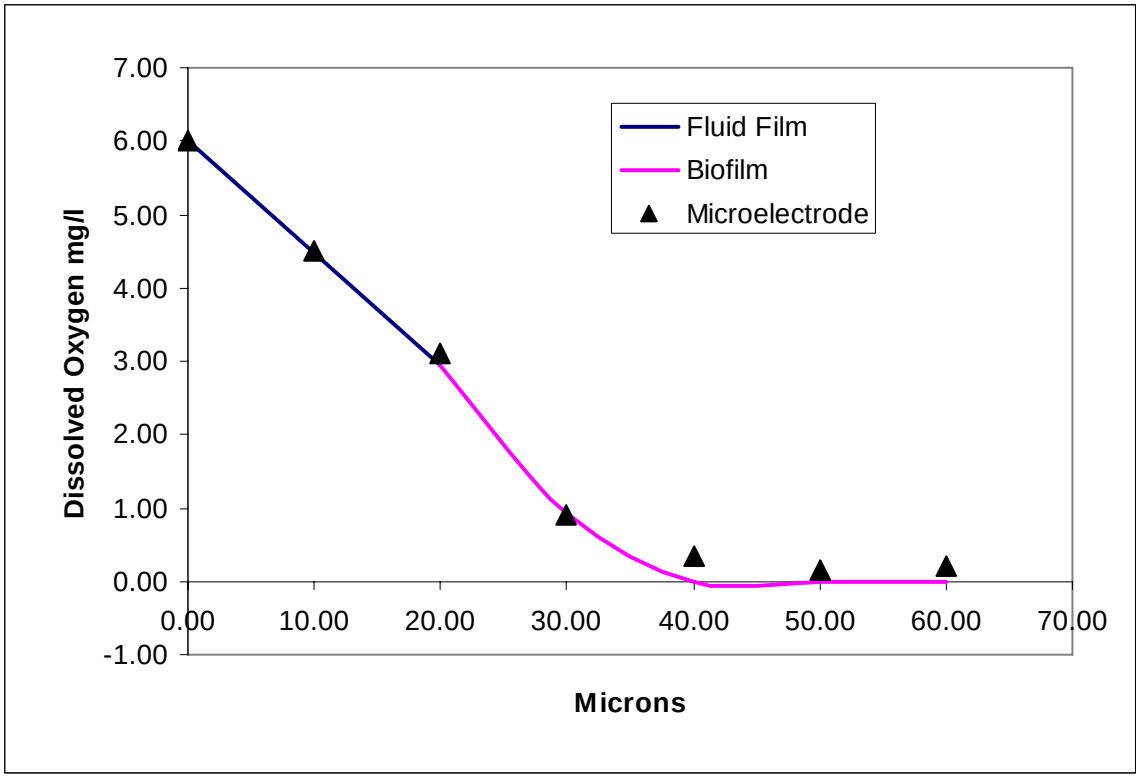

Figure B.9 Graph of a least squares fit to the experimental microelectrode data created by setting the film thickness to 20 μm and varying the biofilm density. This fit was obtained with a biofilm density of 0.077 g of carbon ml^{-1}.

Here we see that with a fluid film thickness of 20 μm and a biofilm density of 0.077g of carbon ml^{-1} a fairly accurate fit can be obtained. It may be that this is closer to

the actual conditions that were present when the microelectrode analysis was performed. Earlier in chapter 2 we explored a theoretical calculation of glucose diffusion into the biofilm and determined that there was adequate glucose available to the biofilm. As further evidence of oxygen being the limiting nutrient in our drip flow biofilms, we will explore the flux of glucose into the biofilm here.

We previously determined the flux of oxygen through the fluid film to be represented by.

$$D_{aq} \frac{d\ C_O^f}{dz} = J$$

Where J = Flux of oxygen through the fluid film. From our oxygen profile we can determine this flux fairly accurately since the slope of the line for the linear fluid film portion is equal to $\frac{d\ C_O^f}{dz}$. Using the first 20 μm of the graph we can get an estimate of the flux of oxygen to be 1.5 mg cm^{-4} multiplied by the diffusion coefficient of Oxygen through water D_{aq} = 26.8*10^{-6} cm^2 s^{-1}. This yields a flux of 4.02*10^{-5} mg cm-^{2} s^{-1}. We can multiply this by the area of the slide which the biofilm is growing on (9.7 cm^2) this is assuming that the surface area of the biofilm is analogous to the area of the slide, i.e. the biofilm covers the entire slide. We get the value 3.9*10^{-4} mg s^{-1}. We can now divide by the flow rate of 50 ml hr^{-1} (0.014 ml s^{-1}) to get 2.8*10^{-2} mg oxygen cm-^{3}. The yield coefficient for glucose consumed per unit of oxygen consumed in 0.89 g glucose carbon g^{-1} oxygen carbon (4). Multiplying by the yield coefficient gives 2.5*10^{-2} mg glucose carbon cm-^{3}, there are .4 grams of carbon per gram of glucose so we get 6.25*10^{-2} mg glucose cm-^{3}. The glucose concentration in our medium was 0.2 mg glucose cm-^{3} so it is

clear that glucose was not limited in our system. And oxygen is in fact the limiting nutrient

Conclusion

This model analysis elucidated a great deal regarding the behavior of oxygen gradients within the biofilm. It was clear from the poor fit using the biofilm density parameters described in the literature that in the system used for microelectrode analysis the density of the biofilm is most likely drastically different than published data. The disparity in the model was most likely due to a difference in both biofilm density and fluid film thickness, although it appears that biofilm density is more important to obtaining a good fit in this situation. The best fit was obtained with a 20 μm thick fluid film above the biofilm and a biofilm density of 0.066 g of carbon ml^{-1}. This is a very useful result since the data obtained for dissolved oxygen concentration using microelectrodes had very few data points and it was difficult to obtain a depth for the fluid film and subsequent oxygen penetration depth. From the analysis here it appears that the fluid film is approximately 20 μm thick and the subsequent penetration depth of oxygen into the biofilm is 30 to 50 μm.

This analysis helps elucidate the need for future research into this area to obtain a more accurate mathematical mode. It would be advantageous to gather more data using dissolved oxygen microelectrodes. By obtaining more data points it would be possible to determine the actual fluid thickness above the biofilm. In addition, and perhaps the most important issue to explore, would be to determine the biofilm density within this system.

From our analysis here, it appears that the density of the biofilm used for microelectrode analysis is drastically different from that recorded in the literature.

REFERENCES

1) de Beer, D.; Stoodley, P.; Lewandowski, Z.; Measurements of local diffusion coefficients in biofilms by micro injection and confocal microscopy. Biotechnology and Bioengineering 1997, 53. 151-158

2) de Beer, D.; Stoodley, P.; Roe, F., Lewandowski, Z.; Effects of biofilm structures on oxygen distribution and mass transport. Biotechnology and Bioengineering 1994, 43, 1131-1138

3) Bird, R.B.; Stewart, W.E.; Lightfoot, E.N.; Transport Phenomena 2nd Edition, John Wiley and Sons Inc. New York, NY, 2002

4) Characklis, W.G.; Energetics and Stoichiometry. Eds. Characklis, W.G.; Marshall, K.C. *in* Biofilms, 1990 John Wiley and Sons inc., New York, pp. 161-192

5) Costerton, J.W.; Lewandowski, Z.; de Beer, D.; Caldwell, D.; Korber, D.; James, G.; Biofilms, the customized microniche. Journal of Bacteriology 1994, 176, 2137-2142

6) Gjaltema, A.; Arts. P.A.M.; van Loosdrecht, M.C.M.; Kuenen, J.G.; Heijnen, J.J.; Heterogeneity of biofilms in rotating annular reactors: Occurrence, structure and consequences. Biotechnology and Bioengineering 1994, 44, 194-204

7) Han, P.; Bartels, D.M.; Temperature dependence of oxygen diffusion in H_20 and D_20. Journal of Physical Chemistry 1996, 100, 5597-5602

8) Kugaprasatham, S.; Nagaoka, H.; Ohgaki, S.; Effect of turbulence on nitrifying biofilms at non-limiting substrate conditions. Water Resources 1992, 26(12), 1629-1638

9) Lawrence, J.R.; Korber, D.R.; Hoyle, B.D.; Costerton, J.W.; Caldwell, D.E.; Optical sectioning of microbial biofilms. Journal of Bacteriology 1991, 173, 6558-6567

10) Massol-Deya, A.A.; Whallon, J.; Hickey, R.F.; Tiedje, J.M.; Channel structures in aerobic biofilms of fixed film reactors treating contaminated ground water. Applied Environmental Microbiology 61(2), 769-777

11) Rasmussen, K.; Lewandowski, Z.; Microelectrode measurements of local mass transport rates in heterogeneous biofilms. Biotechnology and Bioengineering 1998, 59, 302-309

12) Stewart, P.S.; Diffusion in biofilms. Journal of Bacteriology 2003, 185(5), 1485-1491

13) Stewart, P.S.; Biofilm accumulation model that predicts antibiotic resistance of *Pseudomonas aeruginosa* biofilms. Antimicrobial Agents and Chemotherapy 1994, 38(5), 1052-1058

14) Stoodley, P.; Yang, S.; Lappin-Scott, H.; Lewandowski, Z.; Relationship between mass transfer coefficient and liquid flow velocity in heterogenous biofilms using microelectrodes and confocal microscopy. Biotechnology and Bioengineering 1997, 56, 681-688

15) Stoodley, P.; de Beer, D.P.; Lewandowski, Z; Liquid flow in biofilm systems. Applied Environmental Microbiology 1994, 60, 2711-2716

16) Vogt, M.; Flemming, H.C.; Veeman, W.S.; Diffusion in *Pseudomonas aeruginosa* biofilms: a pulsed field gradient NMR study. Journal of Biotechnology 2000, 77, 137-146